Channel Adaptive Transmission of Big Data: A Complete Temporal Characterization and its Application

by

Wen-Jing WANG
B.Sc., Xi'an University of Post & Telecommunications, 2008
M.Sc., Northwestern Polytechnical University, 2013

A Dissertation Submitted in Partial Fulfillment of the
Requirements for the Degree of

DOCTOR OF PHILOSOPHY

in the Department of Electrical & Computer Engineering

Channel Adaptive Transmission of Big Data: A Complete Temporal Characterization and its Application

by

Wen-Jing WANG
B.Sc., Xi'an University of Post & Telecommunications, 2008
M.Sc., Northwestern Polytechnical University, 2013

Supervisory Committee

Dr. Hong-Chuan Yang, Supervisor
(Department of Electrical & Computer Engineering)

Dr. Thomas Aaron Gulliver, Departmental Member
(Department of Electrical & Computer Engineering)

Dr. Kui Wu, Outside Member
(Department of Electrical & Computer Engineering)

Supervisory Committee

Dr. Hong-Chuan Yang, Supervisor
(Department of Electrical & Computer Engineering)

Dr. Thomas Aaron Gulliver, Departmental Member
(Department of Electrical & Computer Engineering)

Dr. Kui Wu, Outside Member
(Department of Electrical & Computer Engineering)

ABSTRACT

We investigate the statistics of transmission time of wireless systems employing adaptive transmission. Unlike traditional transmission systems where the transmission time of a fixed amount of data is typically regarded as a constant, the transmission time with adaptive transmission systems becomes a random variable, as the transmission rate varies with the fading channel condition. To facilitate the design and optimization of wireless transmission schemes, we present an analytical framework to determine statistical characterizations for the transmission time with adaptive transmission. In particular, we derive the exact statistics of transmission time over block fading channels. The probability mass function (PMF) and cumulative distribution function (CDF) of transmission time are obtained for both slow and fast fading scenarios. We further extend our analysis to Markov channels, where the transmission time becomes a sequence of exponentially distributed random-length time slots. Analytical expression for the probability density function (PDF) of transmission time is derived for both fast and slow fading scenarios. Since the energy consumption can be characterized by the product of power consumption and transmission time, we also evaluate the energy consumption for wireless systems with adaptive transmission.

Cognitive radio communication can opportunistically access underutilized spectrum for emerging wireless applications. With interweave cognitive implementation, a secondary user (SU) transmits only if a primary user does not occupy the channel and waits for transmission otherwise. Therefore, secondary packet transmission involves both transmission and waiting periods. The resulting extended delivery time (EDT) is critical to the throughput analysis of secondary system. With the statistical results of transmission time, we derive the PDF of EDT considering random-length SU transmission and waiting periods for continuous spectrum sensing and semi-periodic spectrum sensing. Taking spectrum sensing errors into account, we propose a discrete Markov chain modeling slotted secondary transmission coupled with periodic spectrum sensing. Markov modeling is applied to energy efficiency optimization and queuing performance evaluation.

Contents

Supervisory Committee **ii**

Abstract **iii**

Table of Contents **v**

List of Figures **viii**

Acknowledgements **xii**

1 Introduction **1**

1.1 Background and Motivation 1

1.2 Temporal Characterization of Data Transmission 2

1.3 Thesis Outline 4

2 Transmission Time and Energy Consumption Evaluation for Adaptive Transmission Systems **5**

2.1 Introduction 5

2.2 System Model 7

2.3 Transmission Time Analysis for Block Fading Channels 9

2.3.1 Exact Expression 10

2.3.2 Approximate Distribution 12

2.4 Transmission Time Analysis for Markov Channel 13

2.4.1 Small L 15

2.4.2 Large L 20

2.4.3 What if data transmission experiences medium level fading? . 24

2.5 Energy Consumption Analysis 24

2.6 Numerical Example 26

2.7 Concluding Remarks 36
Appendix: Derivation of Conditional CDF in $F^M_{\mathrm{tr},L}(t)$ 36

3 Extended Delivery Time Analysis for Secondary Transmission with Rate Adaptation 38
3.1 Introduction 38
3.2 System Model 40
3.3 Extended Delivery Time Analysis 42
3.3.1 Continuous Spectrum Sensing 42
3.3.2 Semi-periodic Spectrum Sensing 50
3.3.3 One-shot Transmission 55
3.4 Concluding Remarks 58
Appendix: Derivation of Correlate Coefficient Defined in Eq. (3.12) 60

4 Slotted Secondary Transmission with Rate Adaptation under Interweave Cognitive Implementation 62
4.1 Introduction 62
4.2 System Model 65
4.3 Perfect Sensing Result 66
4.3.1 Markov Model for Secondary Transmission 67
4.3.2 Queuing Analysis of Secondary Packet Transmission 70
4.3.3 EDT analysis for slotted secondary transmission 77
4.4 Imperfect Spectrum Sensing 84
4.4.1 Markov Model of Secondary Transmission with False Alam . . 85
4.4.2 Energy Efficiency of Slotted Secondary Transmission 90
4.4.3 Effect of False Alarm on Queuing Performance 93
4.4.4 Effect of Miss Detection 99
4.5 Concluding Remarks 104
Appendix: Derivation of transition probability for two-dimensional Markov chain 104

5 Conclusions 107

6 Future Work 108
6.1 Secondary Sensor Transmission with RF Energy Harvesting 108

6.2 Performance Evaluation for Multiple PU Multiple SU Cognitive Radio Network 110

List of Publication **112**

Bibliography **114**

List of Figures

Figure 2.1 Adaptive modulation and coding systems over fading channels. 8
Figure 2.2 Transmission time with four-state AMC implementation over block fading channels 9
Figure 2.3 Illustration of continuous-time Markov channels with rate adaptation and corresponding Markov chain model. 14
Figure 2.4 Integral regions when $\frac{1}{R_k} > \frac{1}{R_j} > \frac{1}{R_i}$. 19
Figure 2.5 Illustration of components along the RF chain for adaptive transmission system over fading wireless channels. 25
Figure 2.6 Exact PMF (2.8) of transmission time over block fading channels, where $f_D = 50$ Hz and $\bar{\gamma} = 15$ dB. 27
Figure 2.7 Exact CDF of transmission time over block fading channel versus various Doppler shift, where the channel coherence time is estimated by $T_c = 0.2$ ms, $\bar{\gamma} = 15$ dB, and $H_t = 3.25$ Mb. 28
Figure 2.8 Exact and approximate solution of CDF of T_{tr}^B with different data amount H_t, where $\bar{\gamma} = 15$ dB and $f_D = 20$ Hz. 29
Figure 2.9 Approximate distribution of T_{tr}^B with various channel average value, Doppler shift, and data amount. 31
Figure 2.10 Monte Carlo simulation verification of analytical expression of PDF for T_{tr}^M with adaptive modulation over slow fading (e.g. $f_{\text{tr}}^M(t) \approx f_{\text{tr},1}^M(t) + f_{\text{tr},2}^M(t)$), where $H_t = 0.1$ Mb and $f_D = 50$ Hz. 33
Figure 2.11 Monte Carlo simulation and analytical result in evaluating T_{tr}, where $H_t = 5$ Mb, $f_D = 50$ Hz, and $\bar{\gamma} = 15$ dB. 34
Figure 2.12 PDF of T_{tr} versus different data amount H_t and Doppler shift f_D. 35

Figure 3.1 Secondary transmission with continuous spectrum sensing strategy and semi-periodic spectrum sensing strategy, respectively. . 42

Figure 3.2 Secondary transmission when PU is off and on at the start of secondary transmission with continuous sensing. 43
Figure 3.3 SU transmission with four-state AMC under continuous sensing strategy. 46
Figure 3.4 Monte Carlo simulation verification for the analytical PDF of EDT with continuous sensing ($H_t = 30$ kb, $\bar{\gamma} = 15$ dB, $\mu = 1$ ms, $\lambda = 3$ ms). 49
Figure 3.5 Distribution of EDT for secondary transmission under continuous sensing with various secondary data amount, secondary link quality and PU parameters. 51
Figure 3.6 Monte Carlo simulation verification for the analytical PDF of EDT with periodic sensing,given by Eq. (3.22), where $\lambda = 3$ ms, $\mu = 1$ ms, $\bar{\gamma} = 15$ dB, $T_s = 0.1$ ms, $H_t = 60$ kb in (a) and $H_t = 30$ kb in (b), respectively. 54
Figure 3.7 PDF of EDT for secondary transmission with semi-periodic sensing for various PU parameters, data amount, secondary link quality and the length of sensing period. 57
Figure 3.8 PDF of one-shot transmission ($H_t = 1.2$ kb, $\bar{\gamma} = 15$ dB, $\lambda = 3$ ms, $\mu = 1$ ms). 59

Figure 4.1 Slotted secondary transmission with periodic spectrum sensing strategy and the structure of SU period. 66
Figure 4.2 Markov modeling of secondary slotted transmission and state transition based on PU activity. 67
Figure 4.3 Correspondence of collision probability and sensing period for various PU activities. 69
Figure 4.4 Secondary transmission with AMC for small-size packet. 70
Figure 4.5 Two-dimensional discrete-time finite state Markov chain model for secondary transmission with AMC. 71
Figure 4.6 Queue recursion of secondary transmission. 72
Figure 4.7 Analytical and simulation results on the stationary distribution of queue length with different sensing periods, primary user parameters and secondary channel condition, where $K = 30$ and $p_a = 0.16$. 74

Figure 4.8 Average queuing delay, average throughput and packet drop probability versus various secondary channel quality and primary user parameters. 77
Figure 4.9 EDT sequence conditioning on the first slot is in state W, C and S, respectively. 78
Figure 4.10Monte Carlo verification of T_{ED} analysis ($H_t = 8$ kb, $\lambda = 30$ ms, $\mu = 10$ ms, $\bar{\gamma} = 20$ dB). 81
Figure 4.11PMF of EDT with fixed-rate transmission for various PU activities and secondary packet size. 82
Figure 4.12PMF of EDT for secondary transmission with four-state AMC. 84
Figure 4.13Slotted secondary transmission under false alarm. 85
Figure 4.14Markov model and state transitions of slotted secondary transmission with false alarm. 86
Figure 4.15State transition illustration. 87
Figure 4.16Collision probability/successful transmission probability versus SU period for various false alarm probabilities and PU parameters. 89
Figure 4.17Energy ratio of energy consumed in successful transmission over the total energy consumption, where $p_f = 0.1$, $\lambda = 50$ ms and $\mu = 10$ ms. 91
Figure 4.18Energy ratio versus transmission phase for various false alarm probabilities and PU parameter pairs. 92
Figure 4.19Analytical and simulation results on the stationary distribution of queue length with different PU parameters, where $K = 30$ and $\bar{\gamma} = 20$ dB. 96
Figure 4.20The effect of sensing error on average queuing delay, average throughput and packet drop probability versus various secondary channel quality. 99
Figure 4.21Seven-state Markov model of slotted secondary transmission under spectrum sensing imperfection. 100
Figure 4.22Effect of sensing imperfection on total collision probability, where $\lambda = 50$ ms and $\mu = 30$ ms. 102
Figure 4.23Effect of sensing imperfection on secondary throughput, where $T_{\mathrm{S}} = 2$ ms, $\lambda = 50$ ms and $\mu = 30$ ms. 103

Figure 6.1 Unconstrained/interference constrained secondary sensor transmission with RF harvested energy. 109

ACKNOWLEDGEMENTS

I would like to thank:

My dearest parents for helping me throughout my life and always standing behind me.

Prof. Hong-Chuan Yang, for instruction and support.

Prof. Thomas Aaron Gulliver, for serving as the department member in my thesis supervisory committee.

Prof. Kui Wu, for serving as an outside member in my thesis supervisory committee

Mr. Hao Zhang and Mrs. Shu-Ling Wu for looking after me even my family so well.

Mr. Bai-Yi Li for company, support and thoughtfulness.

I had a mind blank while I started this acknowledge part. All of a sudden, so many names pumped out. Someone said that as a Ph.D student, you must be smart. Others said, you have to be brave. The truth is, you need beloved people showing their support.

Wen-Jing Wang

Chapter 1

Introduction

1.1 Background and Motivation

We are in an era of big data. Data are generated and collected at an accelerating rate. The timely processing, delivery, and analysis of these data will bring huge social and economic benefit. With the intensive ongoing deployment of wireless communication systems, most big data will be transmitted over the air. In fact, smart mobile devices contribute significantly to the generation of big data. The ever-growing Internet of Things (IoT) devices serve as another source of big data for wireless transmission. The supporting of big data transmission presents several technical challenges to wireless system design, including spectrum efficiency enhancement of radio access network (RAN), capacity provision of fronthaul/backhaul links, and network architecture improvement for traffic scalability. To effectively support various big data and IoT applications, future wireless systems need to optimize their transmission strategies for a large amount of data from diverse sources.

Current wireless systems typically apply the same transmission strategy to all transmission sessions over the wireless channel channel. With the application of advanced transmission technologies, the properties of the channel, e.g. average data rate and average error rate, will be improved, which usually translates to better average quality of service experienced by individual sessions. Conventional transmission design ignores the specifics of individual transmission sessions, such as the traffic characteristics and the prevailing network/channel condition. When the transmission sessions are short, the quality of service experienced by individual sessions vary dramatically around the average. With the growing popularity of IoT devices and big

data applications, future wireless systems need to support increasing number of short transmission sessions, initiated for example by sensor nodes.

1.2 Temporal Characterization of Data Transmission

Transmission time refers to the time duration required to transmit a certain amount of data from source to destination. Generally, transmission time over a point-to-point link can be calculated as the ratio of data amount over transmission data rate for constant-rate transmission systems. As a characterization of channel occupancy, transmission time has many applications in wireless communication system analysis and design.

Specifically, the analytical results on transmission time can help investigate the delay performance of various transmission strategies over wireless channels [1]. [2] analyzes transmission time for cognitive radio network with the consideration of primary interference. Transmission time was applied to investigate the extended delivery time of secondary packet transmission with interweave cognitive radio implementation [3]. [4] evaluates the collision probability of communication networks employing random access protocols with the analytical results of transmission time. [5] develops a new scheduling scheme by taking transmission time into account, which results in smaller waiting time. [6] proposes an embedded Markov chain to evaluate the queuing performance of underlay cognitive radio communication assuming that packet is being dropped when transmission time is greater than a pre-determined time-out threshold. Furthermore, as the energy consumption of transmitter can be calculated as the product of transmission time and transmit power, transmission time analysis is instructive in designing energy-efficient wireless communication system. The optimal adaptive modulation strategy to minimize total energy consumption is analyzed for fixed-size packet transmission in [7] and [8]. [9] investigates an on-line algorithms to minimize transmission time for energy harvesting systems.

Previous works typically assume constant transmission time for a fixed amount of data [2–5], which is particularly applicable to constant-rate transmission systems. Specifically, the minimum transmission time for static channel is regarded as a con-

stant and can be estimated as

$$T_{\text{tr min}} = \frac{H_t}{B \log_2(1+\gamma)}, \tag{1.1}$$

where H_t is the data amount, B is the channel bandwidth and γ is the received signal to noise ratio (SNR). However, constant-rate transmission becomes inefficient and unreliable when operating over time varying channels. Assuming slow fading environment, where the data transmission completes within one channel coherence time, the distribution function of transmission time is derived using random variable transformation [10]. For fast fading scenario, where the data transmission experiences many different channel realizations, ergodic channel capacity is used to estimate transmission time as

$$T_{\text{tr}} \approx \frac{H_t}{\bar{C}} = \frac{H_t}{B \int_0^\infty \log_2(1+\gamma) f_\gamma(\gamma) d\gamma}, \tag{1.2}$$

where $\bar{C}$ denotes the ergodic capacity with $f_\gamma(\cdot)$ the probability density function (PDF) of received SNR.

These characterizations of transmission time are insufficient for the following reasons. Firstly, these works use channel capacity in the analysis, which is as upper bound of supportable data rate for reliable communication. These results are, therefore, generally optimistic. Secondly, for large amount of data or a channel with larger Doppler shift, channel realization will vary during transmission. The assumption that channel realization remains constant during the transmission will be invalid. Finally, finite-amount data transmission may not experience all channel realizations resulting in inaccuracy in ergodic capacity based transmission time calculation.

Adaptive transmission is an attractive technology to improve the transmission efficiency with guaranteed reliability. With adaptive transmission, the transceiver can adjust its transmission scheme with the prevailing channel quality, while maintaining an acceptable bit error rate (BER) performance [11,12]. Typically, higher rate transmission schemes are used when the channel condition is favourable, while lower rate or no transmission applies when channel quality is poor. As a result, the transmission rate varies with the instantaneous realization of the received SNR. The optimal rate used and the associated thresholds that maximize the average spectral efficiency is discussed in [13]. In practice, AMC has been incorporated in several current and emerging wireless communication systems [14–17].

1.3 Thesis Outline

Chapter 2 investigates the statistics of transmission time with AMC over block fading channels, where the transmission slot is assumed to be fixed-length channel coherence time and Markov fading channels, where the transmission slot is exponential-length. For block fading channels, the exact and approximate CDF expressions are presented. For Markov channel, assuming data transmission completed within one or two slots, the exact PDF of transmission time is also obtained. If the data transmission experiences medium level fading, we apply the *mixture model* to estimate the PDF of transmission time. If channel introduces fast fading, or equivalently, the data amount is large, we propose an analytical framework to approximately evaluate the statistics of transmission time.

Chapter 3 derives the PDF of EDT of SU transmission with interweave cognitive radio implementation and AMC. The EDT consists of a interleaved sequence of random-length waiting slot and transmission slot. Two spectrum sensing strategies are considered, namely continuous sensing and semi-periodic sensing. For certain application, transmission is accomplished in one SU transmission period. The statistics of EDT for such application is also discussed.

Chapter 4 proposes a discrete-time Markov model to characterize slotted secondary transmission process. Closed-form solution of collision probability is obtained. Assuming SU transmission adopts AMC, we then carry out the queueing analysis based on a two-dimensional-finite-state Markov chain for small-size packet transmission. The optimal length of secondary slot is solved by maximizing energy efficiency subject to a collision probability constraint. For large-size packet transmission, the PMF of EDT for secondary packet transmission is also derived. The effect of sensing imperfection is also discussed.

Chapter 5 concludes the whole thesis

Chapter 2

Transmission Time and Energy Consumption Evaluation for Adaptive Transmission Systems

2.1 Introduction

Data are generated and collected at an accelerating rate. Over the past decade, mobile data traffic has been experiencing a compound annual growth rate of over 40%. This growth rate is expected to accelerate in the coming years as the result of increasing popularity of mobile broadband applications, such as high-resolution video streaming, remote monitoring, real-time control, and broadband downloading [18]. The timely processing, delivery, and analysis of these data can bring huge social and economical benefit [19–21]. With the intensity of ongoing deployment of wireless systems, much of the big data will be transmitted wirelessly. These big data applications bring new challenges to the wireless communication system design [22]. To more effectively support the wireless transmission of big data, a novel data-oriented approach to design and optimize wireless transmission strategies is introduced in [23]. Taking the video traffic as a study case, reference [24] proposes a novel scheduling policy to assist real-time big data delivery in wireless networks.

The fast growing wireless traffics quickly drive up the energy usage of wireless systems. Modern communication systems consume 4.7% global electricity production and it is predicted that 4.4 terawatt-hours energy will be consumed by about

100 million small cells deployed by 2020 [25]. 5G system is expected to achieve up to 90% of energy reduction [26]. While energy consumption has always been a serious concern for wireless transmission, future wireless systems need to achieve even higher energy efficiency. An accurate energy consumption analysis is essential to develop energy-efficient solutions for next generation wireless communication systems [27]. In traditional wireless systems, where the communication distance is usually large ($\geq$ 100 m), circuit power consumption is negligible. However, with the intense ongoing deployment of small cells, WiFi networks, and Wireless Body Area Networks (WBANs), the wireless nodes are densely distributed, resulting in a smaller communication distance ($\leq$ 10 m). In such scenario, the circuit power becomes comparable to the transmit power, or even dominates in the total power consumption. Taking circuit power into account, several work has analyzed the energy consumption of wireless transmission systems. [28] presents a system-level energy model including all the radio frequency (RF) and analog front-end components and shows that, given the quality requirement, the energy consumption of wireless system can be reduced by properly adjusting transmission parameters (e.g. roll-off factor, symbol rate, or signal center frequency). Under a WBANs scenario, [29] proposes an energy consumption model and analyzes the trade-off between circuit power and transmit power with a threshold distance. [30] proposes a novel performance metric in term of the energy consumption per unit distance, which is optimized to achieve energy-efficient cooperative transmission. In [31], an energy-efficient transmission scheduling scheme is developed for delay-limited bursty data under the assumption that the circuit power consumption is non-ideal. [32] presents energy consumption models to characterize Wi-Fi data transmission. The transmission of big data will usually involve multiple channel coherence time, even for slow fading environment.

With AMC, the modulation/coding scheme is adjusted with instantaneous channel condition, while maintaining an acceptable bit error rate (BER) performance. As such, AMC is a suitable candidate for the efficient and reliable transmission of big data over fading wireless channels. Meanwhile, the transmission time/energy consumption of AMC systems is no longer a constant but a random variable depending on channel realization. In this chapter, we propose an analytical framework to investigate the transmission time/energy consumption of wireless big data transmission over fading channels with AMC. We first consider block fading, where transmission rate is adjusted with channel quality every channel coherence time. We derive the exact

distribution function of transmission time for both slow and fast fading scenarios. To reduce the computation complexity, we also obtain an approximate probability mass function (PMF) of the transmission time in fast fading scenario. Then, we generalize the analysis to Markov channel case. The exact PDF is derived for slow fading. For fast fading scenario, the approximate PDF of transmission time is derived. Selected numerical examples are presented and discussed to illustrate the mathematical formulations. We show that the transmission time with adaptive transmission may vary dramatically with the prevailing fading channel condition (i.e. Doppler shift or the average of received SNR).

The statistics of energy consumption for wireless transmission of big data with AMC under slow/fast fading scenario can be similar obtained. If data transmission experiences medium level fading, we apply the mixture model to estimate the PDF of energy consumption. The analytical results will greatly facilitate further analysis of wireless communication systems in terms of delay performance and energy efficiency.

2.2 System Model

We consider a digital transmission system operating over flat fading wireless channel, as shown in Fig. 2.1. Specifically, the information bits s_i are modulated to generate the transmitted signal $x(t)$. The wireless channel introduces flat fading channel gain g and additive white Gaussian noise (AWGN) $n(t)$, which leads to the received signal $y(t) = gx(t) + n(t)$. We assume that the receiver performs coherent detection on the received signal with perfect channel phase estimation. As such, the instantaneous channel quality is characterized by the instantaneous received SNR defined as $\gamma = \frac{|g|^2 E_s}{N_0}$, where E_s denotes the symbol energy and N_0 is the power spectral density of additive noise.

The transmission system adopts constant-power, variable-rate adaptive transmission. In particular, the transmission rate is adaptively adjusted based on the fading channel quality by using different modulation and coding schemes, while the transmission power remains constant. More specifically, the value range of received SNR is divided into N regions, $A_i = [\gamma_{i-1}, \gamma_i),\ i = 1, ..., N$, with $\gamma_0 = 0$ and $\gamma_N = \infty$. When the received SNR γ falls in region A_i, the system will use a modulation and coding scheme with transmission rate R_i bits/symbol, $i = 1, 2, \cdots N$. R_i can be calculated as $R_i = \log_2(M_i)R_{C_i}$, where M_i and R_{C_i} are the constellation size and

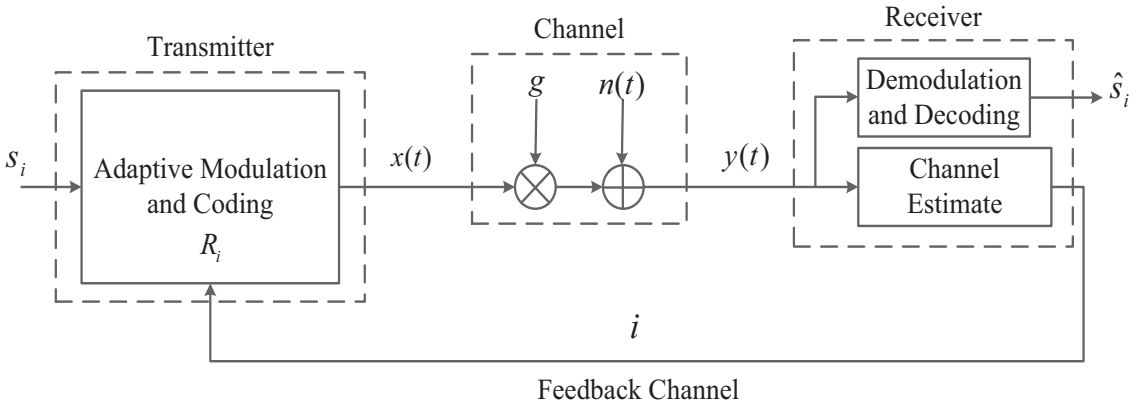

Figure 2.1: Adaptive modulation and coding systems over fading channels.

coding rate of the ith modulation and coding pair, respectively. The boundary SNRs γ_i, $i = 1, 2, \cdots, N-1$, are typically determined such that the instantaneous BER for selected modulation and coding pair is below a target BER value, denoted by BER_{tar} [33][1].

To implement AMC, the receiver needs to estimate the received SNR and determine which SNR region it falls into. The receiver then feeds back the index of the chosen modulation scheme to the transmitter via an error-free feedback channel. After that, the transmitter and the receiver communicate using the chosen modulation scheme. The probability of using transmission rate R_i, denoted by π_i, can then be calculated as the probability that γ falls into region A_i, i.e.

$$\pi_i = \int_{\gamma_{i-1}}^{\gamma_i} f_\gamma(\gamma) d\gamma. \tag{2.1}$$

where $f_\gamma(\cdot)$ represents the PDF of received SNR. The modulation-coding scheme selection should be periodically updated according to the prevailing channel quality, usually once every channel coherence time T_c. As such, when big data is transmitted with AMC, the transmission rate may vary during the transmission. The total transmission time will involve multiple channel coherence time. In the following sec-

[1] As an example, for a general class of uncoded square 2^n-QAM modulation scheme. It has been shown that the instantaneous BER of square 2^n-QAM over an AWGN channel with SNR γ can be approximated by $\text{BER}_n(\gamma) = \frac{1}{5}\exp\left[-\frac{3\gamma}{2(2^n-1)}\right]$, $n = 1, 2, \cdots, N$ [34]. Therefore, the boundary SNR to satisfy a target BER value of BER_{tar} can be determined as $\gamma_i = -\frac{2}{3}\ln(5\text{BER}_{\text{tar}})(2^{i+1}-1)$, $i = 1, 2, \cdots, N-1$.

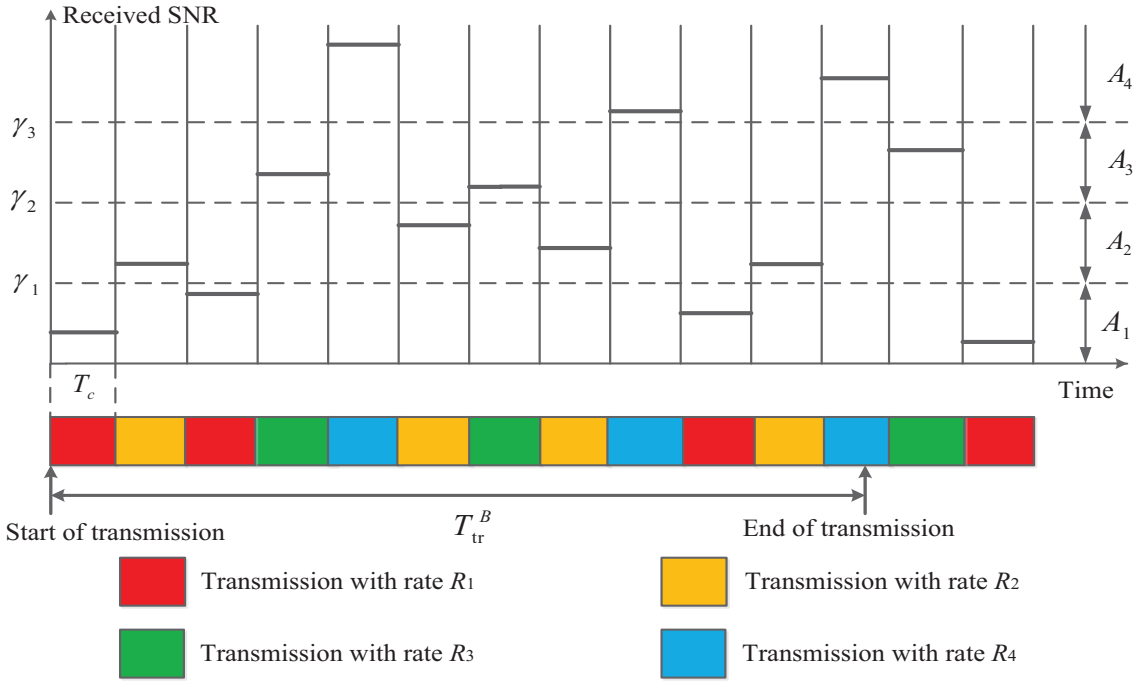

Figure 2.2: Transmission time with four-state AMC implementation over block fading channels

tions, we derive the distribution function of the transmission time for block fading and Markov fading channels.

2.3 Transmission Time Analysis for Block Fading Channels

In this section, we derive the exact and approximate PMF and CDF of transmission time for block fading channels. The channel gain of block fading channels remains constant within a fixed-length time interval in the order of the channel coherence time T_c, which is a measure of the minimum time required for the magnitude change or phase change of the channel to become uncorrelated from its previous value. T_c can be estimated using the maximum Doppler shift, denoted by f_D, as $0.2/f_D$ second to $0.4/f_D$ second empirically. We assume that the transmission rate used in each channel coherence time varies independently from one to another. As such, transmission time for block fading, denoted by T_{tr}^B, is a discrete random variable consisting of random

number of T_cs, as illustrated in Fig. 2.2. Here, we assume that the transmission starts at the beginning of a channel coherence time without loss of generality.

2.3.1 Exact Expression

Specifically, T_{tr}^B is the sum of random number of intact T_cs and one partial T_c. the length of T_{tr}^B depends on the total amount of data H_t and those transmitted over each coherence time. Mathematically, the transmission time can be formulated as

$$T_{\text{tr}}^B = (L-1)T_c + \frac{H_t - \mathbb{H}_{L-1}^B}{R^{(L)}}, \quad L = 1, 2, \cdots, \tag{2.2}$$

where $R^{(L)}$ denotes the transmission rate used in the Lth T_c and $\mathbb{H}_{L-1}^B$ is the amount of data transmitted over the previous $L-1$ T_cs. Note that transmission rate over each T_c is determined by the corresponding channel realization. Let us assume that, during the first $L-1$ channel coherence times, the received SNR falls into region A_i n_i times, $i = 1, 2, \cdots, N$, and as such, transmission rate R_i is used n_i times, where $\sum_{i=1}^N n_i = L-1$. Accordingly, $\mathbb{H}_{L-1}^B$ is given by

$$\mathbb{H}_{L-1}^B = \sum_{i=1}^{N} n_i R_i T_c. \tag{2.3}$$

Let vector $\overrightarrow{\mathbf{n}} = [n_1, n_2, \cdots, n_N]$ represent such channel realization. Applying the block fading assumption, the probability that such channel realization occurs can be calculated as

$$\Pr[\overrightarrow{\mathbf{n}}] = \binom{L-1}{n_1, n_2, \cdots, n_N} \prod_{i=1}^{N} \pi_i^{n_i}, \tag{2.4}$$

where $\binom{L-1}{n_1, n_2, \cdots, n_N} = \frac{(L-1)!}{n_1! n_2! \cdots n_N!}$ denotes the multinomial coefficient. Eq. (2.4) helps us arrive at the following PMF of the amount of data transmitted over the first $L-1$ channel coherence times as

$$\Pr\left[\mathbb{H}_{L-1}^B = T_c \sum_{i=1}^{N} n_i R_i\right] = \binom{L-1}{n_1, n_2, \cdots, n_N} \prod_{i=1}^{N} \pi_i^{n_i}. \tag{2.5}$$

It is important to note that data transmission completes in exact L channel coherence time if and only if the data transmitted over the first $L-1$ coherence time

Algorithm 1 Calculate $F^B_{T_{\rm tr}}(t) = \Pr[T^B_{\rm tr} < t]$

Input H_t, T_c, π_i's, R_i's
Start $cdfTtr = 0$
  for $L = 1 : \lfloor 3L^B_{\rm ave} \rfloor$ **do**
    for $\sum_{i=1}^N n_i = L-1$ **do**
      for $k = 1 : N$ **do**
        $HLn = T_c \sum_{i=1}^N n_i R_i$
        if $H_t - HLn \in (0, R_k T_c]$ **then**
          $\Pr_{\rm temp} = \pi_k \left[\binom{L-1}{n_1, n_2, \cdots, n_N} \prod_{i=1}^N \pi_i^{n_i} \right]$
        else
          $\Pr_{\rm temp} = 0$
        end if
        if $(L-1)T_c + \frac{H_t - HLn}{R_k} < t$ **then**
          $cdfTtr = cdfTtr + \Pr_{\rm temp}$
        end if
      end for
    end for
  end for
Output $cdfTtr$

$\mathbb{H}^B_{L-1}$ falls into the region $(H_t - R_k T_c,\ H_t]$, while rate R_k is used in the Lth T_c. Noting that rate R_k is used in the Lth channel coherence time with probability π_k, we can determine the PMF of $T^B_{\rm tr}$, by considering all L values, as

$$\Pr\left[T^B_{\rm tr} = (L-1)T_c + \frac{H_t - T_c \sum_{i=1}^N n_i R_i}{R_k}\right] = \begin{cases} \pi_k \binom{L-1}{n_1, n_2, ..., n_N} \prod_{i=1}^N \pi_i^{n_i}, \\ \qquad 0 < H_t - T_c \sum_{i=1}^N n_i R_i \le R_k T_c; \\ 0, \qquad\qquad \text{otherwise;} \end{cases} \tag{2.6}$$

For the special case of $L = 1$, we have $\mathbb{H}^B_{L-1} = 0$, which leads to

$$\Pr\left[T^B_{\rm tr} = \frac{H_t}{R_k}\right] = \begin{cases} \pi_k, & 0 < H_t \le R_k T_c; \\ 0, & \text{otherwise.} \end{cases} \tag{2.7}$$

For $L = 2$, we have $\mathbb{H}^B_{L-1} = R^{(1)} T_c$, where $R^{(1)}$ is the rate used in the first T_c and

equal to R_i with probability π_i. The corresponding PMF terms for $L = 2$ are given by

$$\Pr\left[T_{\text{tr}}^{B} = T_c + \frac{H_t - R_i T_c}{R_k}\right] = \begin{cases} \pi_i \pi_k, & 0 < H_t - R_i T_c \leq R_k T_c; \\ 0, & \text{otherwise.} \end{cases} \tag{2.8}$$

Accordingly, the exact CDF of T_{tr}^{B} over block fading channel model, denoted by $F_{\text{tr}}^{B}(t)$, can be calculated as

$$\begin{aligned} F_{\text{tr}}^{B}(t) &= \Pr\left[T_{\text{tr}}^{B} \leq t\right] \\ &= \sum_{L} \sum_{\vec{\mathbf{n}}} \sum_{k=1}^{N} \pi_k \binom{L-1}{n_1, n_2, ..., n_N} \prod_{i=1}^{N} \pi_i^{n_i} \times \mathcal{I}_{(0, R_k T_c]} \left(H_t - T_c \sum_{i=1}^{N} n_i R_i\right) \\ &\quad \times \mathcal{U}\left(t - (L-1)T_c + \frac{H_t - T_c \sum_{i=1}^{N} n_i R_i}{R_k}\right), \end{aligned} \tag{2.9}$$

where $\mathcal{U}[\cdot]$ denotes unit step function, $\mathcal{I}_A(x)$ is an indicator function, equal to 1 if $x \in A$ and zero otherwise, and $\sum_{\vec{\mathbf{n}}}$ is carried over all $n_i \geq 0,\ i = 1, 2, \cdots, N$, subject to $\sum_{i=1}^{N} n_i = L - 1$. In practice, L can not be very large given the increasingly high transmission rate and finite amount of data. As shown in numerical results, taking summation over $L \in [1, \lfloor 3L_{\text{ave}}^{B} \rfloor]$ can achieve sufficient accuracy, where $L_{\text{ave}}^{B} = \frac{H_t}{T_c \sum_{i=1}^{N} R_i \pi_i}$ is the average number of channel coherence time required. Algorithm 1 illustrates the procedure of calculating the exact CDF of T_{tr}^{B}.

2.3.2 Approximate Distribution

When the channel introduces fast fading and T_c is very short compared to total transmission time, we can arrive at more convenient expression for PMF of T_{tr}^{B}, by assuming that data transmission always completes in integer number of channel coherence time, (i.e. $T_{\text{tr}}^{B} = LT_c$,). The probability that transmission completes over L T_c's equals to the joint probability that data transmitted in previous $L-1$ T_c's is less than H_t, and data transmitted in L T_c's is greater than H_t, i.e.

$$\Pr\left[T_{\text{tr}}^{B} = LT_c\right] = \Pr\left[\mathbb{H}_{L-1}^{B} < H_t,\ \mathbb{H}_{L-1}^{B} + R^{(L)} T_c \geq H_t\right]. \tag{2.10}$$

Conditioning on channel realization over L channel coherence time and applying the result in Eq. (2.5), we obtain the approximate PMF of T_{tr}^B as

$$\begin{aligned}\Pr\left[T_{\text{tr}}^B = LT_c\right] &= \sum_{k=1}^{N} \Pr[H_t - R_k T_c \leq \mathbb{H}_{L-1}^B < H_t]\pi_k \\ &= \sum_{k=1}^{N} \left(\sum_{\substack{\overrightarrow{\mathbf{n}} \text{ s.t.} \\ \mathbb{H}_{L-1}^B \in [H_t - R_k T_c, H_t)}} \binom{L-1}{n_1, n_2, ..., n_N} \prod_{i=1}^{N} \pi_i^{n_i} \right) \pi_k. \end{aligned} \tag{2.11}$$

The inner sum in Eq. (2.11) is carried out over all possible $\overrightarrow{\mathbf{n}}$s satisfying that $\mathbb{H}_{L-1}^B$ falls into region $(H_t - R_k T_c,\ H_t]$.

2.4 Transmission Time Analysis for Markov Channel

Inthis section, we derive the PDF of transmission time for Markov channel. We assume that the wireless channel can be modeled as a homogeneous continuous-time finite-state Markov chain. We adopt an N-state Markov chain with the ith state corresponding to the event that the received SNR falls in $A_i,\ i = 1, 2, \cdots, N$, as illustrated in Fig. 2.3. The sojourn time of the Markov chain in state i is an exponential random variable with average λ_i calculated as

$$\lambda_i = \frac{\pi_i}{\text{lcr}_i + \text{lcr}_{i-1}} \quad i = 1, 2, \cdots, N. \tag{2.12}$$

where lcr_i denotes the average level crossing rate with respect to boundary threshold γ_i. For Rayleigh fading, we have

$$\text{lcr}_i = \sqrt{\frac{2\pi\gamma_i}{\bar{\gamma}}} f_D \exp\left(-\frac{\gamma_i}{\bar{\gamma}}\right). \tag{2.13}$$

where $\bar{\gamma}$ is the average received SNR. The PDF of the sojourn time in state i is given by

$$f_{T_i}(t) = \frac{1}{\lambda_i} \exp\left(-\frac{t}{\lambda_i}\right). \tag{2.14}$$

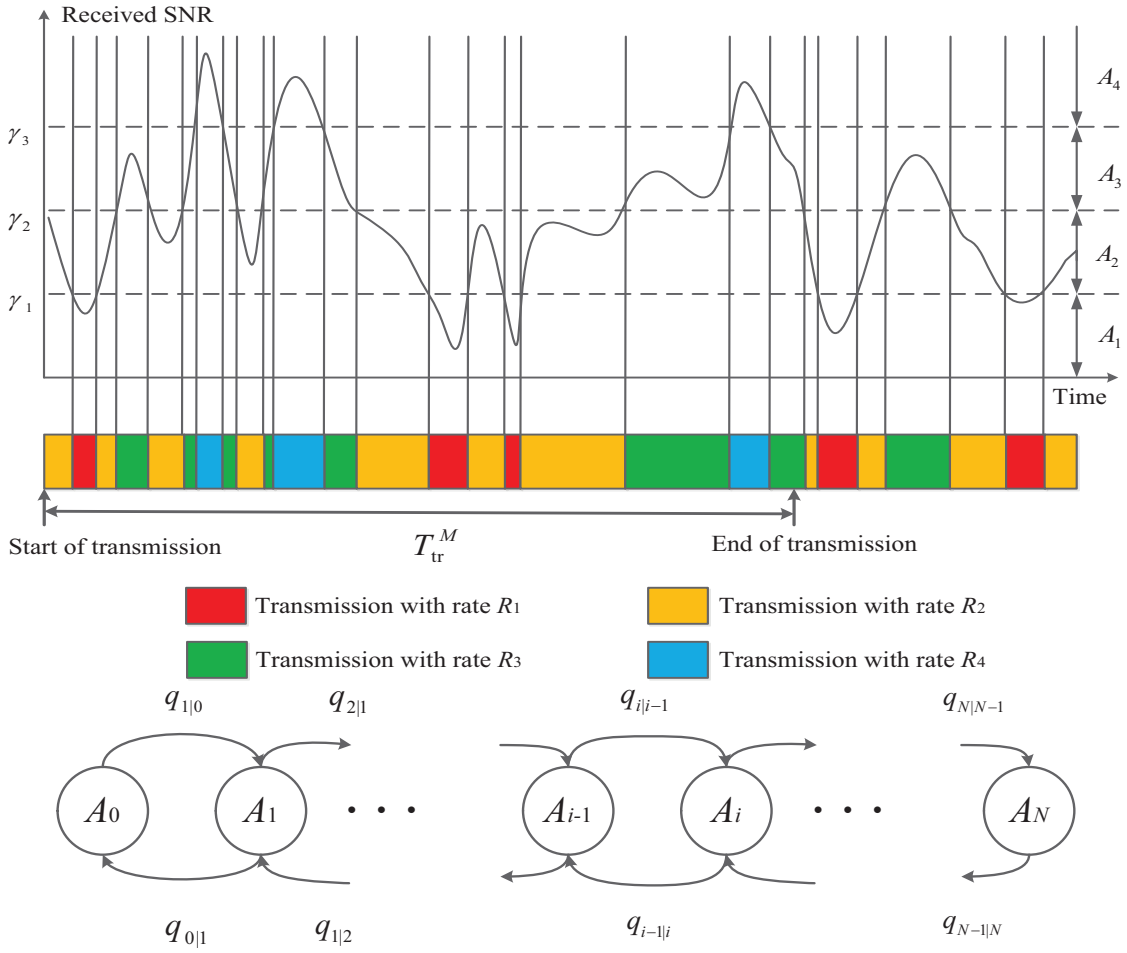

Figure 2.3: Illustration of continuous-time Markov channels with rate adaptation and corresponding Markov chain model.

The transition rate from state i to its neighbouring states, denoted by $q_{i-1|i}$ and $q_{i+1|i}$, can be respectively calculated as

$$q_{i-1|i} = \frac{\text{lcr}_{i-1}}{\pi_i}, \quad q_{i+1|i} = \frac{\text{lcr}_i}{\pi_i}. \tag{2.15}$$

It follows that the transition probability from state i to state $i-1$ and $i+1$ are calculated as

$$\begin{aligned} p_{i-1|i} &= \frac{q_{i-1|i}}{q_{i-1|i} + q_{i+1|i}} = \frac{\text{lcr}_{i-1}}{\text{lcr}_{i-1} + \text{lcr}_i}, \\ p_{i+1|i} &= \frac{q_{i+1|i}}{q_{i-1|i} + q_{i+1|i}} = \frac{\text{lcr}_i}{\text{lcr}_{i-1} + \text{lcr}_i}, \end{aligned} \tag{2.16}$$

respectively.

Transmission time over such Markov channel, denoted by T_{tr}^M, is a sequence of random-length slots, each of which is represented by exponential random variable (See Fig. 2.3). The CDF of T_{tr}^M for a given amount of data H_t is formulated, with the application of total probability theorem, as

$$F_{\text{tr}}^M(t) = \Pr\left[T_{\text{tr}}^M \leq t\right] = \sum_L \Pr\left[T_{\text{tr},L}^M < t,\ L \text{ slots used}\right] \tag{2.17}$$

where $T_{\text{tr},L}^M$ can be in general calculated as

$$T_{\text{tr},L}^M = \sum_{i=1}^{L-1} T^{(i)} + \frac{H_t - \sum_{i=1}^{L-1} R^{(i)} T^{(i)}}{R^{(L)}}. \tag{2.18}$$

Here $R^{(i)}$ denotes the transmission rate over the ith transmission slot and $T^{(i)}$ the duration of the ith slot, which is modeled as exponential random variables for Markov channels. Note that L transmission slots are required to finish transmission if and only if the data transmitted over first $L-1$ transmission slots is less than H_t and that transmitted over L slots is larger than H_t. Therefore, the joint probability $\Pr\left[T_{\text{tr},L}^M < t;\ L \text{ slots used}\right]$, denoted by $F_{\text{tr},L}^M(t)$, can be in general rewritten as

$$F_{\text{tr},L}^M(t) = \Pr\left[\sum_{i=1}^{L-1} T^{(i)} + \frac{H_t - \sum_{i=1}^{L-1} R^{(i)} T^{(i)}}{R^{(L)}} \leq t, \right. \\ \left. \sum_{i=1}^{L-1} R^{(i)} T^{(i)} < H_t,\ \sum_{i=1}^{L-1} R^{(i)} T^{(i)} + R^{(L)} T^{(L)} \geq H_t\right]. \tag{2.19}$$

The corresponding PDF of T_{tr}^M is given by

$$f_{\text{tr}}^M(t) = \sum_L \frac{d}{dt} F_{\text{tr},L}^M(t) = \sum_L f_{\text{tr},L}^M(t). \tag{2.20}$$

We now derive the $F_{\text{tr},L}^M(t)/f_{\text{tr},L}^M(t)$ for small L and general L separately.

2.4.1 Small L

$L = 1$ is a special case. For $L = 1$, the transmission time is equal to $\frac{H_t}{R^{(1)}}$ with probability that data transmitted over the first period is greater than H_t (i.e.

$R^{(1)}T^{(1)} > H_t$). Conditioning on received SNR falls into A_i, $R^{(1)} = R_i$ and $T^{(1)}$ is now an exponential random variable with average λ_i, we have $\Pr\left[T^M_{\text{tr},1} = \frac{H_t}{R_i}\right] = \pi_i e^{-\frac{H_t}{R_i\lambda_i}}$. We can show that

$$F^M_{\text{tr},1}(t) = \sum_{i=1}^{N} \mathcal{U}\left(t - \frac{H_t}{R_i}\right) \pi_i e^{-\frac{H_t}{R_i\lambda_i}}. \tag{2.21}$$

Accordingly, $f^M_{\text{tr},1}(t)$ can be obtained as

$$f^M_{\text{tr},1}(t) = \sum_{i=1}^{N} \delta\left(t - \frac{H_t}{R_i}\right) \pi_i e^{-\frac{H_t}{R_i\lambda_i}}, \tag{2.22}$$

where $\delta(\cdot)$ is the unit impulse function.

For $L = 2$, $F^M_{\text{tr},2}(t)$ is formulated as the joint probability of three events as

$$F^M_{\text{tr},2}(t) = \Pr\Bigg[\left(1 - \frac{R^{(1)}}{R^{(2)}}\right) T^{(1)} + \frac{H_t}{R^{(2)}} \le t, \\ R^{(1)}T^{(1)} < H_t, \quad R^{(1)}T^{(1)} + R^{(2)}T^{(2)} \ge H_t\Bigg]. \tag{2.23}$$

We proceed by conditioning on the channel realization and rewrite $T^M_{\text{tr},2}$ as

$$F^M_{\text{tr},2}(t) = \\ \sum_{i=1}^{N} \Bigg\{ \Pr\left[(R_{i+1} - R_i)T^{(1)} \le tR_{i+1} - H_t,\ R_iT^{(1)} < H_t,\ R_iT^{(1)} + R_{i+1}T^{(2)} \ge H_t\right] p_{i+1|i} \\ + \Pr\left[(R_{i-1} - R_i)T^{(1)} \le tR_{i-1} - H_t,\ R_iT^{(1)} < H_t, \quad R_iT^{(1)} + R_{i-1}T^{(2)} \ge H_t\right] p_{i-1|i} \Bigg\} \pi_i. \tag{2.24}$$

Let $F^+_i(t) = \Pr\left[(R_{i+1} - R_i)T^{(1)} \le tR_{i+1} - H_t,\ R_iT^{(1)} < H_t,\ R_iT^{(1)} + R_{i+1}T^{(2)} \ge H_t\right]$ and $F^-_i(t) = \Pr\left[(R_{i-1} - R_i)T^{(1)} \le tR_{i-1} - H_t,\ R_iT^{(1)} < H_t,\ R_iT^{(1)} + R_{i-1}T^{(2)} \ge H_t\right]$. $F^+_i(t)$ can be further rewritten as

$$F^+_i(t) = \Pr\left[T^{(1)} \le \frac{tR_{i+1} - H_t}{R_{i+1} - R_i},\ T^{(1)} < \frac{H_t}{R_i},\ T^{(2)} \ge \frac{H_t - R_iT^{(1)}}{R_{i+1}}\right]. \tag{2.25}$$

Note that given the channel was in state i in the first transmission slot and then

transit to state $i+1$ in the second slot, the duration of the first slot $T^{(1)}$ will be an exponential random variable with average λ_i and that of the second slot $T^{(2)}$ will be another exponential random variable with average λ_{i+1}. Therefore, applying the PDFs of $T^{(1)}$ and $T^{(2)}$, $F_i^+(t)$ can be calculated as

$$F_i^+(t) = \begin{cases} 0, & t \le \dfrac{H_t}{R_{i+1}}; \\ \displaystyle\int_0^{\frac{tR_{i+1}-H_t}{R_{i+1}-R_i}} \int_{\frac{H_t-R_i x}{R_{i+1}}}^{\infty} f_{T_i}(x) f_{T_{i+1}}(y) dxdy, & \dfrac{H_t}{R_{i+1}} < t \le \dfrac{H_t}{R_i}; \\ \displaystyle\int_0^{\frac{H_t}{R_i}} \int_{\frac{H_t-R_i x}{R_{i+1}}}^{\infty} f_{T_i}(x) f_{T_{i+1}}(y) dxdy, & t > \dfrac{H_t}{R_i} \end{cases}$$

$$F_i^+(t) = \begin{cases} 0, & t \le \dfrac{H_t}{R_{i+1}}; \\ \dfrac{R_{i+1}\lambda_{i+1}}{R_i\lambda_i - R_{i+1}\lambda_{i+1}} e^{-\frac{H_t}{R_{i+1}\lambda_{i+1}}} \left[e^{\frac{(R_i\lambda_i - R_{i+1}\lambda_{i+1})(tR_{i+1}-H_t)}{R_{i+1}\lambda_{i+1}\lambda_i(R_{i+1}-R_i)}} - 1 \right], & \dfrac{H_t}{R_{i+1}} < t \le \dfrac{H_t}{R_i}; \\ \dfrac{R_{i+1}\lambda_{i+1}}{R_i\lambda_i - R_{i+1}\lambda_{i+1}} e^{-\frac{H_t}{R_{i+1}\lambda_{i+1}}} \left[e^{\frac{(R_i\lambda_i - R_{i+1}\lambda_{i+1})H_t}{R_{i+1}\lambda_{i+1}R_i\lambda_i}} - 1 \right], & t > \dfrac{H_t}{R_i}, \end{cases} \tag{2.26}$$

Similarly, $F_i^-(t)$ can be calculated, while noting that $T^{(2)}$ will be an exponential random variables with average λ_{i-1}, as

$$F_i^-(t) = \begin{cases} 0, & t \le \dfrac{H_t}{R_i}; \\ \dfrac{R_{i-1}\lambda_{i-1}}{R_i\lambda_i - R_{i-1}\lambda_{i-1}} e^{-\frac{H_t}{R_{i-1}\lambda_{i-1}}} \left[e^{\frac{(R_i\lambda_i - R_{i-1}\lambda_{i-1})H_t}{R_i\lambda_i R_{i-1}\lambda_{i-1}}} \right. & \\ \qquad \left. - e^{\frac{(R_i\lambda_i - R_{i-1}\lambda_{i-1})(tR_{i-1}-H_t)}{R_{i-1}\lambda_{i-1}\lambda_i(R_{i-1}-R_i)}} \right], & \dfrac{H_t}{R_i} < t \le \dfrac{H_t}{R_{i-1}}; \\ \dfrac{R_{i-1}\lambda_{i-1}}{R_i\lambda_i - R_{i-1}\lambda_{i-1}} e^{-\frac{H_t}{R_{i-1}\lambda_{i-1}}} \left[e^{\frac{(R_i\lambda_i - R_{i-1}\lambda_{i-1})H_t}{R_{i-1}\lambda_{i-1}R_i\lambda_i}} - 1 \right], & t > \dfrac{H_t}{R_{i-1}}, \end{cases} \tag{2.27}$$

After substituting Eq. (2.26) and Eq. (2.27) into Eq. (2.23) and taking the derivative

with respect to t, $f_{\mathrm{tr},2}^{M}(t)$ is given by

$$f_{\mathrm{tr},2}^{M}(t) = \sum_{i=1}^{N} \Bigg\{ \frac{R_{i+1}}{\lambda_i(R_{i+1}-R_i)} e^{-\frac{H_t}{R_{i+1}\lambda_{i+1}}} e^{\frac{(R_i\lambda_i - R_{i+1}\lambda_{i+1})(tR_{i+1}-H_t)}{R_{i+1}\lambda_{i+1}\lambda_i(R_{i+1}-R_i)}} \tag{2.28}$$

$$\left[\mathcal{U}\left(t-\frac{H_t}{R_{i+1}}\right) - \mathcal{U}\left(t-\frac{H_t}{R_i}\right)\right] p_{i+1|i} \tag{2.29}$$

$$+ \frac{R_{i-1}}{\lambda_i(R_i-R_{i-1})} e^{-\frac{H_t}{R_{i-1}\lambda_{i-1}}} e^{\frac{(R_i\lambda_i - R_{i-1}\lambda_{i-1})(tR_{i-1}-H_t)}{R_{i-1}\lambda_{i-1}\lambda_i(R_{i-1}-R_i)}} \tag{2.30}$$

$$\left[\mathcal{U}\left(t-\frac{H_t}{R_i}\right) - \mathcal{U}\left(t-\frac{H_t}{R_{i-1}}\right)\right] p_{i-1|i} \Bigg\} \pi_i. \tag{2.31}$$

For $L = 3$, by conditioning on the channel realization, $F_{\mathrm{tr},3}^{M}(t)$ can be calculated as

$$F_{\mathrm{tr},3}^{M}(t) = \sum_{i=1}^{N} \sum_{j} \sum_{k} \Pr\Bigg[T_i + T_j + \frac{H_t - R_iT_i - R_jT_j}{R_k} \le t, \\ R_iT_i + R_jT_j < H_t, \quad R_iT_i + R_jT_j + R_kT_k \ge H_t \Bigg] \pi_i p_{j|i} p_{k|j}, \tag{2.32}$$

where $j = i + 1/i - 1$ and $k = j + 1/j - 1$. Let $\mathbb{X} = T_i + T_j$ and $\mathbb{Y} = R_iT_i + R_jT_j$. It can be rewritten by

$$F_{\mathrm{tr},3}^{M}(t) = \sum_{i=1}^{N} \sum_{j} \sum_{k} \Pr\left[\mathbb{X} + \frac{H_t - \mathbb{Y}}{R_k} \le z,\ \mathbb{Y} \le H_t,\ \mathbb{Y} + R_kT_k \ge H_t \right] \pi_i p_{j|i} p_{k|j}. \tag{2.33}$$

The joint PDF of $\mathbb{X}$ and $\mathbb{Y}$, denoted by $f_{\mathbb{X}\mathbb{Y}}(x,y)$, is solved via its Jacobian and given by

$$f_{\mathbb{X}\mathbb{Y}}(x,y) = \frac{f_{T_i}\left(\frac{R_jx-y}{R_j-R_i}\right) f_{T_j}\left(\frac{R_ix-y}{R_i-R_j}\right)}{|R_j-R_i|} = \frac{\exp\left[-\frac{R_jx-y}{\lambda_i(R_j-R_i)}\right] \exp\left[-\frac{R_ix-y}{\lambda_j(R_i-R_j)}\right]}{\lambda_i\lambda_j|R_j-R_i|}. \tag{2.34}$$

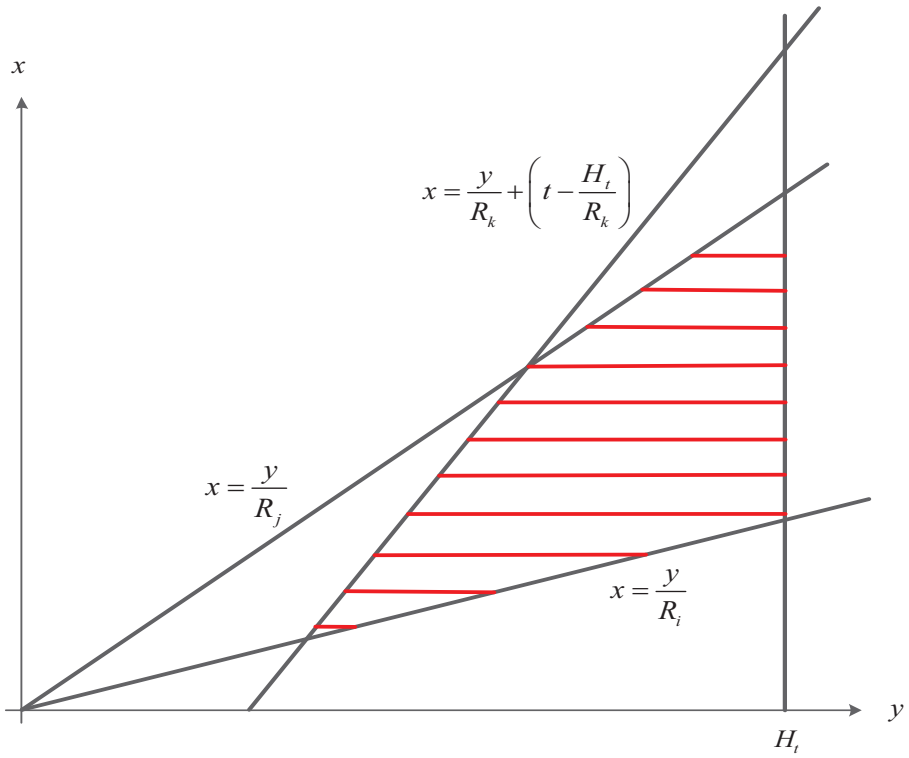

Figure 2.4: Integral regions when $\frac{1}{R_k} > \frac{1}{R_j} > \frac{1}{R_i}$.

The support set for Eq. (2.34) can be determined as

$$\begin{aligned} 0 < \frac{y}{R_j} < x < \frac{y}{R_i} < +\infty \quad \text{if } \frac{1}{R_i} > \frac{1}{R_j}, \\ 0 < \frac{y}{R_i} < x < \frac{y}{R_j} < +\infty \quad \text{if } \frac{1}{R_j} > \frac{1}{R_i}. \end{aligned} \tag{2.35}$$

In general, conditioning on the independent random variable T_k, we obtain

$$\begin{aligned} \Pr\left[\mathbb{X} + \frac{H_t - \mathbb{Y}}{R_k} \le z,\ \mathbb{Y} \le H_t,\ \mathbb{Y} + R_k T_k \ge H_t\right] &= \int\int_{\mathbb{R}} f_{\mathbb{X}\mathbb{Y}}(x,y) \exp\left(-\frac{H_t - y}{R_k \lambda_k}\right) d\mathbb{R} \\ &= \int\int_{\mathbb{R}} K \exp(Ax + By) d\mathbb{R}, \end{aligned} \tag{2.36}$$

with $A = \frac{\lambda_i R_i - \lambda_j R_j}{\lambda_i \lambda_j (R_j - R_i)}$, $B = \frac{\lambda_j - \lambda_i}{\lambda_i \lambda_j (R_j - R_i)} + \frac{1}{\lambda_k R_k}$, and $K = \frac{\exp\left(-\frac{H_t}{\lambda_k R_k}\right)}{\lambda_i \lambda_j |R_j - R_i|}$. The exact solution

depends on the rate used in the first, the second, and the third slot determining the integral region $\mathbb{R}$. Suppose that $\frac{1}{R_k} > \frac{1}{R_j} > \frac{1}{R_i}$, the integral region is illustrated in Fig. 2.4. As such, the corresponding conditional probability, denoted by $F^M_{\mathrm{tr},3|k>j>i}(t)$, can be solved as

$$F^M_{\mathrm{tr},3|k>j>i}(t) = \begin{cases} 0, & t \le \frac{H_t}{R_i}; \\ \int_{\frac{R_iR_k}{R_k-R_i}\left(t-\frac{H_t}{R_k}\right)}^{H_t} \int_{\frac{y}{R_i}}^{\frac{y}{R_k}+\left(t-\frac{H_t}{R_k}\right)} K\exp(Ax+By)dxdy, & \frac{H_t}{R_i} < t < \frac{H_t}{R_j}; \\ \int_{\frac{R_iR_k}{R_k-R_i}\left(t-\frac{H_t}{R_k}\right)}^{\frac{R_jR_k}{R_k-R_j}\left(t-\frac{H_t}{R_k}\right)} \int_{\frac{y}{R_i}}^{\frac{y}{R_k}+\left(t-\frac{H_t}{R_k}\right)} K\exp(Ax+By)dxdy, & \\ \quad + \int_{\frac{R_jR_k}{R_k-R_j}\left(t-\frac{H_t}{R_k}\right)}^{H_t} \int_{\frac{y}{R_i}}^{\frac{y}{R_j}} K\exp(Ax+By)dxdy & \frac{H_t}{R_j} < t < \frac{H_t}{R_k}; \\ \int_0^{H_t} \int_{\frac{y}{R_i}}^{\frac{y}{R_j}} K\exp(Ax+By)dxdy, & t > \frac{H_t}{R_k} \end{cases} \tag{2.37}$$

The formulas for other cases can be obtained by adjusting the integral boundaries accordingly.

2.4.2 Large L

For the general cases where $L \ge 3$, $F^M_{\mathrm{tr},L}(t)$, is formulated as

$$F^M_{\mathrm{tr},L}(t) = \Pr\left[\mathbb{T}^M_{L-1} + \frac{H_t - \mathbb{H}^M_{L-1}}{R^{(L)}} \le t,\ \mathbb{H}^M_{L-1} < H_t,\ \mathbb{H}^M_{L-1} + R^{(L)}T^{(L)} \ge H_t\right], \tag{2.38}$$

where $\mathbb{T}^M_{L-1} = \sum_{i=1}^{L-1} T^{(i)}$ and $\mathbb{H}^M_{L-1} = \sum_{i=1}^{L-1} R^{(i)}T^{(i)}$. To proceed further, we again condition on the channel realization. Let us consider a particular channel realization over L transmission slots, where the channel ends in state k over the Lth slot. As such, $R^{(L)}$ will be equal to R_k based on the mode of operation and $T^{(L)}$ will be an exponential random variable with mean λ_k. Suppose also that rate R_j is used n_j times over the first $L-1$ slots, where $\sum_{j=1}^{N} n_j = L-1$. Then, the time duration of the first

$L-1$ transmission slots $\mathbb{T}^M_{L-1}$ will be the sum of n_1 random variables with PDF $f_{T_1}(t)$, n_2 random variables with PDF $f_{T_2}(t)$, ..., and n_N random variables with PDF $f_{T_N}(t)$. Furthermore, $\mathbb{H}^M_{L-1}$ will be the sum of n_1 random variables with PDF $f_{T_1}(t/R_1)/R_1$, n_2 random variables with PDF $f_{T_2}(t/R_2)/R_2$, ..., and n_N random variables with PDF $f_{T_N}(t/R_N)/R_N$. These relationships apply to all channel realizations that leads to same vector $\overrightarrow{\mathbf{n}} = [n_1, n_2, \cdots, n_N]$ and channel state in Lth slot. By conditioning on the channel realization leading to the same $\overrightarrow{\mathbf{n}}$ and Lth slot state, we arrive at

$$F^M_{\mathrm{tr},L}(t) = \sum_{k=1}^{N}\sum_{\overrightarrow{\mathbf{n}}} \Pr\left[\mathbb{T}^M_{L-1|\overrightarrow{\mathbf{n}}} + \frac{H_t - \mathbb{H}^M_{L-1|\overrightarrow{\mathbf{n}}}}{R_k} \le t,\ \mathbb{H}^M_{L-1|\overrightarrow{\mathbf{n}}} < H_t,\ \mathbb{H}^M_{L-1|\overrightarrow{\mathbf{n}}} + R_k T^{(L)} \ge H_t\right] \times \Pr[\overrightarrow{\mathbf{n}} \text{ and slot } L \text{ in state } k]. \tag{2.39}$$

Let $F^M_{\mathrm{tr},L|\overrightarrow{\mathbf{n}},k}(t)$ denote $\Pr\left[\mathbb{T}^M_{L-1|\overrightarrow{\mathbf{n}}} + \frac{H_t - \mathbb{H}^M_{L-1|\overrightarrow{\mathbf{n}}}}{R_k} \le t, \mathbb{H}^M_{L-1|\overrightarrow{\mathbf{n}}} < H_t,\ \mathbb{H}^M_{L-1|\overrightarrow{\mathbf{n}}} + R_k T^{(L)} \ge H_t\right]$. In general, calculating $F^M_{\mathrm{tr},L|\overrightarrow{\mathbf{n}},k}(t)$ is challenging since it is the joint probability involving correlated events. Essentially, $\mathbb{T}^M_{L-1|\overrightarrow{\mathbf{n}}} = \sum_{i=1}^{L-1} T^{(i)}$ and $\mathbb{H}^M_{L-1|\overrightarrow{\mathbf{n}}} = \sum_{i=1}^{L-1} R^{(i)} T^{(i)}$ are two linear combinations of one identical set of $L-1$ i.n.d. exponential random variables, whose joint PDF is unknown even in the statistic literature, to the best of authors' knowledge. To proceed further, assuming multiple transmission slots are usually needed to complete transmission, we apply central limit theory to obtain an approximate expression of $F^M_{\mathrm{tr},L|\overrightarrow{\mathbf{n}},k}(t)$ for moderate value of L. Specifically, we approximate that $\mathbb{T}^M_{L-1|\overrightarrow{\mathbf{n}}}$ and $\mathbb{H}^M_{L-1|\overrightarrow{\mathbf{n}}}$ are jointly Gaussian distributed random variables (i.e. $(\mathbb{T}^M_{L-1|\overrightarrow{\mathbf{n}}},\ \mathbb{H}^M_{L-1|\overrightarrow{\mathbf{n}}}) \sim \mathcal{N}(\eta_x,\ \sigma_x^2,\ \eta_y,\ \sigma_y^2,\ \rho)$), whose parameters are derived in Appendix A. The joint PDF of $\mathbb{T}^M_{L-1|\overrightarrow{\mathbf{n}}}$ and $\mathbb{H}^M_{L-1|\overrightarrow{\mathbf{n}}}$ is given by

$$f_{\mathbb{T}^M_{L-1|\overrightarrow{\mathbf{n}}},\mathbb{H}^M_{L-1|\overrightarrow{\mathbf{n}}}}(x,y) = \frac{1}{2\pi\sigma_x\sigma_y\sqrt{1-\rho^2}} \times \exp\left(-\frac{1}{2(1-\rho^2)}\left(\frac{(x-\eta_x)^2}{{\sigma_x}^2} - 2\rho\frac{(x-\eta_x)(y-\eta_y)}{\sigma_x\sigma_y} + \frac{(y-\eta_y)^2}{{\sigma_y}^2}\right)\right). \tag{2.40}$$

By conditioning on the independent random variable $T^{(L)}$, $F^M_{\mathrm{tr},L|\overrightarrow{\mathbf{n}},k}(t)$ can now be calculated as

$$F^M_{\mathrm{tr},L|\overrightarrow{\mathbf{n}},k}(t) = \int_0^{H_t}\int_{-\infty}^{t-\frac{H_t-y}{R_k}} f_{\mathbb{T}^M_{L-1|\overrightarrow{\mathbf{n}}},\mathbb{H}^M_{L-1|\overrightarrow{\mathbf{n}}}}(x,y)\, e^{\left(-\frac{H_t-y}{\lambda_k R_k}\right)} dxdy. \tag{2.41}$$

For Markov channels, the probability of all channel realizations that lead to a vector $\overrightarrow{\mathbf{n}}$ over first $L-1$ slots and state k in the last slot, is challenging to calculate exactly due to the correlation between channel states over subsequent transmission slots. In other words, the duration of two consecutive slots is not necessarily independent due to the memory property of Markov process. In the following, we assume that the number of transmission slots is large and as such, the possible channel realizations lead to the same vector $\overrightarrow{\mathbf{n}}$ are huge. Then the joint probability $\Pr[\overrightarrow{\mathbf{n}}$ and slot L in state $k]$ can be approximately calculated by neglecting the correlation as

$$\Pr[\overrightarrow{\mathbf{n}} \text{ and slot } L \text{ in state } k] = \pi_k \binom{L-1}{n_1, n_2, \cdots, n_N} \prod_{j=1}^{N} \pi_j^{n_j}. \tag{2.42}$$

After substituting Eq. (2.40) and Eq. (2.42) into Eq. (2.41), taking derivative with respect to t and much manipulations with the help of [35], we obtain the PDF of the transmission time when L transmission slots are needed, $T_{\mathrm{tr},L}^{M}$, as

$$f_{\mathrm{tr},L}^{M}(t) = \sum_{k=1}^{N} \sum_{\overrightarrow{\mathbf{n}}} f_{\mathrm{tr},L|\overrightarrow{\mathbf{n}},k}^{M}(t) \pi_k \binom{L-1}{n_1, n_2, \cdots, n_N} \prod_{j=1}^{N} \pi_j^{n_j}, \tag{2.43}$$

where

$$
\begin{aligned}
f^{M}_{\mathrm{tr},L|\vec{\mathbf{n}},k}(t) = {} & \frac{\exp\left(-\frac{H_t}{R_k}\right)\exp\left(-\frac{(t-\frac{H_t}{R_k}-\eta_x)^2{\sigma_y}^2+2\rho\eta_y\sigma_x\sigma_y(t-\frac{H_t}{R_k}-\eta_x)+{\sigma_x}^2{\eta_y}^2}{2(1-\rho^2){\sigma_x}^2{\sigma_y}^2}\right)}{4\pi\sigma_x\sigma_y\sqrt{1-\rho^2}} \\
& \times\sqrt{\frac{2\pi(1-\rho^2){\sigma_x}^2{\sigma_y}^2}{\left(\frac{{\sigma_y}^2}{R_k^2}-2\rho\frac{\sigma_x\sigma_y}{R_k}+{\sigma_x}^2\right)}} \\
& \times\exp\left(\frac{\left(\frac{(t-\frac{H_t}{R_k}-\eta_x){\sigma_y}^2+\rho\eta_y\sigma_x\sigma_y}{R_k}-\frac{(1-\rho^2){\sigma_x}^2{\sigma_y}^2}{R_k\lambda_k}-\rho\sigma_x\sigma_y(t-\frac{H_t}{R_k}-\eta_x)-{\sigma_x}^2\eta_y\right)^2}{\left(\frac{{\sigma_y}^2}{R_k^2}-2\rho\frac{\sigma_x\sigma_y}{R_k}+{\sigma_x}^2\right)2(1-\rho^2){\sigma_x}^2{\sigma_y}^2}\right) \\
& \times\left\{\mathrm{erf}\left[\frac{\left(\frac{(t-\frac{H_t}{R_k}-\eta_x){\sigma_y}^2+\rho\eta_y\sigma_x\sigma_y}{R_k}-\frac{(1-\rho^2){\sigma_x}^2{\sigma_y}^2}{R_k\lambda_k}-\rho\sigma_x\sigma_y(t-\frac{H_t}{R_k}-\eta_x)-{\sigma_x}^2\eta_y\right)}{\sqrt{\left(\frac{{\sigma_y}^2}{R_k^2}-2\rho\frac{\sigma_x\sigma_y}{R_k}+{\sigma_x}^2\right)2(1-\rho^2){\sigma_x}^2{\sigma_y}^2}}\right.\right. \\
& \qquad\left.\left.+\sqrt{\frac{2(1-\rho^2){\sigma_x}^2{\sigma_y}^2}{\left(\frac{{\sigma_y}^2}{R_k^2}-2\rho\frac{\sigma_x\sigma_y}{R_k}+{\sigma_x}^2\right)}}H_t\right]\right. \\
& \left.-\mathrm{erf}\left(\frac{\left(\frac{(t-\frac{H_t}{R_k}-\eta_x){\sigma_y}^2+\rho\eta_y\sigma_x\sigma_y}{R_k}-\frac{(1-\rho^2){\sigma_x}^2{\sigma_y}^2}{R_k\lambda_k}-\rho\sigma_x\sigma_y(t-\frac{H_t}{R_k}-\eta_x)-{\sigma_x}^2\eta_y\right)}{\sqrt{\left(\frac{{\sigma_y}^2}{R_k^2}-2\rho\frac{\sigma_x\sigma_y}{R_k}+{\sigma_x}^2\right)2(1-\rho^2){\sigma_x}^2{\sigma_y}^2}}\right)\right\},
\end{aligned}
\tag{2.44}
$$

where $\mathrm{erf}(\cdot)$ is the Gauss error function.

Finally, the distribution function of transmission time, T^{M}_{tr}, can be evaluated by substituting Eq. (2.43) into Eq. (2.20) and taking summation over an appropriate range of integer L. In fact, the average number of slots required can be estimated by $L_{\mathrm{ave}} = \frac{H_t}{\sum_{j=1}^{N} R_j\lambda_j\pi_j}$. We can achieve satisfactory accuracy by taking summation over $L \in [1, \lfloor 3L_{\mathrm{ave}} \rfloor]$ as shown in numerical examples.

2.4.3 What if data transmission experiences medium level fading?

When the channel introduces medium level fading or the data amount is relatively large, data transmission completes in several slots. In such scenario, the accurate mathematical analysis of transmission time becomes very challenging and the condition for the central limit theorem is not satisfied. Hence, we apply the mixture model to directly estimate $f_{\text{tr}}^{M}(t)$. Specifically, we use *Gamma Mixture Model* (ΓMM) [36] as

$$f_{\text{tr}}^{M}(t) = \sum_{i=1}^{I} w_i f_{\Gamma_i}(t), \tag{2.45}$$

where $f_{\Gamma_i}(t) = \frac{\beta_i^{\alpha_i}}{\Gamma(\alpha_i)} t^{\alpha_i - 1} e^{-\beta_i t}$ is the Gamma PDF and $\Gamma(\cdot)$ is the Gamma function. The weights for each Gamma component w_i's satisfying $0 \leq w_i \leq 1$ and $\sum_{i=1}^{I} w_i = 1$, α_i and β_i are the shape parameter and rate parameter for the ith Gamma component, respectively. Provided a training data set of size K (e.g. $\mathbf{t} = [t_1, \cdots, t_K]$), the log-likelihood function for $f_{\text{tr}}^{M}(t)$ is given by

$$\mathcal{L}_{f_{\text{tr}}^{M}}(\mathbf{t}, w_1, \cdots w_I, \alpha_1, \cdots, \alpha_I, \beta_1, \cdots, \beta_I) = \log \left[\sum_{k=1}^{K} \sum_{i=1}^{I} w_i \left(\frac{\beta_i^{\alpha_i}}{\Gamma(\alpha_i)} t_k^{\alpha_i - 1} e^{-\beta_i t_k} \right) \right]. \tag{2.46}$$

It can be easily seen that the resulting likelihood function for estimating the $3I - 1$ parameters $w_1, \cdots w_{I-1}$, $\alpha_1, \cdots, \alpha_I$, $\beta_1, \cdots, \beta_I$ is non-linear and has no closed-form solution. As such, one can resort to the *Expectation Maximization* (EM) algorithm [37] or its variants [38].

2.5 Energy Consumption Analysis

In this section, we present the energy consumption analysis with the framework proposed in previous sections. We assume that the power consumed in the RF chain dominates the overall transmitter power consumption. Each component along the RF chain consumes a certain amount of energy as illustrated in Fig. 2.5. The RF power consumption is divided into two parts: PA power P_{AMP} and other component power P_{ci}. P_{AMP} depends on the target transmit power P_{tr} and can be calculated as

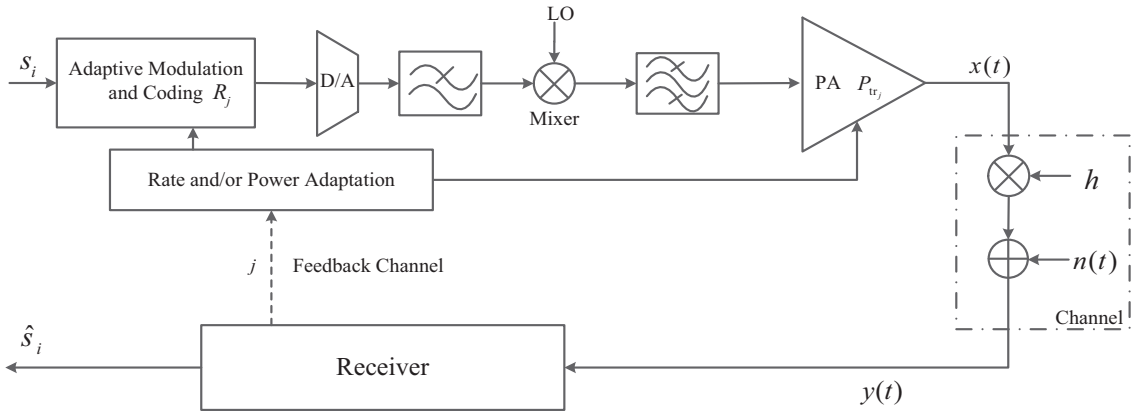

Figure 2.5: Illustration of components along the RF chain for adaptive transmission system over fading wireless channels.

$P_{\mathrm{AMP}} = \left(\frac{\xi}{\eta}\right) P_{\mathrm{tr}}$, where $\xi > 1$ is the peak-to-average power ratio of RF signal, which depends on the chosen modulation scheme, and $\eta < 1$ is the draining efficiency of the PA [39]. P_{ci} characterizes the power consumption of other components, including filter P_{FIL}, mixer P_{MIX}, and D/A P_{D2A}.

We consider the energy consumption of variable rate adaptation assuming that the transmission power is fixed to P_{tr}. The energy consumption for wireless transmission of big data depends on the number of random-length time slots required to complete transmission. The total energy consumption, denoted by $\mathcal{E}$, is the sum of the energy consumed in each slot. The CDF of $\mathcal{E}$ for a given amount of data H_t is formulated using the total probability theorem as

$$F_{\mathcal{E}}(z) = \sum_{L} \Pr\left[\mathcal{E}_L < z;\ L \text{ transmission slots used}\right], \tag{2.47}$$

where $\mathcal{E}_L$ denotes the total energy consumed when L transmission slots are required for transmission.

Energy consumption over the ith slot $\mathcal{E}^{(i)}$ can be calculated as the product of the transmitter power consumption level over the ith slot $P^{(i)}$ and the duration of the ith slot $T^{(i)}$ as

$$\mathcal{E}^{(i)} = P^{(i)} T^{(i)}. \tag{2.48}$$

When the channel gain g falls into region j over the ith slot, $T^{(i)}$ is an exponential random variable with average value λ_j, and $P^{(i)} = P_j$. P_j is the power consumption

when the $j$rh transmission mode is used, depending on the modulation scheme used since the peak-to-average ratio ξ is a function of modulation constellation size. For squared MQAM, $\xi_j = 3\left(\frac{\sqrt{M_j}-1}{\sqrt{M_j}+1}\right)$ with M_j being the number of symbols in the constellation [40]. Specifically, the transmitter power consumption when the jth transmission mode is adopted is

$$P_j = \frac{\xi_j}{\eta} P_{\text{tr}} + P_{\text{ci}},\ j = 1, 2, \cdots, N. \tag{2.49}$$

When L slots are required to finish transmission, $\mathcal{E}_L$ is the sum of energy consumed over the first $L-1$ intact slots and that consumed in the last partial slot and hence

$$\mathcal{E}_L = \sum_{i=1}^{L-1} \mathcal{E}^{(i)} + \frac{H_t - \sum_{i=1}^{L-1} R^{(i)} T^{(i)}}{R^{(L)}} P^{(L)}. \tag{2.50}$$

The energy consumption over slow/fast block/Markov fading channels can be similarly evaluated.

2.6 Numerical Example

We now present numerical results for the analytical solution. All the analytical and simulating results are carried out based on the received SNR divided into four regions corresponding to BPSK, QPSK, 8PSK, 16QAM transmission, (i. e. $[R_1, R_2, R_3, R_4] = [1, 2, 3, 4]$ bits/symbol). The symbol period is 1 μs. The threshold of each region is calculated using Rayleigh fading ($\gamma \sim \text{Exp}(\bar{\gamma})$, where $\bar{\gamma}$ is the average received SNR).

Fig. 2.6 reveals the exact PMF of T_{tr}^B over fast fading channel for different data amount H_t. We notice that T_{tr}^B varies dramatically around its average value.

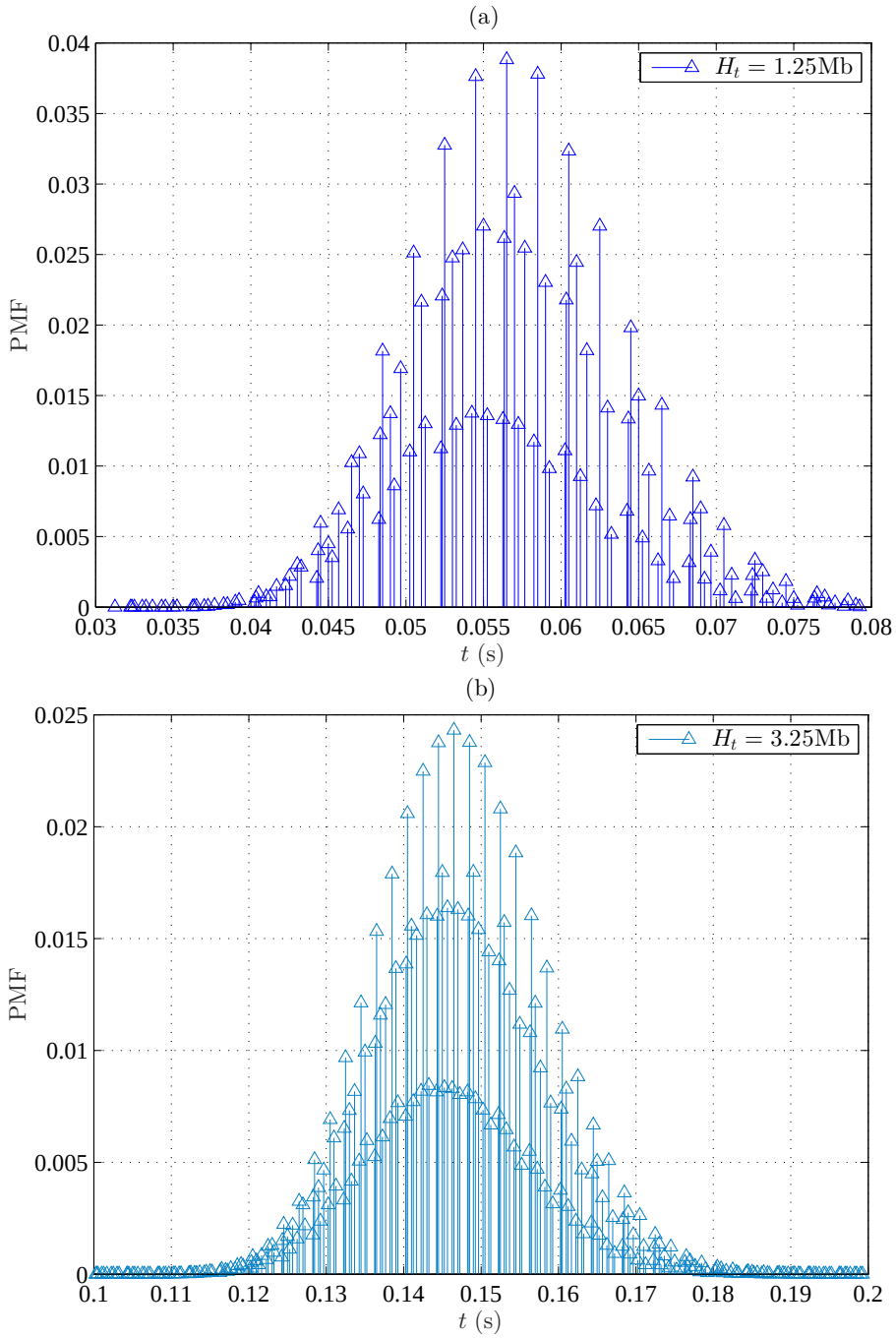

Figure 2.6: Exact PMF (2.8) of transmission time over block fading channels, where $f_D = 50$ Hz and $\bar{\gamma} = 15$ dB.

Fig. 2.7 plots the analytical results of approximate PMF of T_{tr}^{B} and its Monte Carlo simulation, where a large number of trials were simulated, and the results were compiled to estimate the PMF of T_{tr}^{B}. The perfect match between analytical and simulation results verify our analytical approach.

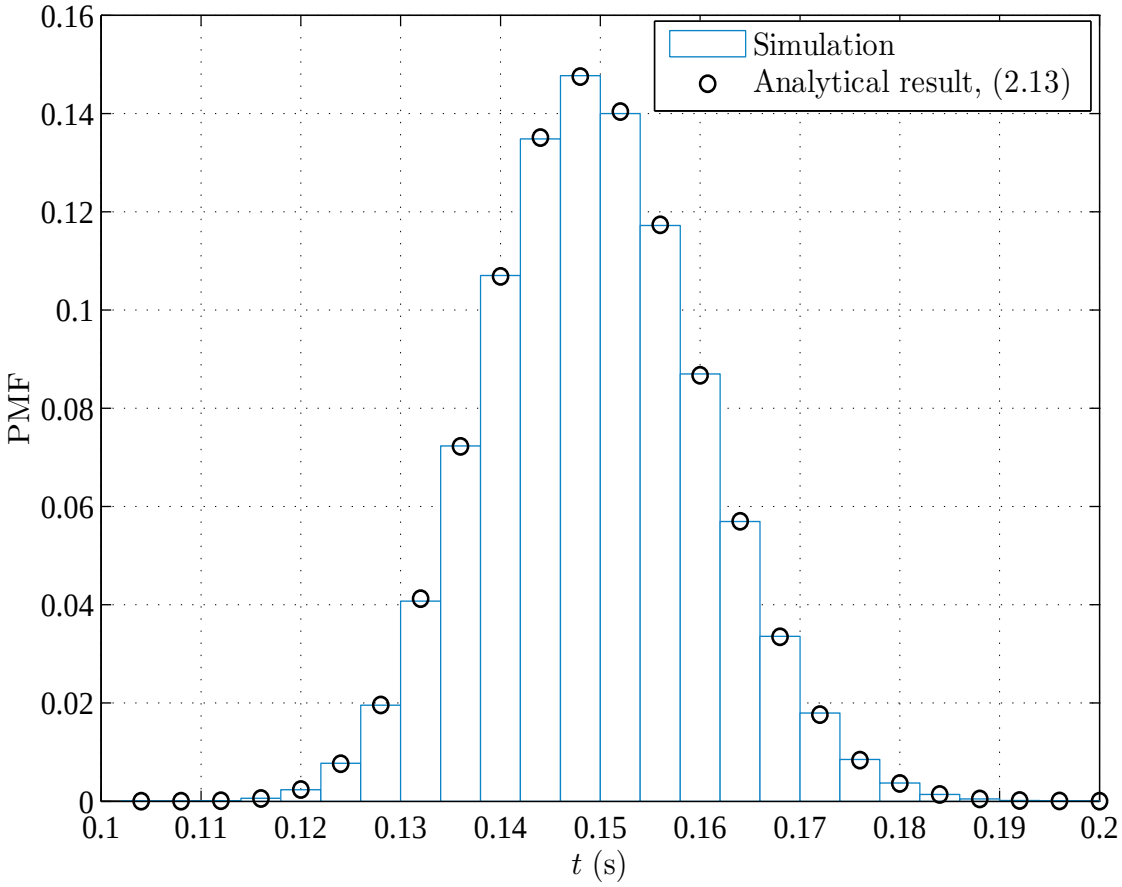

Figure 2.7: Exact CDF of transmission time over block fading channel versus various Doppler shift, where the channel coherence time is estimated by $T_c = 0.2$ ms, $\bar{\gamma} = 15$ dB, and $H_t = 3.25$ Mb.

Fig. 2.8 compares the exact CDF expression of T_{tr}^{B} in Eq. (2.9) and its approximation assuming fast fading for various data amount. We observe that the approximate CDF matches the exact CDF well at integer channel coherence time. As such, the approximate solution can be an effective alternative in T_{tr}^{B} analysis.

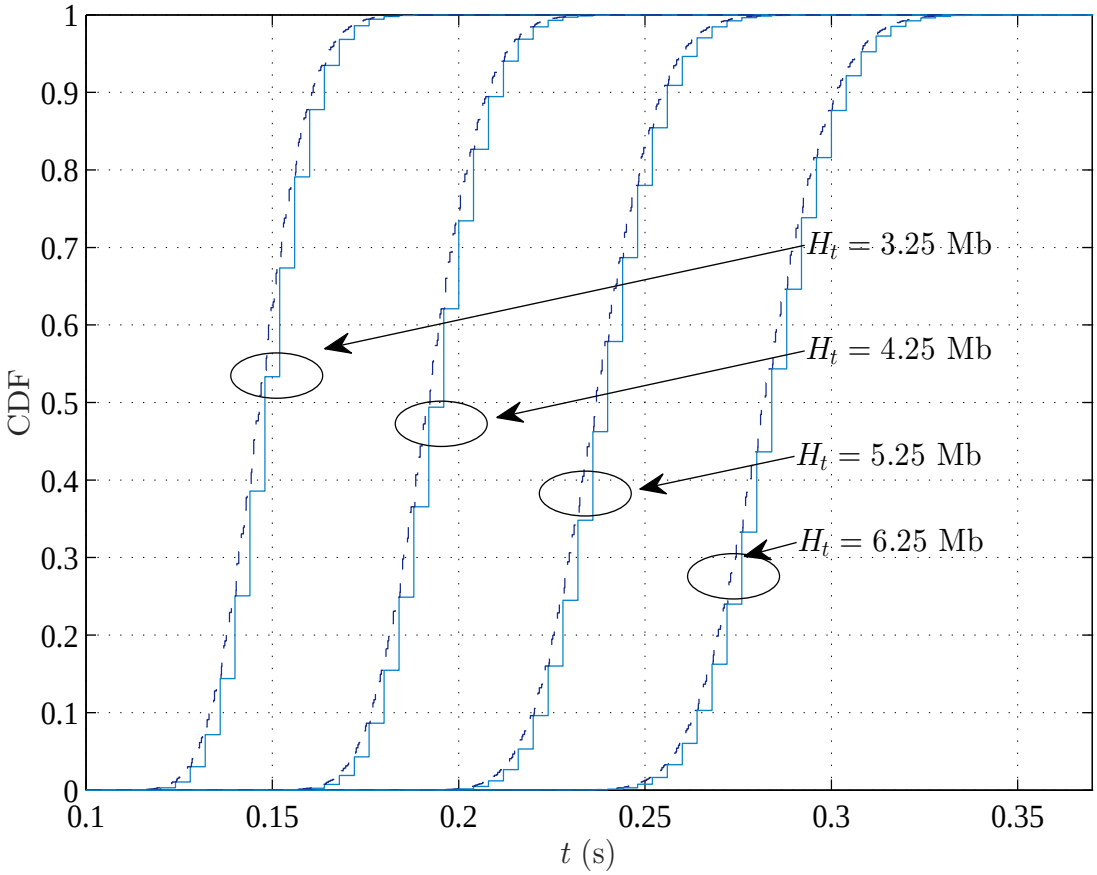

Figure 2.8: Exact and approximate solution of CDF of T_{tr}^{B} with different data amount H_t, where $\bar{\gamma} = 15$ dB and $f_D = 20$ Hz.

The distribution of T_{tr}^B greatly depends on the average received SNR $\bar{\gamma}$, Doppler shift f_D and the data amount H_t. We examine the behaviour of the analytical results with different parameter settings in Fig. 2.9. The average value of T_{tr}^B increases as H_t gets larger as the probability of transmission completed within fewer T_c's decreases. In fact, the variance of T_{tr}^B slightly increases as well when H_t becomes larger. When channel quality improves, higher order modulation schemes have more chance to be used, resulting in smaller values for both the average and variance of T_{tr}^B since the amount of T_c required decreases (see Fig. 2.9(a)). As Doppler shift reduces, the length of T_c increases and fewer T_c's are required. Thus, the variance of T_{tr}^B increases. However, the average value barely change given the data amount and channel condition, which is shown in Fig. 2.9(b).

(a)

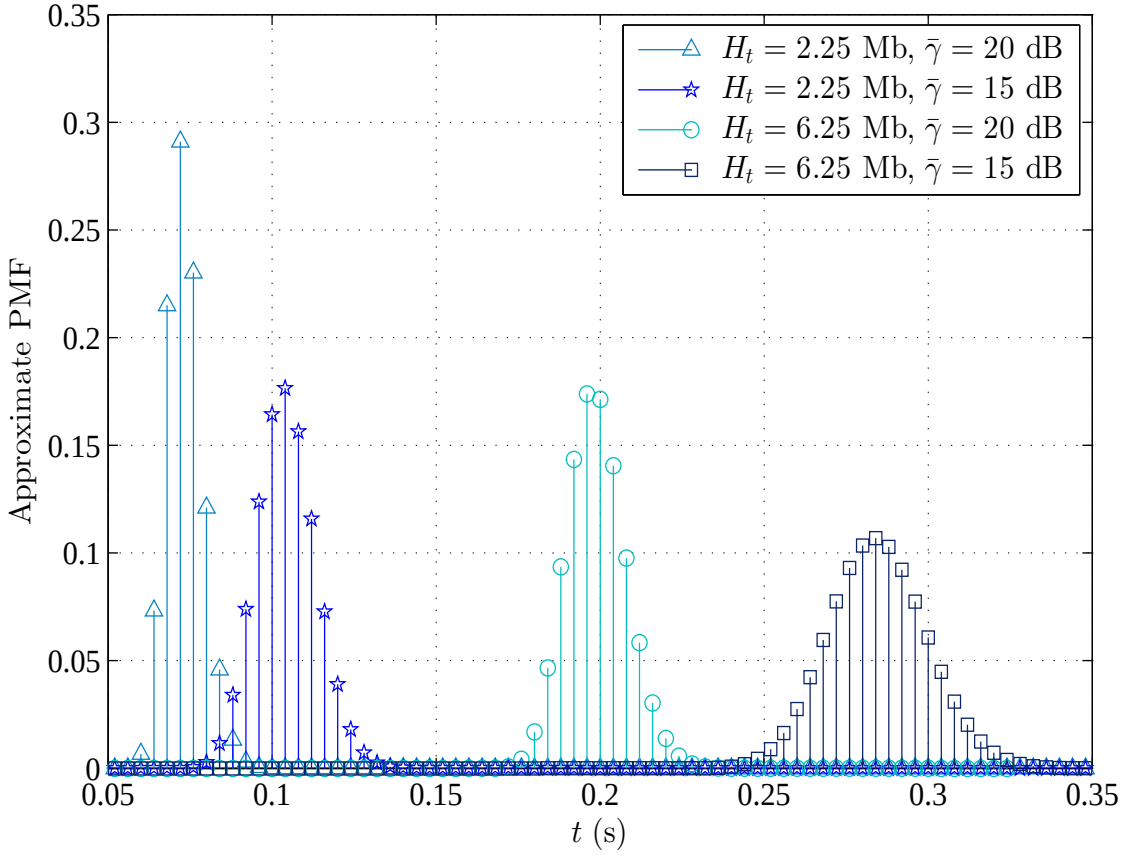

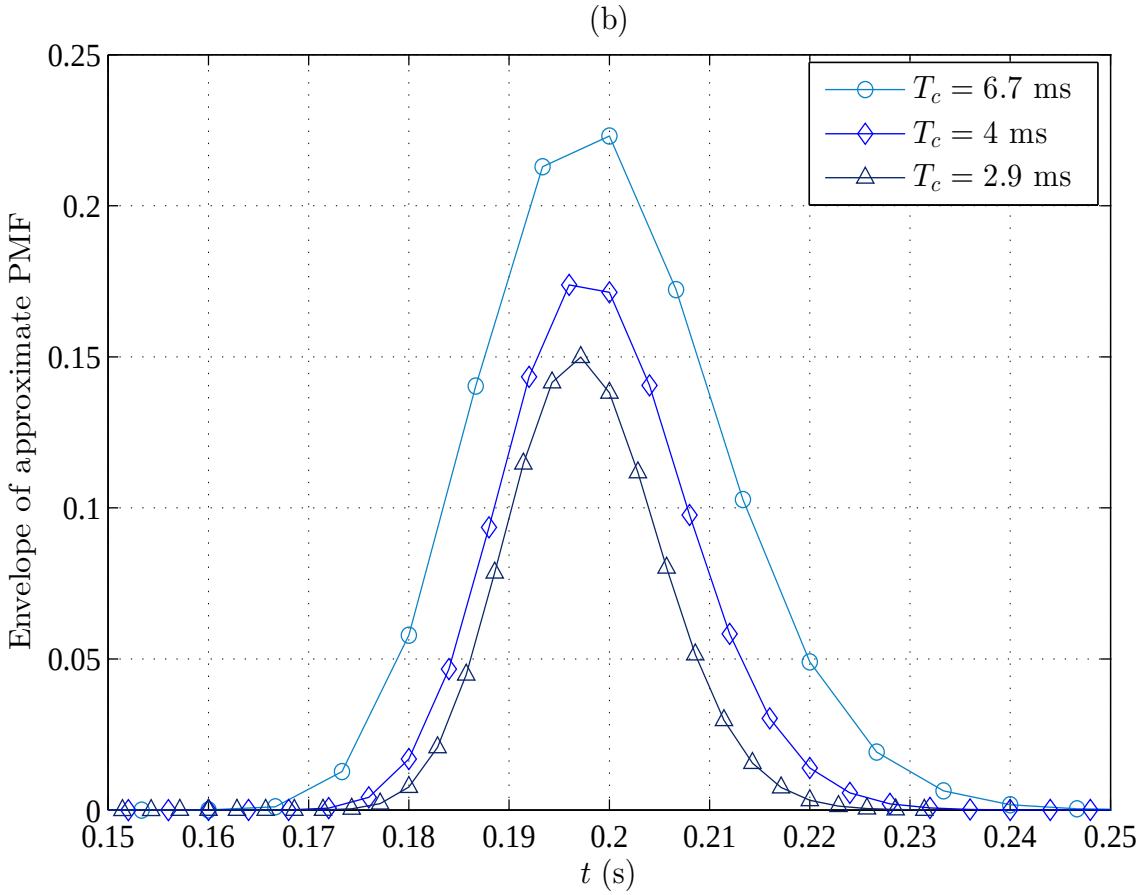

Figure 2.9: Approximate distribution of T_{tr}^{B} with various channel average value, Doppler shift, and data amount.

For Markov channels, the transmission slot is exponentially distributed. If the channel introduces slow fading and the transmission rate is high, data transmission will most likely complete over two time slots. The overall PDF of transmission time can be approximated by $f_{\text{tr},1}^{M}(t) + f_{\text{tr},2}^{M}(t)$. Fig. 2.10 plots the analytical PDF and corresponding simulation results of transmission time for slow fading scenario versus various average received SNR. The perfect match between the analytical formulation and Monte Carlo simulation validates our investigation. We observe that the probability distribution of T_{tr}^{M} over each sub-region $[H_t/R_{i+1},\ H_t/R_i]$ varies w.r.t. channel condition. The average value of T_{tr}^{M} approaches minimum transmission time, $\frac{H_t}{R_N}$ while average received SNR increases.

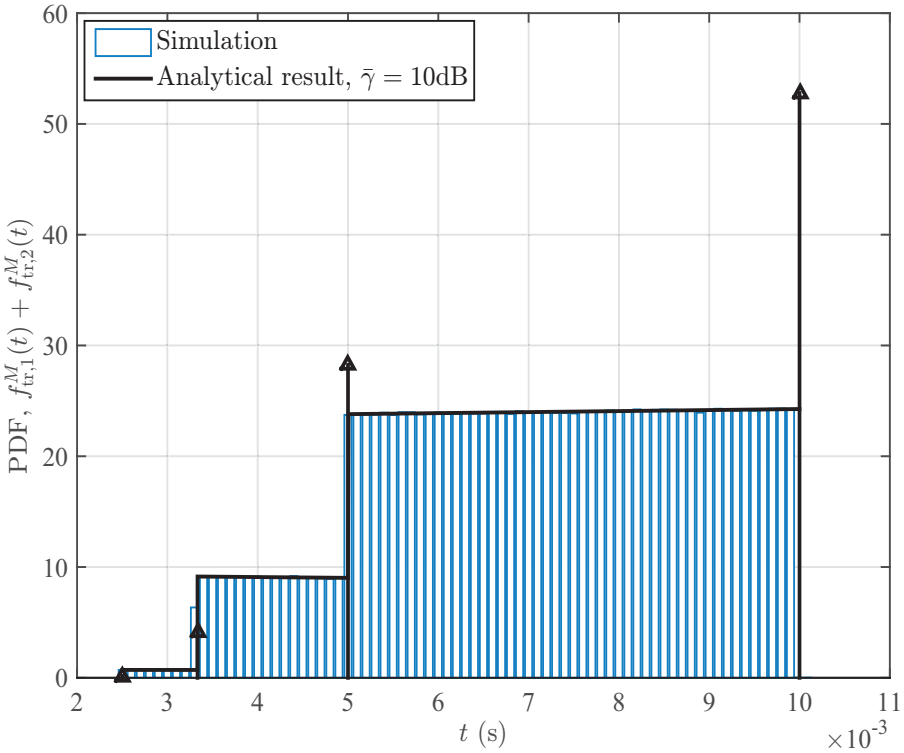
Simulation
Analytical result, $\bar{\gamma} = 10$dB
PDF, $f^M_{\mathrm{tr},1}(t) + f^M_{\mathrm{tr},2}(t)$
t (s)
$\times 10^{-3}$

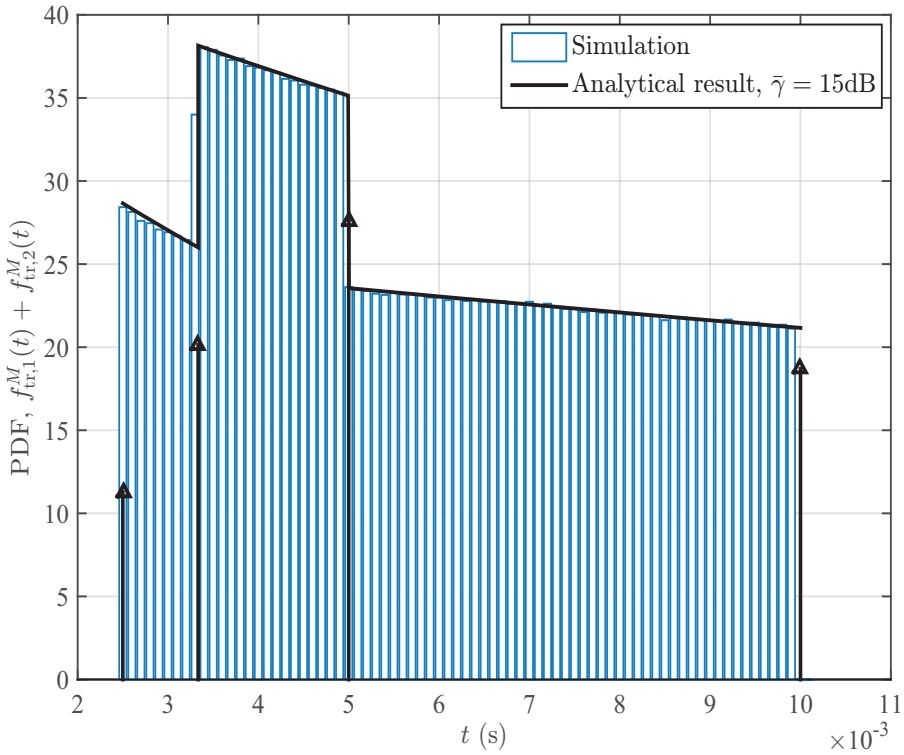
Simulation
Analytical result, $\bar{\gamma} = 15$dB
PDF, $f^M_{\mathrm{tr},1}(t) + f^M_{\mathrm{tr},2}(t)$
t (s)
$\times 10^{-3}$

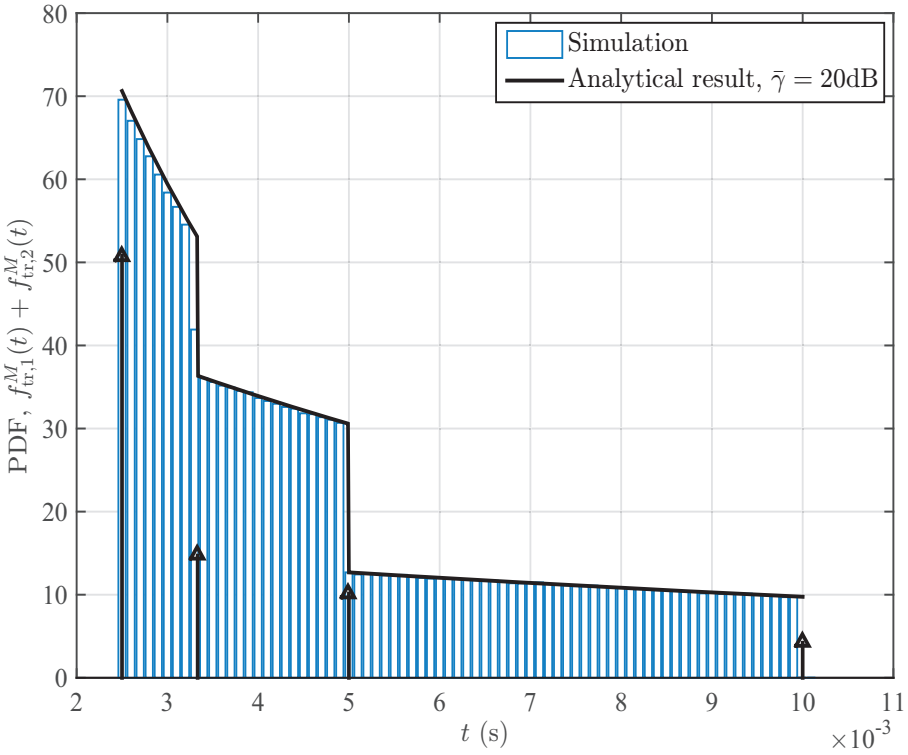

Figure 2.10: Monte Carlo simulation verification of analytical expression of PDF for T^M_{tr} with adaptive modulation over slow fading (e.g. $f^M_{\mathrm{tr}}(t) \approx f^M_{\mathrm{tr},1}(t) + f^M_{\mathrm{tr},2}(t)$), where $H_t = 0.1$ Mb and $f_D = 50$ Hz.

Fig. 2.11 plots both Monte Carlo simulation and analytical expression of PDF of T^M_{tr}. The good match between simulation and analytical results validate our analytical framework in evaluating transmission time. As the range of the summation over L gets larger, the approximation becomes more accurate. However, the computation grows fast accordingly.

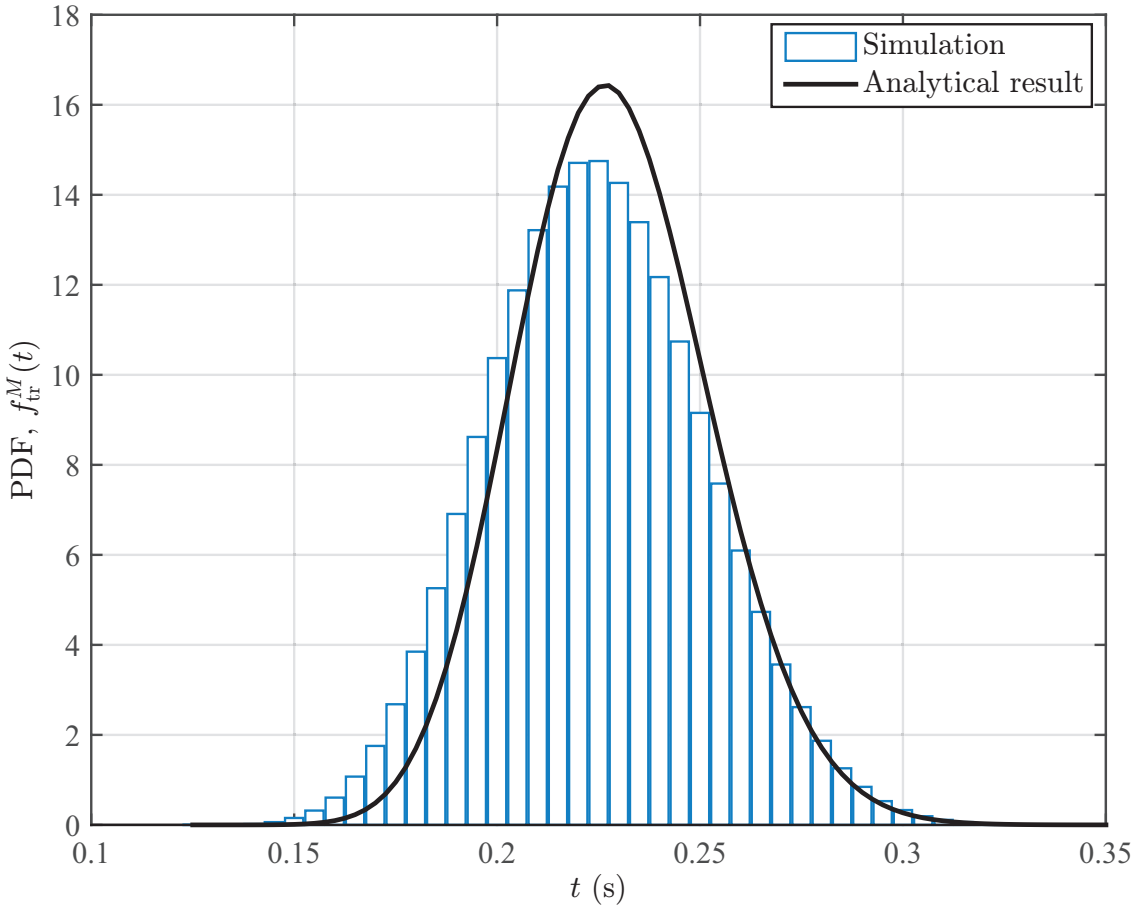

Figure 2.11: Monte Carlo simulation and analytical result in evaluating $T_{\rm tr}$, where $H_t = 5$ Mb, $f_D = 50$ Hz, and $\bar{\gamma} = 15$ dB.

It is obvious that the transmission time depends on the channel average value $\bar{\gamma}$, Doppler shift f_D and the data amount H_t. Typically, more transmission slots are required for large-amount data transmission, the average value and variance of $T_{\rm tr}^M$ increases with increasing H_t. On the other hand, as Doppler shift becomes smaller, the length of transmission slot increases and less transmission slots are required. Thus, the variance of $T_{\rm tr}^M$ increases. However, since $T_{\rm tr}^M = \sum_i T_i$, the average value barely changes given H_t as revealed in Fig. 2.12.

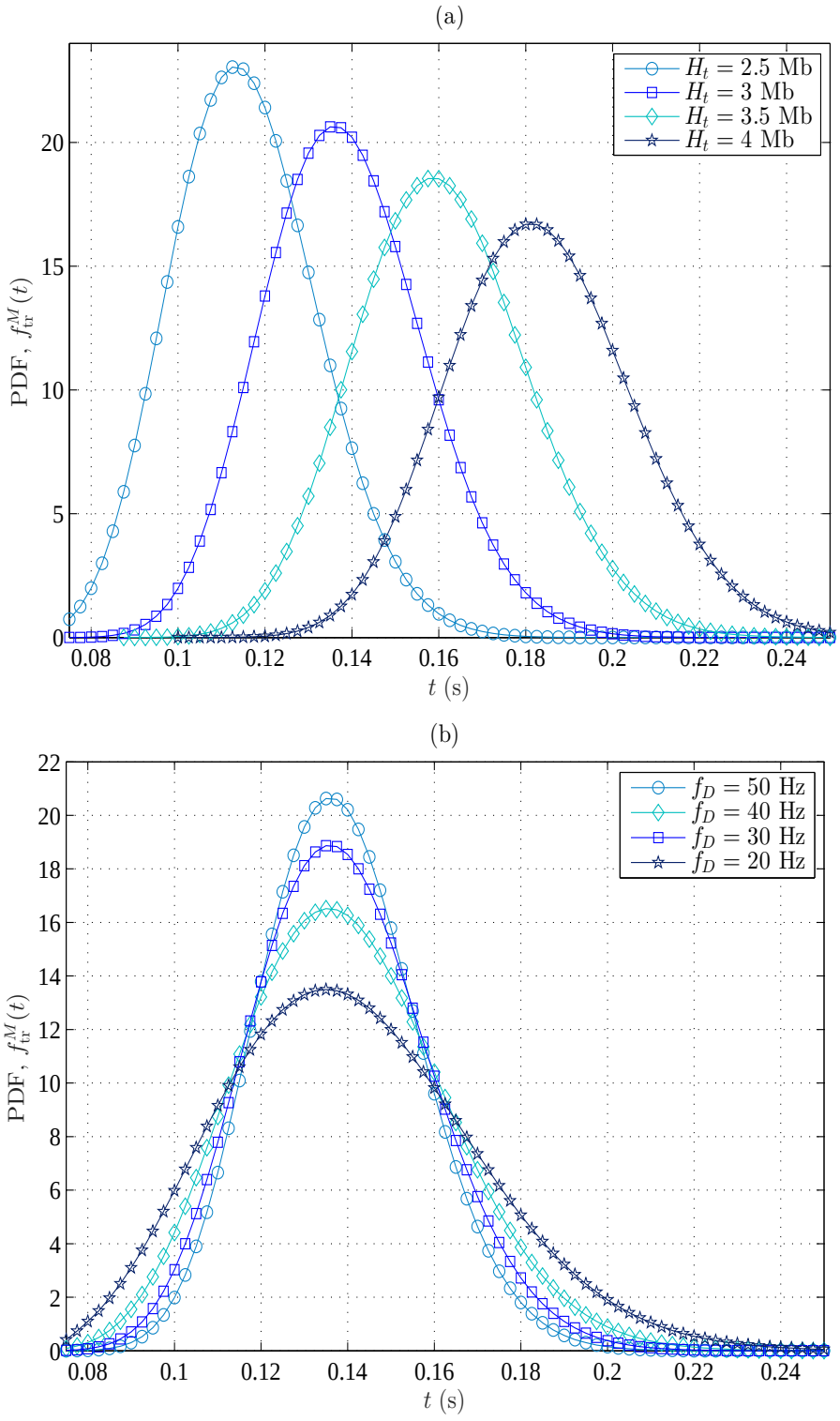

Figure 2.12: PDF of $T_{\rm tr}$ versus different data amount H_t and Doppler shift f_D.

2.7 Concluding Remarks

In this chapter, we proposed an analytical approach to investigate the transmission time of wireless system with adaptive modulation. Assuming the transmission slot is of the order of channel coherence time, the exact and approximate PMF and CDF of the transmission time are derived under block fading model. Then we generalized our analysis into continuous-time Markov channel, where transmission slots have random length. We first assume that channel experiences slow fading or, equivalently, data amount is small. The PDFs of $T_{\mathrm{tr},L}^{M}$ for one-slot and two-slot transmission are derived. By applying central limit theory, the approximate PDF of $T_{\mathrm{tr},L}^{M}$ is also derived for larger L. Transmission time evaluation can be helpful in both system design and performance analysis. The statistical results in this work can directly apply to designing energy efficient communication system or evaluating the delay performance of various communication systems.

Derivation of Conditional CDF in $F_{\mathrm{tr},L}^{M}(t)$

$\mathbb{T}_{L-1|\overrightarrow{n}}^{M} = \sum_{i=1}^{L-1} T^{(i)}$ and $\mathbb{H}_{L-1|\overrightarrow{n}}^{M} = \sum_{i=1}^{L-1} R^{(i)}T^{(i)}$ are two linear combination of $L-1$ independently non-identically distributed exponential random variables $T_l,\ l = 1, \cdots, L-1$. We approximate that $\mathbb{T}_{L-1|\overrightarrow{n}}^{M}$ and $\mathbb{H}_{L-1|\overrightarrow{n}}^{M}$ are jointly Gaussian distributed random variables. Specifically, $(\mathbb{T}_{L-1|\overrightarrow{n}}^{M}\ \mathbb{H}_{L-1|\overrightarrow{n}}^{M}) \sim \mathcal{N}(\eta_x,\ \sigma_x^2,\ \eta_y,\ \sigma_y^2,\ \rho)$. Given the channel realization, we can directly calculate their marginal first and second order statistics as $\eta_x = \mathbb{E}\left[\mathbb{T}_{L-1|\overrightarrow{n}}^{M}\right] = \sum_{i=1}^{N} n_i\lambda_i$, $\sigma_x^2 = \mathbb{V}\left[\mathbb{T}_{L-1|\overrightarrow{n}}^{M}\right] = \sum_{i=1}^{N} n_i\lambda_i^2$, $\eta_y = \mathbb{E}\left[\mathbb{H}_{L-1|\overrightarrow{n}}^{M}\right] = \sum_{i=1}^{N} n_i R_i\lambda_i$ and $\sigma_y^2 = \mathbb{V}\left[\mathbb{H}_{L-1|\overrightarrow{n}}^{M}\right] = \sum_{i=1}^{N} n_i\left(R_i\lambda_i\right)^2$, where $\mathbb{E}[\cdot]$ and $\mathbb{V}[\cdot]$ denote the expectation and variance, respectively. The covariance of $\mathbb{T}_{L-1|\overrightarrow{n}}^{M}$

and $\mathbb{H}^M_{L-1|\overrightarrow{n}}$, denoted by $\mathbb{C}_{\mathbb{T}^M_{L-1|\overrightarrow{n}}\mathbb{H}^M_{L-1|\overrightarrow{n}}}$, can be calculated as

$$\begin{aligned}\mathbb{C}_{\mathbb{T}^M_{L-1|\overrightarrow{n}}\mathbb{H}^M_{L-1|\overrightarrow{n}}} &= \mathbb{E}\left[\mathbb{T}^M_{L-1|\overrightarrow{n}}\mathbb{H}^M_{L-1|\overrightarrow{n}}\right] - \mathbb{E}\left[\mathbb{T}^M_{L-1|\overrightarrow{n}}\right]\mathbb{E}\left[\mathbb{H}^M_{L-1|\overrightarrow{n}}\right] \\ &= \mathbb{E}\left[\left(\sum_{l=1}^{L-1} T^{(l)}\right)\left(\sum_{j=1}^{L-1} R^{(j)}T^{(j)}\right)\right] - \mathbb{E}\left[\sum_{l=1}^{L-1} T^{(l)}\right]\mathbb{E}\left[\sum_{j=1}^{L-1} R^{(j)}T^{(j)}\right] \\ &= \mathbb{E}\left[\sum_{l=1}^{L-1}\sum_{j=1}^{L-1} R^{(j)}T^{(j)}T^{(l)}\right] - \left(\sum_{l=1}^{L-1}\mathbb{E}[T^{(l)}]\right)\left(\sum_{j=1}^{L-1}\mathbb{E}[R^{(j)}T^{(j)}]\right) \\ &= \sum_{l=1}^{L-1}\sum_{j=1}^{L-1} R^{(j)}\mathbb{E}[T^{(j)}T^{(l)}] - \sum_{l=1}^{L-1}\sum_{j=1}^{L-1} R^{(j)}\mathbb{E}[T^{(j)}]\mathbb{E}[T^{(l)}]. \end{aligned} \tag{2.51}$$

If the number of transmission slots is large and as such, the possible channel realizations lead to the same vector $\overrightarrow{n}$ are huge. By neglecting the correlation, $T^{(l)}$ and $T^{(j)}$ are independent when $l \neq j$, as such $\mathbb{E}[T^{(l)}T^{(j)}] - \mathbb{E}[T^{(l)}]\mathbb{E}[T^{(j)}] = 0$ for $l \neq j$. Therefore, $\mathbb{C}_{\mathbb{T}^M_{L-1|\overrightarrow{n}}\mathbb{H}^M_{L-1|\overrightarrow{n}}}$ can be rewritten as

$$\begin{aligned}\mathbb{C}_{\mathbb{T}^M_{L-1|\overrightarrow{n}}\mathbb{H}^M_{L-1|\overrightarrow{n}}} &= \sum_{l=1}^{L-1} R^{(l)}\mathbb{E}[(T^{(l)})^2] - \sum_{l=1}^{L-1} R^{(l)}\mathbb{E}^2[T^{(l)}] = \sum_{l=1}^{L-1} R^{(l)}(\mathbb{E}[(T^{(l)})^2] - \mathbb{E}^2[T^{(l)}]) \\ &= \sum_{l=1}^{L-1} R^{(l)}\mathbb{V}[T^{(l)}] = \sum_{i=1}^{N} n_i R_i \lambda_i^2. \end{aligned} \tag{2.52}$$

Hence, by definition, the correlation coefficient can be calculated as

$$\rho = \frac{\mathbb{C}_{\mathbb{T}^M_{L-1|\overrightarrow{n}}\mathbb{H}^M_{L-1|\overrightarrow{n}}}}{\sqrt{\mathbb{V}\left[\mathbb{T}^M_{L-1|\overrightarrow{n}}\right]}\sqrt{\mathbb{V}\left[\mathbb{H}^M_{L-1|\overrightarrow{n}}\right]}} = \frac{\sum_{i=1}^{N} n_i R_i \lambda_i^2}{\sqrt{\sum_{i=1}^{N} n_i \lambda_i^2}\sqrt{\sum_{i=1}^{N} n_i (R_i\lambda_i)^2}}. \tag{2.53}$$

As such, $F^M_{\mathrm{tr},L|\overrightarrow{n},k}(t)$ can be rewritten as

$$\begin{aligned}&F^M_{\mathrm{tr},L|\overrightarrow{n},k}(t) \\ &= \Pr\left[\mathbb{T}^M_{L-1|\overrightarrow{n}} \leq t - \frac{H_t - \mathbb{H}^M_{L-1|\overrightarrow{n}}}{R_k},\ 0 \leq \mathbb{H}^M_{L-1|\overrightarrow{n}} \leq H_t,\ T^{(L)} \geq \frac{H_t - \mathbb{H}^M_{L-1|\overrightarrow{n}}}{R_k}\right], \end{aligned} \tag{2.54}$$

where we restrict data transmitted to be non-negative.

Chapter 3

Extended Delivery Time Analysis for Secondary Transmission with Rate Adaptation

3.1 Introduction

Radio spectrum scarcity is one of the most significant problems faced by wireless communication industry nowadays. By exploring existing licensed frequency bands opportunistically, cognitive radio becomes a promising solution to such problem. Various implementation strategies exist for opportunistic spectrum sharing [41–47]. With underlay cognitive implementation, primary user (PU) and secondary user (SU) can utilize the same spectrum simultaneously as long as the SU-to-PU interference satisfies a certain interference constraint. As such, SU transmitter needs to know the SU-to-PU channel condition, which can be very challenging in practice. With interweave cognitive implementation, the SU can access the licensed frequency band only when PU does not occupy it and must vacate the spectrum when PU starts transmission. Therefore, SU transmission causes no interference to PU. Meanwhile, SU needs to monitor PU activity on the target frequency band and perform spectrum hand-off adaptively for relinquishing or reaccessing the channel. Typically, multiple spectrum handoffs are involved to complete the secondary transmission of a given amount of data, resulting in extra delay. The total information delivery time, termed as extended delivery time (EDT) [48], would consist of waiting time and transmission

time. We analyse the EDT of interweave cognitive radio system and investigate its statistical characteristics, which is essential to delay performance evaluation for SU transmission.

The concept of EDT was first introduced to derive the throughput bounds and delay performance of SU in cognitive radio transmission system [48]. Generally, EDT consists of an interleaved sequence of transmission periods and waiting periods. By taking into account of the waiting time during secondary packet transmission, EDT is an important performance metric for cognitive systems. [49] investigates EDT considering the spectrum sensing error. [50] studies EDT for cognitive radio system with multiple available channels and multiple SUs. The statistical characteristics of EDT depend on both spectrum sharing strategy and packet transmission policy. SU can adopt either work-preserving strategy [49,50], where SU restarts the transmission from the breaking point without wasting the previous transmission, or non-work-preserving strategy, where the SU retransmits the whole packet after reaccessing to the channel. Work-preserving strategy is achievable with the help of rateless codes [10,51,52], and also applies to the transmission of individually-coded small packets. In [3], the exact PDF of EDT for secondary packet transmission is derived for work-preserving strategy.

The delay and throughput analysis for secondary transmission is closely related to EDT, especially for interweave implementation. [53] investigates the average waiting time and average service time of the SU in one transmission slot with general primary traffic model. [54] derives a probability distribution of the service time available to SU within a fixed period of time. To evaluate the delay performance for secondary users, [55] proposes a priority virtual queue model. In cooperative wireless communication scenarios, [56] investigates the probability of successful data transmission with the hard delay constraints. [57] analyses the end-to-end delay performance of an interweave cognitive radio network in terms of the quality of service parameters. [58] carries out a queueing performance analysis for secondary users with dynamic spectrum access. A dynamic channel selection method is proposed in [59] to minimize the delay for secondary transmission in a pre-emptive resume M/G/1 queueing network.

With AMC, which can guarantee reliability, the transmission rate will change with the channel condition, leading to varying transmission time for fixed-amount data. Specifically, the implementation of AMC in an underlay fashion was investigated in [13]. In [60], achievable capacity gain by implementing AMC was analyzed for

an underlay cognitive radio system. Assuming transmission completes in one SU transmission period, the BER performance and spectral efficiency for an interweave cognitive radio system with AMC was investigated in [61] considering PU traffic and imperfect spectrum sensing. We extend previous work on EDT analysis for secondary data transmission with AMC. AMC can take advantage of better channel conditions, resulting in data throughput improvement, with a guaranteed BER [62]. Since SU can only access the channel when PU is off, throughput improvement is critical in secondary system design.

In general, the EDT of secondary data transmission depends on the spectrum sharing policy, data transmission policy, and spectrum sensing strategy. We focus on analyzing the EDT performance of the secondary data transmission with work-preserving strategy, practical spectrum sensing, and AMC under an interweave implementation. In particular, we consider the transmission of both large amount of data, which requires multiple secondary transmission periods, and data of small amount, which can be delivered in one period. For the first case, noting the difficulties in obtaining the exact solution, we derive the approximate PDF of the transmission time by applying the central limit theorem.

3.2 System Model

We consider a cognitive transmission system with interweave implementation. Specifically, SU opportunistically explores a licensed PU channel by transmitting when PU does not utilize the channel and stopping its transmission whenever PU transmission occurs. We use a continuous-time two-state Markov chain to describe PU activity with state space being PU busy and PU idle. The duration of busy and idle periods are, therefore, modelled as independent, non-identical exponential random variables with average busy duration λ and average idle duration μ, respectively[1].

The transmission decision of SU depends on channel sensing strategy. Here we focus on two sensing strategies, namely *continuous sensing technique* [66] and *semi-periodic sensing technique*, to guarantee no interference caused by secondary trans-

[1]Empirical and experimental studies on IEEE 802.11 Wireless LAN (WLAN) support a semi-Markovian model for various traffic types. Therefore, Markovian model serves as a reasonable approximation and is widely used in evaluating the performance of secondary packet transmission in various scenarios [63–65].

mission. With continuous sensing, SU transmitter continuously senses PU channel while transmitting and waiting, which could be implemented with matched filter or energy detector [66]. SU starts its transmission immediately when the channel becomes available. Similarly, SU stops its transmission as soon as PU re-occupies the channel. Continuous spectrum sensing can fully utilize PU channel at the cost of higher energy consumption and system complexity. For semi-periodic sensing, SU senses the channel periodically with a fixed period T_s to explore transmission opportunity. When the channel is sensed free, SU will start or continue its transmission. Otherwise, SU will wait T_s time period and sense the channel again. In order to avoid any interference to PU transmission, SU continuously monitors the channel during its transmission. For both spectrum sensing strategies, the continuous time period during which SU transmits is referred to as a SU transmission period. Similarly, the continuous time period during which SU waits is referred to as a waiting period. For semi-periodic sensing case, the SU waiting period also includes the time when the channel is available, but the SU has not performed sensing yet. As being illustrated in Fig. 3.1, the whole time line, in term of secondary transmission, has been classified as SU transmission period and SU waiting period. With adopted PU model and sensing strategy, SU transmission period and SU waiting period are exponential length with average μ and λ, respectively. We assume that the sensing result is perfect, and as such, no interference is caused to PU transmission.

We consider a wireless communication system operating over flat fading channels, as illustrated in previous chapter. We also assume that secondary transmission adopts AMC, where the transmission rate measured in bits/symbol remains unchanged within each SU transmission period. However, between different transmission periods, the transmission rate can be varied on the basis of the secondary channel quantity. As such, suppose that SU received SNR is divided into N regions, rate R_i is selected when falls into region A_i with probability π_i.

To implement adaptive modulation, SU transmitter sends a pilot signal once the spectrum sensed free. The receiver estimates the received SNR from the pilot signal and determines which SNR region it falls into. Then, the receiver feeds back the index of the selected modulation scheme to the transmitter via an error-free feedback channel. After that, the transmitter and the receiver will be configured to use identical modulation scheme.

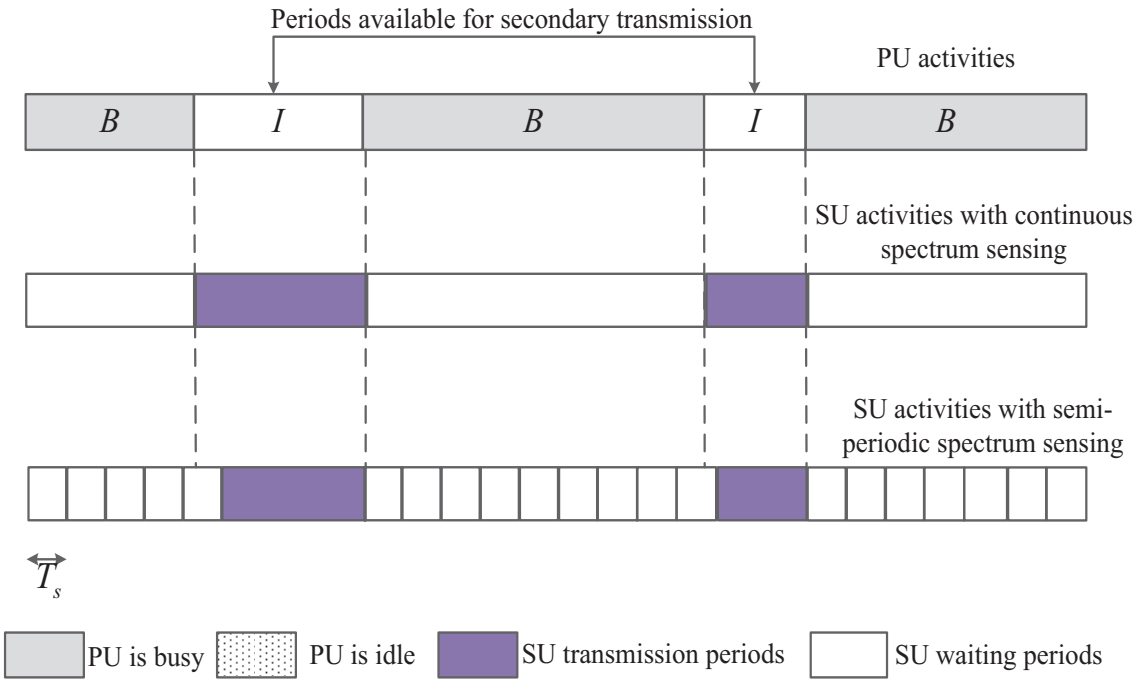

Figure 3.1: Secondary transmission with continuous spectrum sensing strategy and semi-periodic spectrum sensing strategy, respectively.

3.3 Extended Delivery Time Analysis

We consider a SU is intended to transmit certain amount of data. The secondary transmission starts at a random point in time. The EDT of a fixed-amount SU data transmission can be formulated as: $T_{\mathrm{ED}} = T_{\mathrm{tr}} + T_{\mathrm{w}}$, where T_{tr} is data transmission time and T_{w} is total waiting time. Notice that, in general, T_{w} and T_{tr} are random variables. Typically, T_{w} depends on T_{tr}, primary user activity and sensing strategies. T_{tr}, in turn, relies on data amount and secondary channel condition when PU channel is available. In the following two subsections, we derive the PDF of EDT considering both continuous spectrum sensing and semi-periodic spectrum sensing strategies.

3.3.1 Continuous Spectrum Sensing

With Markov PU activities and continuous spectrum sensing, The SU transmission period, denoted by T, is exponentially distributed with average μ. Similarly, the SU waiting period, denoted by W, is an exponential random variable with average λ.

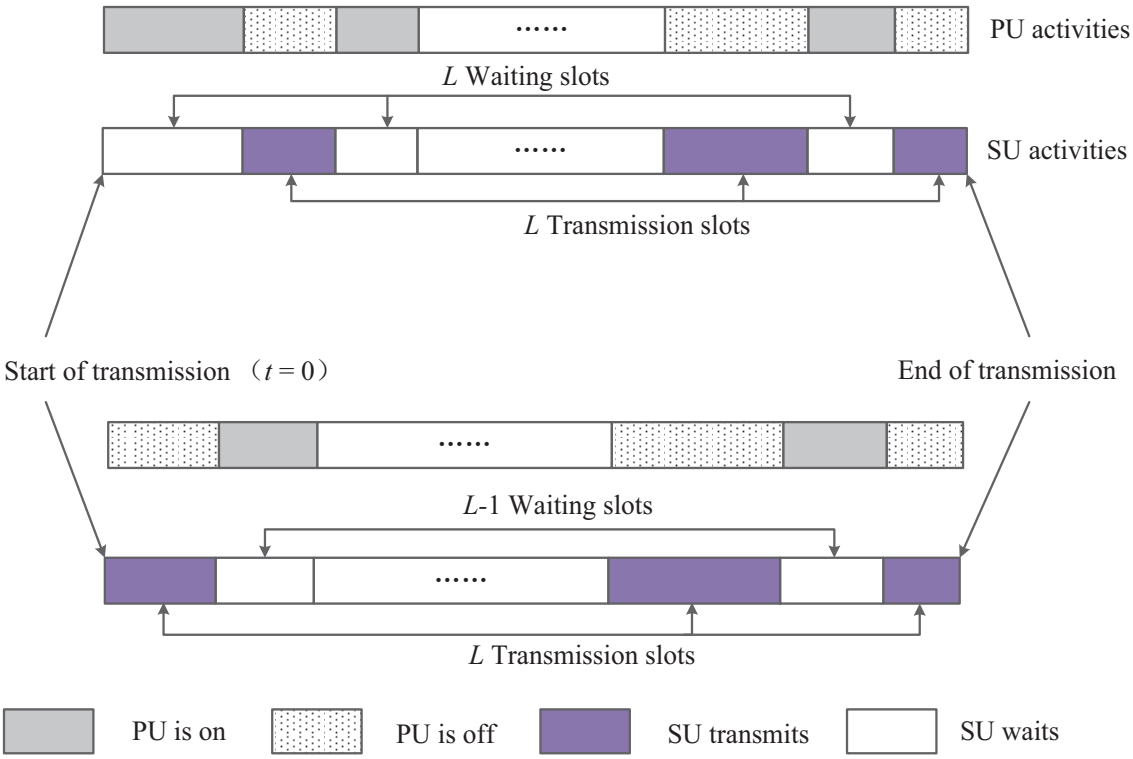

Figure 3.2: Secondary transmission when PU is off and on at the start of secondary transmission with continuous sensing.

The PDF of EDT with continuous sensing, denoted by $f^C_{T_{\rm ED}}(t)$, depends on PU is on or off at the start of secondary transmission as revealed in Fig. 3.2. We denote the conditional PDF of EDT when PU is on and off at the beginning of transmission by $f^C_{T_{\rm ED}|{\rm on}}(t)$ and $f^C_{T_{\rm ED}|{\rm off}}(t)$, respectively, and corresponding CDF by $F^C_{T_{\rm ED}|{\rm on}}(t)$ and $F^C_{T_{\rm ED}|{\rm off}}(t)$. We have

$$\begin{aligned} f^C_{T_{\rm ED}}(t) &= \frac{\lambda}{\lambda+\mu} f^C_{T_{\rm ED}|{\rm on}}(t) + \frac{\mu}{\lambda+\mu} f^C_{T_{\rm ED}|{\rm off}}(t) \\ &= \frac{\lambda}{\lambda+\mu} \frac{dF^C_{T_{\rm ED}|{\rm on}}(t)}{dt} + \frac{\mu}{\lambda+\mu} \frac{dF^C_{T_{\rm ED}|{\rm off}}(t)}{dt}, \end{aligned} \tag{3.1}$$

where $\frac{\lambda}{\lambda+\mu}$ and $\frac{\mu}{\lambda+\mu}$ are the probabilities that the PU is on or off at the transmission start for secondary transmission. The number of waiting periods is same as the number of transmission periods when PU is on at the beginning of secondary transmission. Hence, $T_{\rm w}$ includes L waiting periods if L transmission periods are required to complete transmission as illustrated in Fig. 3.2. Given the data amount H_t, $F^C_{T_{\rm ED}|{\rm on}}(t)$

can be formulated as

$$F^{C}_{T_{\mathrm{ED}}|\mathrm{on}}(t) = \sum_{L} \Pr\left[\mathbb{T}_{\mathrm{tr},L} + \mathbb{T}_{\mathrm{w},L} \leq t;\ \mathbb{H}_{L-1} \leq H_t;\ \mathbb{H}_{L} \geq H_t\right], \tag{3.2}$$

where $\mathbb{T}_{\mathrm{tr},L}$ and $\mathbb{T}_{\mathrm{w},L}$ are the total transmission time and waiting time when L transmission periods are needed. $\mathbb{H}_{L-1}$ and $\mathbb{H}_{L}$ denote the amount of data transmitted over $L-1$ and L transmission periods, respectively. It can be easily shown that $\mathbb{H}_{L-1}$ and $\mathbb{H}_{L}$ are given by

$$\mathbb{H}_{L-1} = \sum_{j=1}^{L-1} R^{(j)} T_j, \quad \mathbb{H}_{L} = \mathbb{H}_{L-1} + R^{(L)} T_L, \tag{3.3}$$

respectively, where $R^{(j)}$ is the transmission rate adopted in the jth transmission period without the information of channel realization, which is a random variable (e.g. $R^{(j)} = R_i$ with probability $\pi_i,\ i = 1, 2, \cdots, N$). T_j is the jth SU transmission period and $R^{(L)}$ is the transmission rate used in the last transmission period. Meanwhile, $\mathbb{T}_{\mathrm{tr},L}$ depends on the data amount and secondary channel realization. Specifically, $\mathbb{T}_{\mathrm{tr},L}$ is a sequence of $L-1$ intact transmission periods plus one partial transmission period, since secondary transmission may stop anywhere within the last transmission period depending on H_t and data transmitted over previous $L-1$ transmission periods. Hence, we obtain

$$\begin{aligned} \mathbb{T}_{\mathrm{tr},L} &= \sum_{j=1}^{L-1} T_j + \frac{H_t - \mathbb{H}_{L-1}}{R^{(L)}} \\ &= \mathbb{T}_{L-1} + \frac{H_t - \mathbb{H}_{L-1}}{R^{(L)}} \leq \mathbb{T}_{L}, \end{aligned} \tag{3.4}$$

where $\mathbb{T}_{L-1} = \sum_{j=1}^{L-1} T_j$ represents the total length of $L-1$ transmission periods. Similarly, $\mathbb{T}_{\mathrm{w},L}$ can be mathematically expressed as

$$\mathbb{T}_{\mathrm{w},L} = \sum_{l=1}^{L} W_l, \tag{3.5}$$

where W_l represents the length of the lth waiting slot. After proper substitution, we can rewrite the CDF of SU data transmission time as

$$F^C_{T_{\mathrm{ED}}|\mathrm{on}}(t) = \sum_L \Pr\left[\sum_{j=1}^{L-1} T_j + \sum_{l=1}^{L} W_l + \frac{H_t - \sum_{j=1}^{L-1} R^{(j)} T_j}{R^{(L)}} \le t;\ \sum_{j=1}^{L-1} R^{(j)} T_j \le H_t;\ \sum_{j=1}^{L-1} R^{(j)} T_j + R^{(L)} T_L \ge H_t\right]. \tag{3.6}$$

To simplify the representation, let $F^C_{T_{\mathrm{ED}},L|\mathrm{on}}(t)$ denote the probability that $\Pr\big[\sum_{j=1}^{L-1} T_j + \sum_{l=1}^{L} W_l + \frac{H_t - \sum_{j=1}^{L-1} R^{(j)} T_j}{R^{(L)}} \le t;\ \sum_{j=1}^{L-1} R^{(j)} T_j \le H_t;\ \sum_{j=1}^{L-1} R^{(j)} T_j + R^{(L)} T_L \ge H_t\big]$. With AMC, if the received SNR of the secondary link, denoted by γ_{SU}, falls in region A_i over the jth transmission period, then rate R_i is used. The secondary transmission with adaptive modulation is revealed in Fig. 3.3. Suppose that packet transmission completes over L transmission periods and γ_{SU} falls into the ith region n_i times over the first $L-1$ transmission periods. Hence, rate R_i is used n_i times $i = 1, 2, \cdots, N$. Here, let us define the vector $\overrightarrow{\mathbf{n}} = [n_1, ..., n_N]$, where $\sum_{i=1}^{N} n_i = L-1$. $\mathbb{H}_{L-1}$, given a certain channel realization represented by $\overrightarrow{\mathbf{n}}$, can be rewritten as

$$\mathbb{H}_{L-1|\overrightarrow{\mathbf{n}}} = \sum_{j=1}^{L-1} R^{(j)} T_j = \sum_{i=1}^{N} R_i \left(\sum_{d=1}^{n_i} T_d\right). \tag{3.7}$$

Note that, R_j is the rate used in the jth transmission period provided channel realization, which is considered constant. Therefore, $\mathbb{H}_{L-1|\overrightarrow{\mathbf{n}}}$ is the summation of $L-1$ independent but not necessarily identical exponential random variables. Furthermore, if γ_{SU} falls into region A_k over the last transmission period, then R_k is used (i.e. $R^{(L)} = R_k$). By conditioning on the channel realization of the L SU transmission periods, $F^C_{T_{\mathrm{ED}},L|\mathrm{on}}(t)$ can be rewritten as

$$F^C_{T_{\mathrm{ED}},L|\mathrm{on}}(t) = \sum_{\overrightarrow{\mathbf{n}}} \sum_{k=1}^{N} \Pr\left[\sum_{j=1}^{L-1} T_j + \sum_{l=1}^{L} W_l + \frac{H_t - \mathbb{H}_{L-1|\overrightarrow{\mathbf{n}}}}{R_k} \le t;\ \mathbb{H}_{L-1|\overrightarrow{\mathbf{n}}} \le H_t;\ \mathbb{H}_{L-1|\overrightarrow{\mathbf{n}}} + R_k T_L \ge H_t\right] \times \Pr\left[\bigcup_{i=1}^{N} (\gamma_{\mathrm{SU}} \in A_i)^{n_i};\ \gamma_{\mathrm{SU}} \in A_k\right] \tag{3.8}$$

where $\sum_{\overrightarrow{\mathbf{n}}}$ represents the summation of all the possible combinations of n_i's satisfying $\sum_{i=1}^{N} n_i = L-1$, $\big[\bigcup_{i=1}^{N} (\gamma_{\mathrm{SU}} \in A_i)^{n_i}\ , \gamma_{\mathrm{SU}} \in A_k\big]$ denotes the event that the received

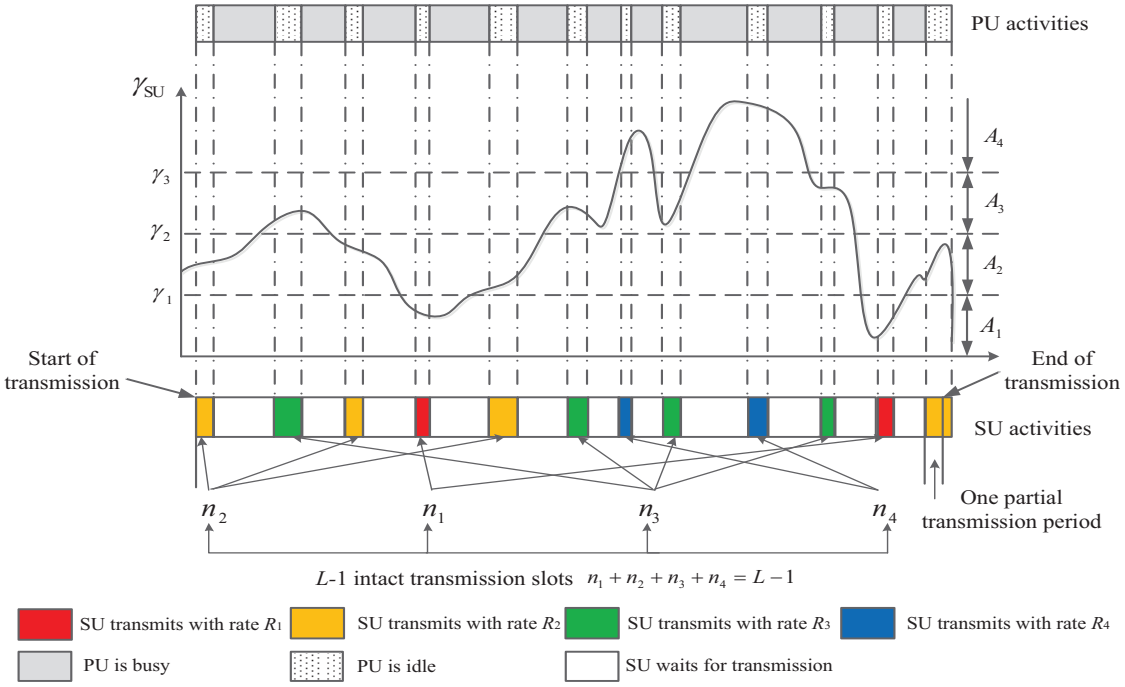

Figure 3.3: SU transmission with four-state AMC under continuous sensing strategy.

SNR of secondary channel falls into region A_i totally n_i times, $i = 1, 2, \cdots N$, over the first $L-1$ periods and region A_k in the last transmission period. Note that, due to the existence of waiting period, the duration of transmission periods is modeled by independent, not necessarily identical exponential random variables. After applying multinomial distribution with the independent fading assumption, we can show that

$$\Pr\left[\bigcup_{i=1}^{N}(\gamma_{\mathrm{SU}} \in A_i)^{n_i},\ \gamma_{\mathrm{SU}} \in A_k\right] = \pi_k \binom{L-1}{n_1, ..., n_N} \prod_{i=1}^{N} \pi_i^{n_i}. \tag{3.9}$$

Thus, $F^C_{T_{\mathrm{ED}}|\mathrm{on}}(t)$ can be expressed as

$$F^C_{T_{\mathrm{ED}}|\mathrm{on}}(t) = \sum_{L} F^C_{T_{\mathrm{ED}},L|\mathrm{on}}(t) = \sum_{L}\sum_{k=1}^{N}\sum_{\vec{\mathbf{n}}} F^C_{T_{\mathrm{ED}},L|\vec{\mathbf{n}},k,\mathrm{on}}(t) \times \pi_k \binom{L-1}{n_1, ..., n_N} \prod_{i=1}^{N} \pi_i^{n_i}, \tag{3.10}$$

where $F^C_{T_{\mathrm{ED}},L|\vec{\mathbf{n}},k,\mathrm{on}}(t)$ denotes the joint probability that $\Pr\left[\sum_{j=1}^{L-1} T_j + \sum_{l=1}^{L} W_l + \frac{H_t - \mathbb{H}_{L-1|\vec{\mathbf{n}}}}{R_k} \leq t;\ \mathbb{H}_{L-1|\vec{\mathbf{n}}} \leq H_t;\ \mathbb{H}_{L-1|\vec{\mathbf{n}}} + R_k T_L \geq H_t\right]$. The corresponding PDF,

$f^C_{T_{\rm ED}|{\rm on}}(t)$, is given by

$$f^C_{T_{\rm ED}|{\rm on}}(t) = \frac{dF^C_{T_{\rm ED}|{\rm on}}(t)}{dt} = \sum_L \sum_{k=1}^{N} \sum_{\vec{\mathbf{n}}} f^C_{T_{\rm ED},L|\vec{\mathbf{n}},k,{\rm on}}(t) \times \pi_k \binom{L-1}{n_1,...,n_N} \prod_{i=1}^{N} \pi_i^{n_i}, \quad (3.11)$$

where $f^C_{T_{\rm ED},L|\vec{\mathbf{n}},k,{\rm on}}(t) = \frac{dF^C_{T_{\rm ED},L|\vec{\mathbf{n}},k,{\rm on}}(t)}{dt}$.

Note the difficulties obtaining the exact solution of $F^C_{T_{\rm ED},L|\vec{\mathbf{n}},k,{\rm on}}(t)$, assuming that multiple secondary transmission slots are needed to complete transmission, we apply the central limit theory to approximate the time duration required and data transmitted by two jointly Gaussian random variables as $\mathcal{X}_{L|{\rm on}} = \sum_{j=1}^{L-1} T_j + \sum_{l=1}^{L} W_l$; $\mathcal{Y}_{L|\vec{\mathbf{n}},{\rm on}} = \sum_{j=1}^{L-1} R_j T_j$. Then, $\mathcal{X}_{L|{\rm on}}$ and $\mathcal{Y}_{L|\vec{\mathbf{n}},{\rm on}}$ are jointly Gaussian distributed whose first and second order moments are $\eta_x = (L-1)\mu + L\lambda$, ${\sigma_x}^2 = (L-1)\mu^2 + L\lambda^2$, $\eta_y = \mu \sum_{i=1}^{N} n_i R_i$ and ${\sigma_y}^2 = \mu^2 \sum_{i=1}^{N} n_i R_i^2$. The correlate coefficient, denoted by ρ, can be calculated as (See Appendix A)

$$\rho = \frac{\mu^2 \sum_{i=1}^{N} n_i R_i}{\sqrt{(L-1)\mu^2 + L\lambda^2} \sqrt{\mu^2 \sum_{i=1}^{N} n_i R_i^2}}. \quad (3.12)$$

Then $F^C_{T_{\rm ED},L|\vec{\mathbf{n}},k,{\rm on}}(t)$ can be rewritten as

$$F^C_{T_{\rm ED},L|\vec{\mathbf{n}},k,{\rm on}}(t) = \Pr\left[\mathcal{X}^{on}_L \le t - \frac{H_t - \mathcal{Y}^{on}_{L|\vec{\mathbf{n}}}}{R_k};\ 0 \le \mathcal{Y}^{on}_{L|\vec{\mathbf{n}}} \le H_t;\ T_L \ge \frac{H_t - \mathcal{Y}^{on}_{L|\vec{\mathbf{n}}}}{R_k}\right], \quad (3.13)$$

where we restrict the data transmitted to be non-negative.

Consequently, conditioning on the independent random variable T_L, the conditional PDF $f^{on}_{T_{\rm ED}|L,\vec{\mathbf{n}}}(t)$ can be calculated as

$$\begin{aligned} f^C_{T_{\rm ED},L|\vec{\mathbf{n}},k,{\rm on}}(t) &= \frac{dF^C_{T_{\rm ED},L|\vec{\mathbf{n}},k,{\rm on}}(t)}{dt} \\ &= \int_0^{H_t} f_{\mathcal{X}_{L|{\rm on}},\mathcal{Y}_{L|\vec{\mathbf{n}},{\rm on}}}\left(t - \frac{H_t - y}{R_k}, y\right) f_{T_L}\left(-\frac{H_t - y}{\mu R_k}\right) dy, \end{aligned} \quad (3.14)$$

where $f_{\mathcal{X}_{L|{\rm on}},\mathcal{Y}_{L|\vec{\mathbf{n}},{\rm on}}}(\cdot,\cdot)$ is the PDF of two jointly Gaussian random variables. With

the help of [35], the conditional PDF is given by

$$f^{C}_{T_{\mathrm{ED}},L|\vec{\mathbf{n}},k,\mathrm{on}}(t) = \frac{\exp\left(-\frac{H_t}{R_k}\right)\exp\left(-\frac{(t-\frac{H_t}{R_k}-\eta_x)^2{\sigma_y}^2+2\rho\eta_y\sigma_x\sigma_y(t-\frac{H_t}{R_k}-\eta_x)+{\sigma_x}^2{\eta_y}^2}{2(1-\rho^2){\sigma_x}^2{\sigma_y}^2}\right)}{4\pi\sigma_x\sigma_y\sqrt{1-\rho^2}}$$
$$\times\sqrt{\frac{2\pi(1-\rho^2){\sigma_x}^2{\sigma_y}^2}{\left(\frac{{\sigma_y}^2}{R_k^2}-2\rho\frac{\sigma_x\sigma_y}{R_k}+{\sigma_x}^2\right)}}$$
$$\times\exp\left(\frac{\left(\frac{(t-\frac{H_t}{R_k}-\eta_x){\sigma_y}^2+\rho\eta_y\sigma_x\sigma_y}{R_k}-\frac{(1-\rho^2){\sigma_x}^2{\sigma_y}^2}{R_k\mu}-\rho\sigma_x\sigma_y(t-\frac{H_t}{R_k}-\eta_x)-{\sigma_x}^2\eta_y\right)^2}{\left(\frac{{\sigma_y}^2}{R_k^2}-2\rho\frac{\sigma_x\sigma_y}{R_k}+{\sigma_x}^2\right)2(1-\rho^2){\sigma_x}^2{\sigma_y}^2}\right)$$
$$\times\left\{\mathrm{erf}\left[\frac{\left(\frac{(t-\frac{H_t}{R_k}-\eta_x){\sigma_y}^2+\rho\eta_y\sigma_x\sigma_y}{R_k}-\frac{(1-\rho^2){\sigma_x}^2{\sigma_y}^2}{R_k\mu}-\rho\sigma_x\sigma_y(t-\frac{H_t}{R_k}-\eta_x)-{\sigma_x}^2\eta_y\right)}{\sqrt{\left(\frac{{\sigma_y}^2}{R_k^2}-2\rho\frac{\sigma_x\sigma_y}{R_k}+{\sigma_x}^2\right)2(1-\rho^2){\sigma_x}^2{\sigma_y}^2}}\right.\right.$$
$$\left.\left.+\sqrt{\frac{2(1-\rho^2){\sigma_x}^2{\sigma_y}^2}{\left(\frac{{\sigma_y}^2}{R_k^2}-2\rho\frac{\sigma_x\sigma_y}{R_k}+{\sigma_x}^2\right)}}H_t\right]\right.$$
$$\left.-\mathrm{erf}\left(\frac{\left(\frac{(t-\frac{H_t}{R_k}-\eta_x){\sigma_y}^2+\rho\eta_y\sigma_x\sigma_y}{R_k}-\frac{(1-\rho^2){\sigma_x}^2{\sigma_y}^2}{R_k\mu}-\rho\sigma_x\sigma_y(t-\frac{H_t}{R_k}-\eta_x)-{\sigma_x}^2\eta_y\right)}{\sqrt{\left(\frac{{\sigma_y}^2}{R_k^2}-2\rho\frac{\sigma_x\sigma_y}{R_k}+{\sigma_x}^2\right)2(1-\rho^2){\sigma_x}^2{\sigma_y}^2}}\right)\right\}, \tag{3.15}$$

where erf[·] is the Gaussian error function.

When PU is off at the instant of packet arrival, the only difference here is that total waiting time has one less waiting slot as illustrated in Fig. 3.2. One can directly obtain $f^{C}_{T_{\mathrm{ED}},L|\vec{\mathbf{n}},k,\mathrm{off}}(t)$ by replacing η_x, ${\sigma_x}^2$ and ρ in Eq. (3.15) accordingly. The PDF

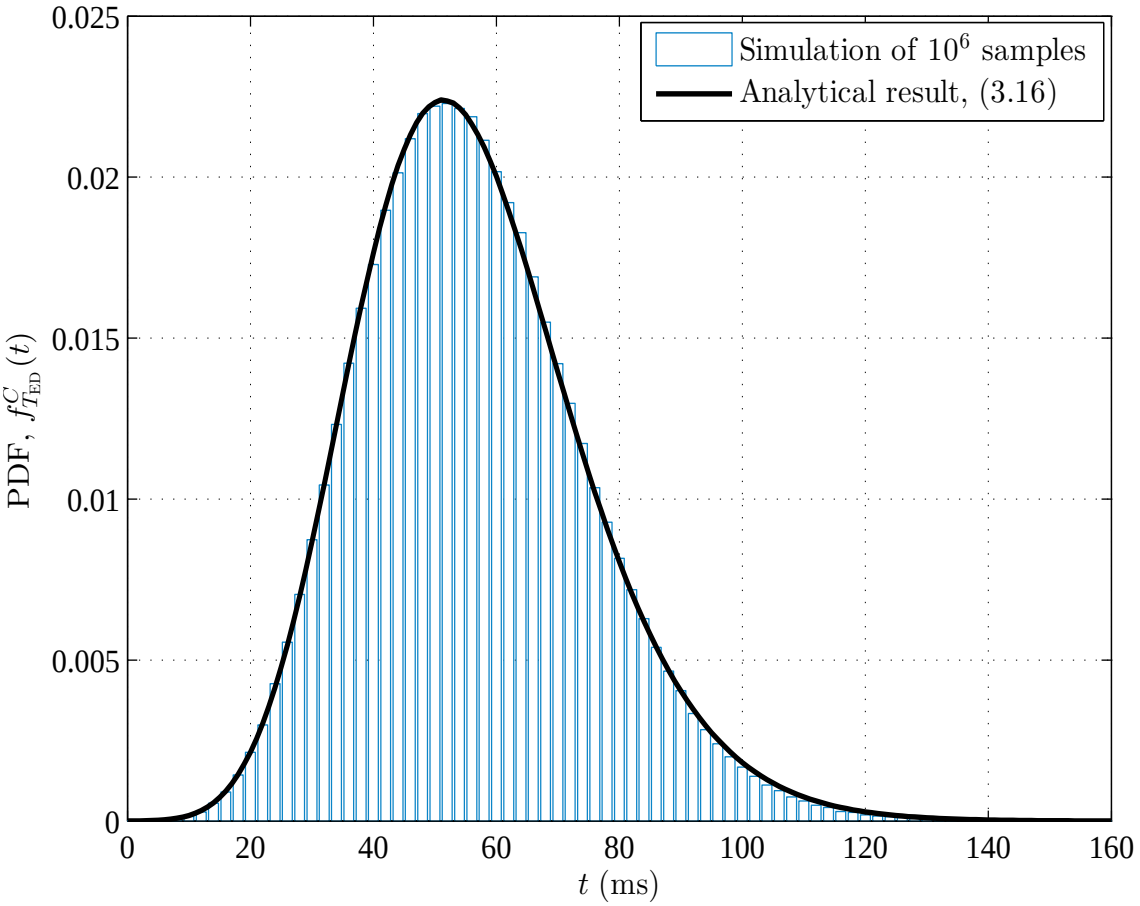

Figure 3.4: Monte Carlo simulation verification for the analytical PDF of EDT with continuous sensing ($H_t = 30$ kb, $\bar{\gamma} = 15$ dB, $\mu = 1$ ms, $\lambda = 3$ ms).

of EDT for secondary packet transmission with AM is finally obtained as

$$f^C_{T_{\rm ED}}(t) = \sum_{L} \sum_{\vec{\mathbf{n}}} \sum_{k=1}^{N} \left(\frac{\lambda}{\lambda+\mu} f^C_{T_{\rm ED},L|\vec{\mathbf{n}},k,\rm on}(t) + \frac{\mu}{\lambda+\mu} f^C_{T_{\rm ED},L|\vec{\mathbf{n}},k,\rm off}(t) \right) \times \pi_k \binom{L-1}{n_1,...,n_N} \prod_{i=1}^{N} \pi_i^{n_i}. \tag{3.16}$$

We then present selected numerical results to verify and illustrate our analytical solutions. We assume that the secondary system adopts an AMC system with transmission rates $[R_1,\ R_2,\ R_3,\ R_4] = [1,\ 2,\ 3,\ 4]$ bits/symbol, corresponding to BPSK, QPSK, 8PSK and 16QAM modulation schemes, respectively. The symbol period is

1μs. We also assume that the channel gain of secondary link follows Rayleigh distribution. As such, SU received SNR follows exponential distribution with average $\bar{\gamma}$, (i.e. $\gamma_{\mathrm{SU}} \sim \mathrm{Exp}(\bar{\gamma})$). Identical AMC implementation is applied throughout the whole chapter.

Fig. 3.4 compares the analytical results for the PDF of EDT for SU packet transmission with those obtained by Monte Carlo simulation, where a cognitive radio system is simulated with randomly generated PU on/off duration decided by parameter μ and λ. The simulation and the analytical results match well, which validates our analytical approach for moderate value of L. In fact, the EDT of SU transmission greatly depends on PU activity and transmission slots required. Fig. 3.5(a) reveals the PDF of T_{ED} with different packet size H_t and secondary link quality $\bar{\gamma}$. Intuitively, as H_t increases, more transmission slots are required, thus, both average value and variance of T_{ED} increase. Higher order modulation and coding schemes are used more frequently for larger $\bar{\gamma}$, which results in shorter T_{ED}. As shown in Fig 3.5(b), for large value of λ, SU wastes more time in waiting for transmission. For large value of μ, SU can access the channel for longer duration, resulting in shorter EDT.

3.3.2 Semi-periodic Spectrum Sensing

With semi-periodic spectrum sensing, SU continuously monitors the PU channel while transmitting and periodically senses for transmission availability with constant period T_s. Therefore, T_{ED} is the summation of a continuous random variable T_{tr} and discrete random variable T_{w}. Noting that, total waiting time T_{w} depends on total transmission time T_{tr}, the PDF of T_{ED} can be obtained by taking the distribution of T_{w} into account while conditioning on the distribution of T_{tr}. Hence, the PDF of EDT with semi-periodic spectrum sensing, denoted by $f^{P}_{T_{\mathrm{ED}}}(t)$ can be calculated by

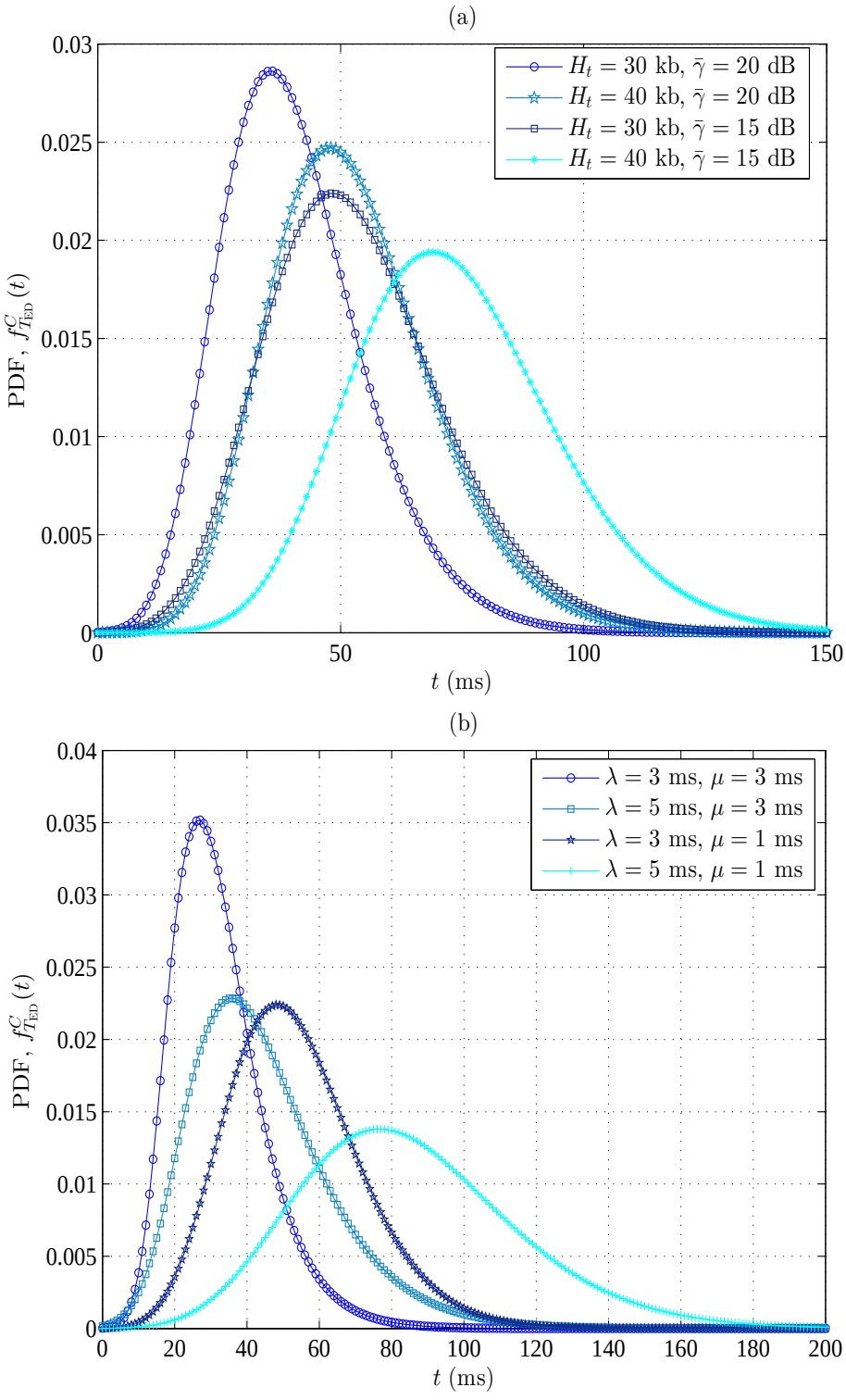

Figure 3.5: Distribution of EDT for secondary transmission under continuous sensing with various secondary data amount, secondary link quality and PU parameters.

conditioning on the transmission time as

$$
\begin{aligned}
& f_{T_{\mathrm{ED}}}^{P}(t) \\
&= \sum_{L} f_{T_{\mathrm{ED},L}}^{P}(t) \\
&= \sum_{L} \sum_{m=1}^{\infty} f_{T_{\mathrm{ED},L}}^{P}(t|T_{\mathrm{w},L} = mT_s) \Pr\left[T_{\mathrm{w},L} = mT_s\right] \\
&= \sum_{L} \sum_{m=1}^{\infty} f_{T_{\mathrm{tr},L}}^{M}(t - mT_s) \Pr\left[T_{\mathrm{w},L} = mT_s\right] \\
&= \sum_{L} \sum_{m=1}^{\infty} \left[\sum_{k=1}^{N} \sum_{\vec{\mathbf{n}}} \pi_k \binom{L-1}{n_1, ..., n_N} \prod_{i=1}^{N} \pi_i^{n_i} f_{T_{\mathrm{tr},L|\vec{\mathbf{n}},k}}^{M}(t - mT_s) \right] \Pr\left[T_{\mathrm{w},L} = mT_s\right],
\end{aligned}
\tag{3.17}
$$

where $f_{T_{\mathrm{tr},L|\vec{\mathbf{n}},k}}^{M}(t)$ is given by Eq. (2.44). $\Pr\left[T_{\mathrm{w},L} = mT_s\right]$ denotes the probability that $T_{\mathrm{w},L}$ is equal to m sensing periods. Specifically, the probability mass function (PMF) of $T_{\mathrm{w},L}$ depends on whether the primary user is transmitting or not at the start of secondary transmission. The number of sensing periods in $T_{\mathrm{w},L}$ when PU is off is one less than those when PU is on. Conditioning on that PU is on and off at the start of secondary transmission, we can calculate $\Pr\left[T_{\mathrm{w},L} = mT_s\right]$ as

$$
\Pr\left[T_{\mathrm{w},L} = mT_s\right] = \frac{\lambda}{\lambda + \mu} \Pr\left[T_{\mathrm{w},L|\mathrm{on}} = mT_s\right] + \frac{\mu}{\lambda + \mu} \Pr\left[T_{\mathrm{w},L|\mathrm{off}} = mT_s\right], \tag{3.18}
$$

where $T_{\mathrm{w},L|\mathrm{on}}$ and $T_{\mathrm{w},L|\mathrm{off}}$ denote the total waiting time given that PU is on or off at the start of secondary transmission, respectively. $\Pr\left[T_{\mathrm{w},L|\mathrm{on}} = mT_s\right]$ is actually the probability that it takes m sensing periods to find out exactly L times that PU is off. Applying the result of negative binomial distribution, we can compute $\Pr\left[T_{\mathrm{w},L|\mathrm{on}} = mT_s\right]$ as

$$
\Pr\left[T_{\mathrm{w},L|\mathrm{on}} = mT_s\right] = \binom{m-1}{L-1} (1 - \beta_{\mathrm{on}})^{L} \beta_{\mathrm{on}}^{m-L}, \tag{3.19}
$$

where β_{on} is the probability that provided PU was on at the previous sensing instant, PU is also on at current sensing instant. While PU is modelled by a continuous-time Markov chain with transition rate μ and λ, β_{on} does not equal to the stationary probability that PU on. The reason is that SU will sense the channel again at current

instant only after the channel is sensed busy at the previous sensing instant. Hence, β_{on} is calculated as the probability that given PU was on at certain point in time, the PU is again on after a time interval T_s. Note that there is a chance that PU turns off and then turns back to on between two sensing instants. According to the property of two-state-continuous-time Markov chain model for PU, β_{on} can be calculated as [67]

$$\beta_{\text{on}} = \frac{\lambda}{\lambda+\mu} + \frac{\mu}{\lambda+\mu} e^{\left(-\frac{\mu+\lambda}{\mu\lambda} T_s\right)}. \tag{3.20}$$

Similarly, in case of PU is off at the instant of packet arrival, the number of waiting periods is one less than the number of transmission periods. Thus, we can compute $\Pr\left[T_{\text{w},L|\text{off}} = mT_s\right]$ as

$$\Pr\left[T_{\text{w},L|\text{off}} = mT_s\right] = \binom{m-1}{L-2} (1-\beta_{\text{on}})^{L-1} \beta_{\text{on}}^{m-L+1}. \tag{3.21}$$

After substituting Eq. (3.18) into Eq. (3.17) and several carrying out manipulations, the PDF of EDT for secondary transmission with AMC and semi-periodic spectrum sensing strategy under interweave cognitive radio implementation is obtained as

$$\begin{aligned} f_{T_{\text{ED}}}^{P}(t) = & \sum_{L} \sum_{\vec{\mathbf{n}}} \sum_{k=1}^{N} \left[\pi_k \binom{L-1}{n_1, ..., n_N} \prod_{i=1}^{N} \pi_i^{n_i} \sum_{m=1}^{\infty} f_{T_{\text{tr}},L|\vec{n},k}^{M}(t - mT_s) \right] \\ & \times \left[\frac{\lambda}{\lambda+\mu} \binom{m-1}{L-1} (1-\beta_{\text{on}})^{L} \beta_{\text{on}}^{m-L} + \frac{\mu}{\lambda+\mu} \binom{m-1}{L-2} (1-\beta_{\text{on}})^{L-1} \beta_{\text{on}}^{m-L+1} \right]. \end{aligned} \tag{3.22}$$

Fig. 3.6 compares the analytical results for the PDF of EDT for secondary data transmission with those obtained by Monte Carlo simulation, where a cognitive radio system is simulated with randomly generated PU on/off duration decided by parameter μ and λ. We observe that when L_{ave} is large, the simulation and the analytical results match well, which validates our analytical approach. When the parameters H_t, $\bar{\gamma}$ and μ lead to small L_{ave}, the secondary packet transmission completes in a few periods, resulting in inaccurate analytical PDF of T_{tr}, as shown in Fig. 3.6 (b).

Fig. 3.7(a) plots the PDF of EDT for SU transmission with various parameters for PU activities. As we can see, increasing λ causes the mass of the PDF move to the right, which implies larger T_{ED} on average, since larger λ leads to longer waiting

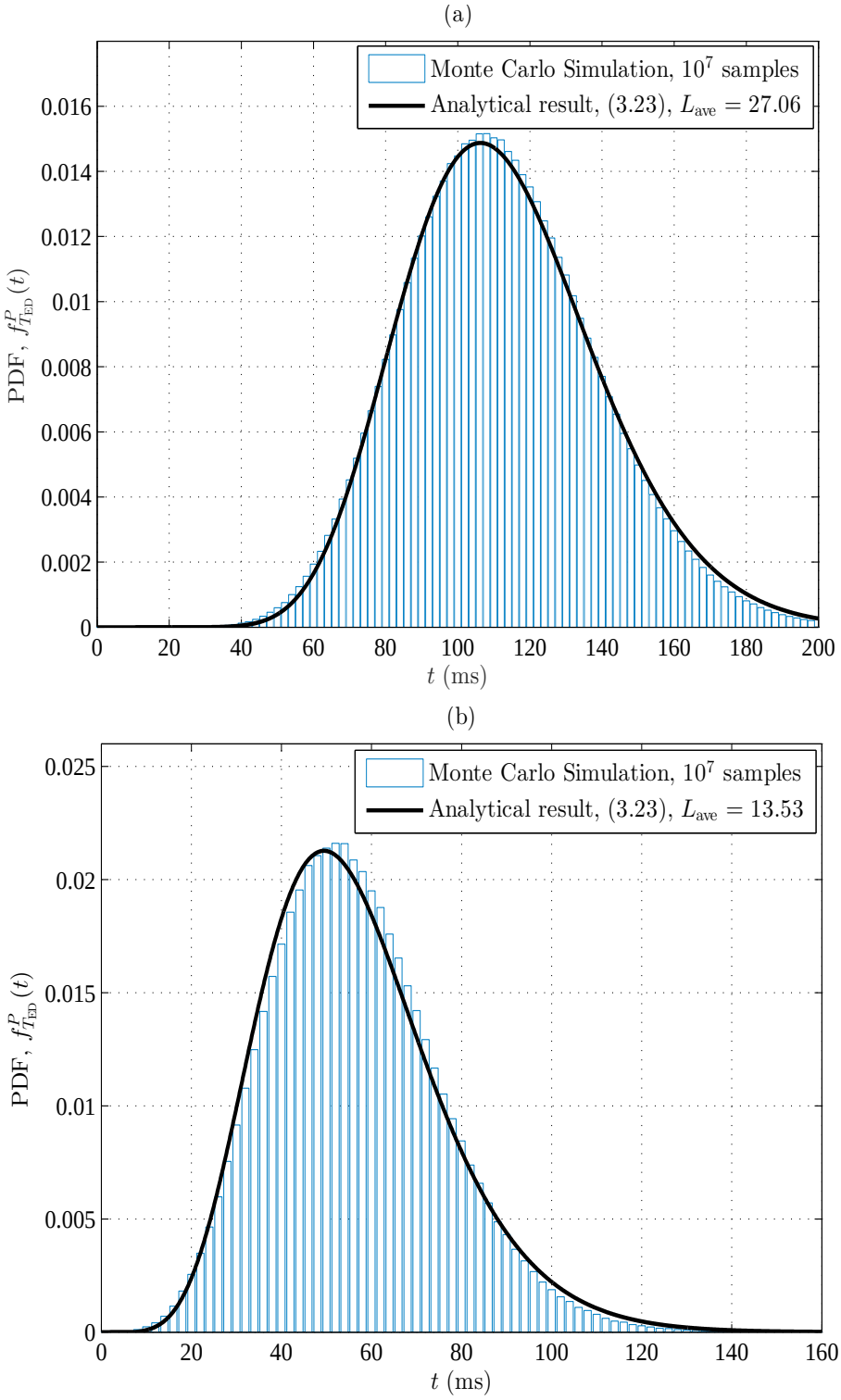

Figure 3.6: Monte Carlo simulation verification for the analytical PDF of EDT with periodic sensing,given by Eq. (3.22), where $\lambda = 3$ ms, $\mu = 1$ ms, $\bar{\gamma} = 15$ dB, $T_s = 0.1$ ms, $H_t = 60$ kb in (a) and $H_t = 30$ kb in (b), respectively.

time. On the other hand, larger μ helps reduce the T_{ED} as SU transmission period becomes longer on average. The PDF of T_{ED} with various H_t and $\bar{\gamma}$ is revealed in Fig. 3.7(b). It can be clearly seen that as secondary channel condition becomes better, the EDT reduced. This is because there are more chances that modulation and coding schemes with higher rates are used, resulting in fewer transmission periods. As H_t increases, both average value and variance of T_{ED} increase. In fact, for larger H_t, the average value and variance of both T_{tr} and T_{w} increase as more SU transmission periods are required to complete secondary data transmission. Fig. 3.7(c) shows the packet delivery time with periodic sensing for various sensing period T_s. It is interesting to observe that the expectation and variance of T_{ED} decreases as T_s gets smaller. This is because that smaller T_s helps reduce the time lag that PU has vacated the channel already, but SU has not sensed the channel yet. Note that T_s only effects the waiting time. Mathematically, for each L, the expectation and variance of $T_{\mathrm{w}|L}$ slightly decrease with decreasing T_s.

3.3.3 One-shot Transmission

In certain cognitive radio application, the data amount can be so small that one SU transmission period is sufficient to complete its transmission. Such data may only contain temperature or humidity measurement, or some other environment index. In this subsection, we derive the PDF of EDT for small amount data transmission. Note that, the transmission time is equal to $\frac{H_t}{R_i}$, where transmission rate R_i depends on secondary channel realization. When PU is off at the instant of transmission initiation, there is no waiting time. The PDF of EDT for one-period transmission with semi-periodic sensing when PU is off can be calculated as

$$f^{P}_{T_{\mathrm{ED}},1|\mathrm{off}}(t) = \sum_{i=1}^{N} \delta\left(t - \frac{H_t}{R_i}\right) \pi_i, \tag{3.23}$$

where $\delta(\cdot)$ is the impulse function. Otherwise, when PU is on at the start of secondary transmission, a sequence of m sensing periods should be included as waiting time. Following similar derivation in previous subsections, we derive the PDF of T_{ED} for

(a)

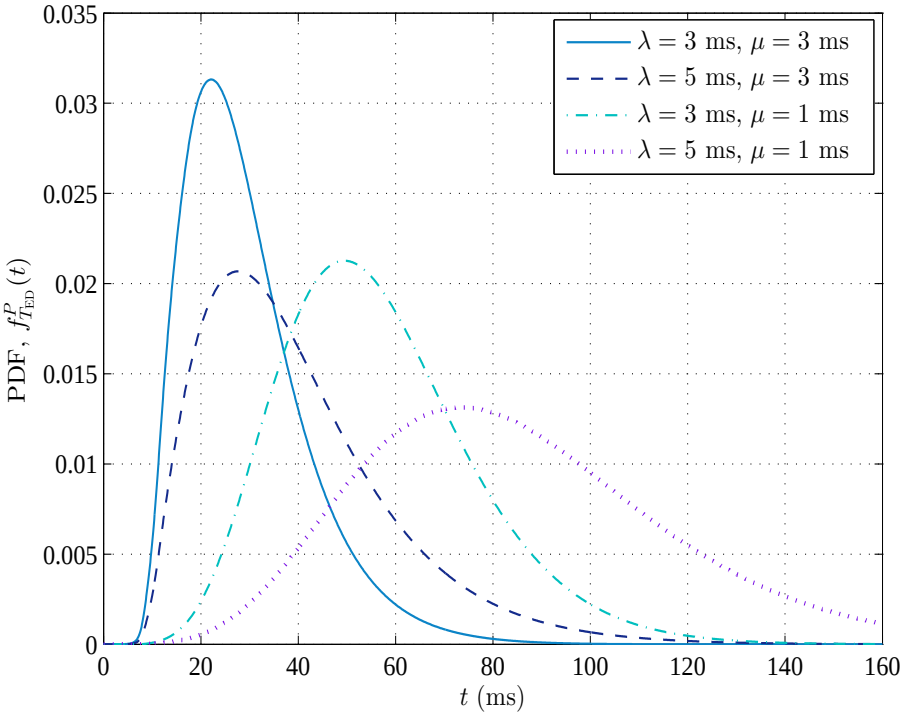
0.035
0.03
0.025
0.02
0.015
0.01
0.005
0
PDF, $f^P_{T_{\rm ED}}(t)$
0
20
40
60
80
100
120
140
160
t (ms)
$\lambda = 3$ ms, $\mu = 3$ ms
$\lambda = 5$ ms, $\mu = 3$ ms
$\lambda = 3$ ms, $\mu = 1$ ms
$\lambda = 5$ ms, $\mu = 1$ ms

(b)

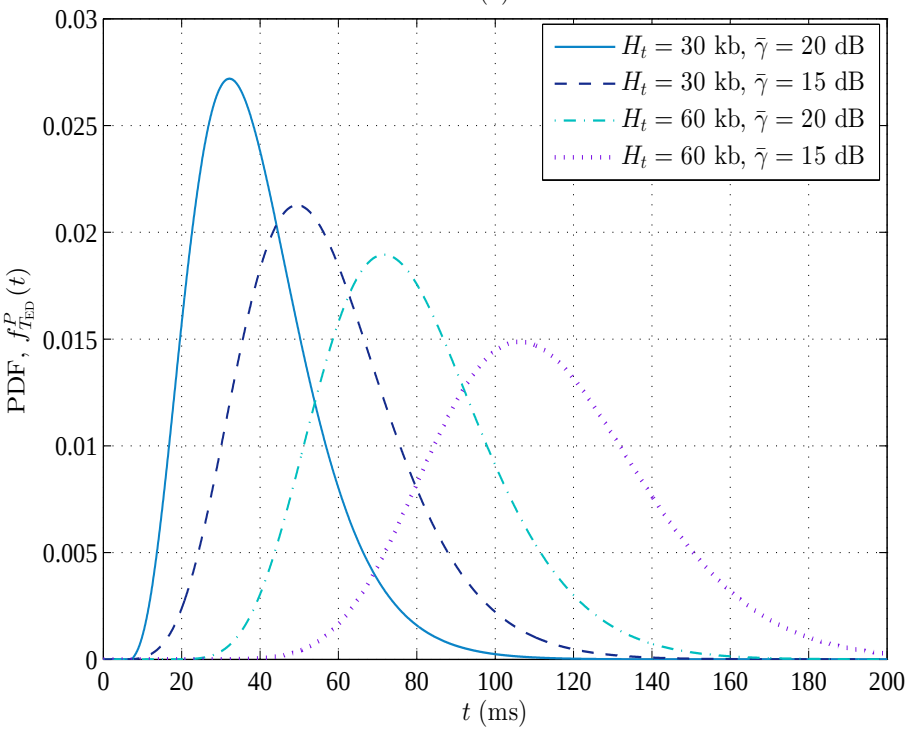
0.03
0.025
0.02
0.015
0.01
0.005
0
PDF, $f^P_{T_{\rm ED}}(t)$
0
20
40
60
80
100
120
140
160
180
200
t (ms)
$H_t = 30$ kb, $\bar{\gamma} = 20$ dB
$H_t = 30$ kb, $\bar{\gamma} = 15$ dB
$H_t = 60$ kb, $\bar{\gamma} = 20$ dB
$H_t = 60$ kb, $\bar{\gamma} = 15$ dB

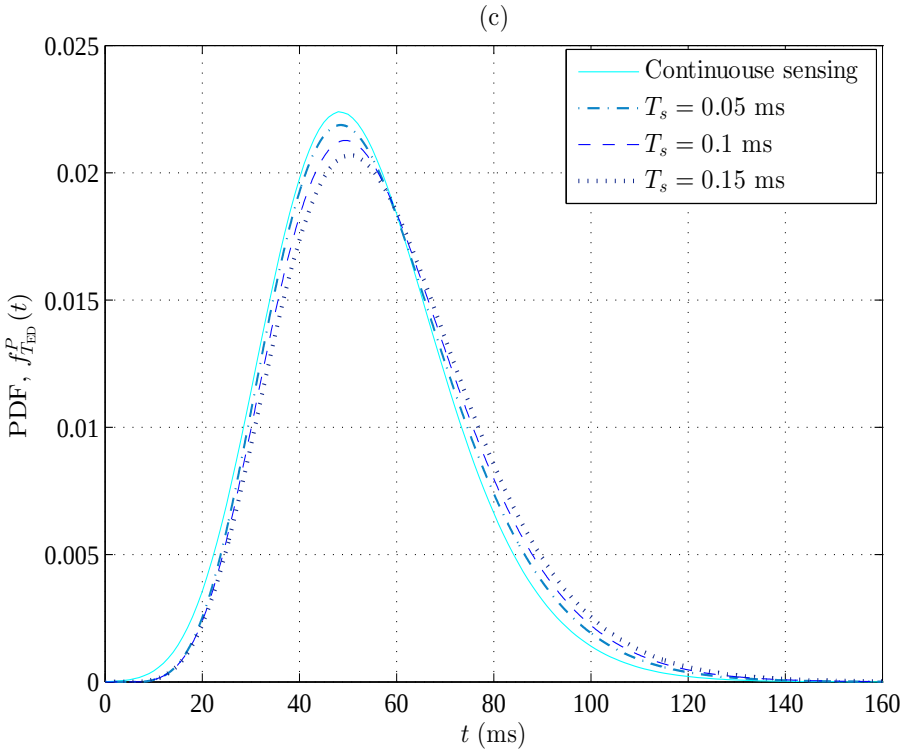

Figure 3.7: PDF of EDT for secondary transmission with semi-periodic sensing for various PU parameters, data amount, secondary link quality and the length of sensing period.

this case as

$$f^P_{T_{\rm ED},1|{\rm on}}(t) = \sum_{i=1}^{N} \left[\sum_{m=1}^{\infty} \delta\left(t - \frac{H_t}{R_i} - mT_s\right) (1-\beta_{\rm on})\beta_{\rm on}^{m-1} \right] \pi_i. \tag{3.24}$$

Thus, the PDF of EDT for one-shot transmission is given by

$$\begin{aligned} f^P_{T_{\rm ED},1}(t) &= \frac{\lambda}{\lambda+\mu} f_{T_{\rm ED},1|{\rm on}}(t) + \frac{\mu}{\lambda+\mu} f_{T_{\rm ED},1|{\rm off}}(t) \\ &= \sum_{i=1}^{N} \left\{ \frac{\lambda}{\lambda+\mu} \left[\sum_{m=1}^{\infty} \delta\left(t - \frac{H_t}{R_i} - mT_s\right) (1-\beta_{\rm on})\beta_{\rm on}^{m-1} \right] + \frac{\mu}{\lambda+\mu} \delta\left(t - \frac{H_t}{R_i}\right) \right\} \pi_i. \end{aligned}$$

Similarly, the PDF of EDT for one shot transmission with continuous sensing can

be calculated as:

$$\begin{aligned} f^{C}_{T_{\mathrm{ED}},1}(t) &= \sum_{i=1}^{N} \left[\frac{\mu}{\lambda+\mu}\delta\left(t-\frac{H_t}{R_i}\right) + \frac{\lambda}{\lambda+\mu} f_W\left(t-\frac{H_t}{R_i}\right)\right]\pi_i \\ &= \sum_{i=1}^{N} \left[\frac{\mu}{\lambda+\mu}\delta\left(t-\frac{H_t}{R_i}\right) + \frac{1}{\lambda+\mu}\exp\left(-\frac{t-\frac{H_t}{R_i}}{\lambda}\right)\mathcal{U}\left(t-\frac{H_t}{R_i}\right)\right]\pi_i \end{aligned} \tag{3.25}$$

where $\mathcal{U}(\cdot)$ represents the unit step function. The PDF of one-shot transmission with semi-periodic sensing when PU is on at the start of secondary transmission is given in Fig. 3.8. The discrete distribution indicates that T_{tr} for one-period transmission is discrete distributed once the corresponding transmission rate is given. In fact, distribution of T_{ED} is actually obtained shifting the distribution of T_{tr} by mT_s, $m = 1, 2, \cdots$ and scaling it by the probability $\Pr[T_{\mathrm{w},1} = mT_s]$. For continuous sensing, the peaks attribute to the application of AMC.

3.4 Concluding Remarks

We propose an analytical framework to evaluate the extended deliver time of secondary data transmission with adaptive modulation and coding in this chapter. The analysis is carried out assuming that SU performs continuous or semi-periodic spectrum sensing strategy with work-preserving transmission. Specifically, for continuous sensing, both transmission time and waiting time are continuous random variables. The approximate PDF of T_{ED} is obtained applying the central limit theorem assuming that service time and data transmitted are jointly Gaussian random variables. For semi-periodic sensing, the approximate PDF packet transmission time T_{tr} for a fixed-amount data transmission is derived by applying the central limit theory. Then conditioning on the distribution of T_{tr}, the PDF of EDT is obtained by taking the discrete distributed waiting time into account.

For certain application with very small data amount, distribution of EDT of one-shot transmission is also derived in this chapter. Monte Carlo simulation and numerical results are also included. Simulation results validate our analytical results. These results will facilitate the design and optimization of secondary systems for diverse target applications, such as deriving throughput bounds [48] or evaluating secondary queuing performance by investigating the first and second order moment of EDT

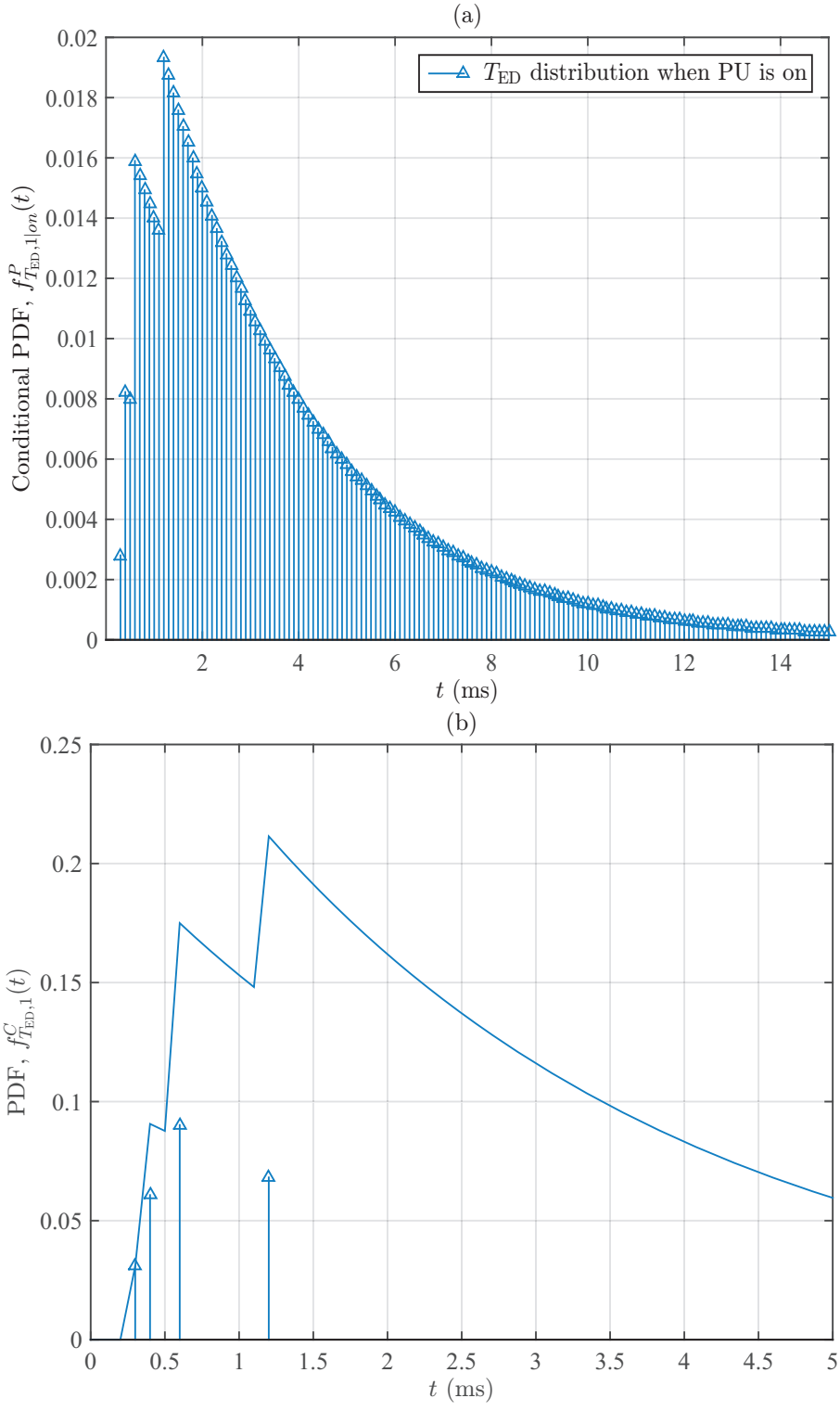

Figure 3.8: PDF of one-shot transmission ($H_t = 1.2$ kb, $\bar{\gamma} = 15$ dB, $\lambda = 3$ ms, $\mu = 1$ ms).

following the same analytical procedure in [3].

Derivation of Correlation Coefficient Defined in Eq. (3.12)

We can calculate the correlate coefficient by calculating the covariance, denoted by $\mathbb{C}_{xy}$, first.

$$\begin{aligned}
&\mathbb{C}_{xy} \\
&= \mathbb{E}\left[\mathcal{X}_L^{on}\mathcal{Y}_{L|\overrightarrow{n}}^{on}\right] - \mathbb{E}\left[\mathcal{X}_L^{on}\right]\mathbb{E}\left[\mathcal{Y}_{L|\overrightarrow{n}}^{on}\right] \\
&= \mathbb{E}\left[\left(\sum_{j=1}^{L-1} T_j\right)\left(\sum_{d=1}^{L-1} R_d T_d\right) + \left(\sum_{l=1}^{L} W_l\right)\left(\sum_{d=1}^{L-1} R_d T_d\right)\right] \\
&\qquad\qquad - \mathbb{E}\left[\sum_{j=1}^{L-1} T_j + \sum_{l=1}^{L} W_l\right]\mathbb{E}\left[\sum_{d=1}^{L-1} R_d T_d\right] \\
&= \mathbb{E}\left[\left(\sum_{j=1}^{L-1} T_j\right)\left(\sum_{d=1}^{L-1} R_d T_d\right)\right] - \mathbb{E}\left[\sum_{j=1}^{L-1} T_j\right]\mathbb{E}\left[\sum_{d=1}^{L-1} R_d T_d\right], \qquad (3.26)
\end{aligned}$$

where $\mathbb{E}[\ \ ]$ denotes the statistical average. The last equality follows $\sum_{l=1}^{L} W_l$ and $\sum_{d=1}^{L-1} R_d T_d$ are independent. Eq. (3.26) can be further simplified into

$$\begin{aligned}
\mathbb{C}_{xy} &= \mathbb{E}\left[\sum_{j=1}^{L-1}\sum_{d=1}^{L-1} R_d T_j T_d\right] - \left(\sum_{j=1}^{L-1}\mathbb{E}[T_j]\right)\left(\sum_{d=1}^{L-1}\mathbb{E}[R_d T_d]\right) \\
&= \sum_{j=1}^{L-1}\sum_{d=1}^{L-1} R_d \mathbb{E}[T_j T_d] - \sum_{j=1}^{L-1}\sum_{d=1}^{L-1} R_d \mathbb{E}[T_j]\mathbb{E}[T_d]. \qquad (3.27)
\end{aligned}$$

When $j \neq d$, we notice that T_j and T_d are independent, leading to $\mathbb{E}[T_j T_d] = \mathbb{E}[T_j]\mathbb{E}[T_d]$. Eq. (4.3.2) can be rewritten as

$$\mathbb{C}_{xy} = \sum_{i=1}^{L-1} R_i \left(\mathbb{E}[T_i^2] - \mathbb{E}^2[T_i]\right) = \mu^2 \sum_{i=1}^{N} n_i R_i. \qquad (3.28)$$

Hence, by definition, the correlation coefficient can be calculated as

$$\rho = \frac{\mathbb{C}_{xy}}{\sigma_x \sigma_y} = \frac{\mu^2 \sum_{i=1}^{N} n_i R_i}{\sqrt{(L-1)\mu^2 + L\lambda^2}\sqrt{\mu^2 \sum_{i=1}^{N} n_i R_i^2}}. \tag{3.29}$$

Chapter 4

Slotted Secondary Transmission with Rate Adaptation under Interweave Cognitive Implementation

4.1 Introduction

In cognitive radio communication, SU is allowed to communicate over the under-utilized licensed frequency bands of primary system with opportunistic spectrum access strategies. Meanwhile, interference caused by secondary transmission must be appropriately controlled so that the PU's communication is not significantly affected. To seek the transmission availability, SU transmitter has to sense PU activity on the target frequency band. Ideally, SU continuously monitors the target spectrum while transmitting and waiting [68]. With perfect continuous monitoring, secondary transmission causes no interference to PU, at the cost of higher energy consumption and implementation complexity. However, it is challenging that SU performs transmission and spectrum sensing simultaneously. As such, SU can also perform spectrum sensing on a periodic basis, which leads to lower complexity and at the same time occasional interference to PU.

In this chapter, we construct Markov models to evaluate SU performance (collision probability, energy consumption, and queuing performance) under perfect/imperfect

spectrum sensing, where SU applies a sense-then-transmit protocol and perform spectrum sensing on a periodic basis. Such slotted secondary transmission leads to lower complexity but, at the same time, occasional collision with PU transmission. Substantial amount of previous work has been carried out in developing practical accessing strategies with various PU and SU models. Assuming that all the primary users and secondary user share the same slotted transmission structure, [44] designs a novel MAC protocol based on optimal and suboptimal spectrum sensing and accessing strategies, where the optimization problem is formulated as a partially observable Markov decision process. [45] proposes optimal and suboptimal access protocol by maximizing the throughput of secondary transmission subject to the collision probability constraint, where the SU adopts slotted transmission coupled with periodic sensing strategy. [69] investigates the average system throughput for a slotted ALOHA based cognitive system. [70] designs a combined channel sensing and access scheme for a cognitive ALOHA network and evaluates the performance based on a five-dimensional Markov model. [71] proposes an optimal sensing order selection strategy for multiple PUs and multiple SUs cognitive radio network, where the proposed sensing strategy converges to the collision free channel sensing order when the number of SUs is less than the number of the channels.

The delay and throughput analysis for secondary transmission is also of considerable current research interests. Assuming SU continuously monitors the spectrum when PU is on and periodically senses while PU is off, [53] investigates the average waiting time and average service time of SU in one transmission period, under general heavy tail and light tail PU traffic models. [54] derives the distribution function of SU service time over a fixed-length time duration. The analytical result is then applied to the average delay evaluation for real-time constant-bit-rate traffic. In [58], a queuing performance analysis is carried out for two-server-single-queue and single-server-two-queue cases, under a Markov PU traffic model. The maximum arrival rate that stabilizes the queue with respect to different service rates and interruption parameters is obtained via a numerical approach. The energy consumption evaluation and energy efficiency analysis are also of great interest. In [72], a stochastic, energy-aware model is proposed to investigate the optimal spectrum sensing interval by exploring the tradeoffs between energy consumption and SU throughput. In [73], the average energy efficiency maximization problem in fading channels is solved as a joint optimization problem of the spectrum sensing duration and the SU transmit

power, where collision might occur due to miss detection.

Spectrum sensing is performed before each transmission period as secondary user transmits with a slotted structure. Thus, sensing error could impact the performance of secondary transmission. The analytical formulations of the throughput of cognitive multi-channel MACs with perfect and imperfect sensing are presented in [74], where a discrete time Markov chain is used to model the number of communicating node pairs in the MAC protocols. The authors in [75] precisely analyzed the effect of imperfect sensing on the stability region of the multi-user cognitive radio system. The condition with sensing errors, for which the identical stability region achieved with perfect sensing, is also presented. The effects of imperfect channel sensing decisions, interference from the primary user, are studied in [76] using a Gaussian mixture model. Joint algorithm for sensing adaptation and opportunistic resource allocation is proposed in [77] to minimize the total expected cost of the throughput loss and utilization of unused frequency bands.

Previous work on queuing performance evaluation concentrate on waiting time analysis while assuming that the packet transmission rate is constant. With adaptive modulation and coding (AMC), the transmission data rate will be adaptively adjusted with the channel condition [62]. The queuing performance with AMC in conventional communication system is studied in [78]. However, with cognitive implementation, the analytical approach is different since SU has to wait for transmission opportunities and SU transmission may fail due to collision. In [60], achievable capacity gain by implementing AMC was analyzed for an underlay cognitive radio system. Assuming transmission completes in one SU transmission period and imperfect spectrum sensing, the bit error rate (BER) performance and spectral efficiency for an interweave cognitive radio system with AMC was investigated in [61]. With continuous spectrum sensing, the statistics of packet service time for SU packet transmission with adaptive modulation is studied in [79]. In this work, we study the queuing performance for slotted secondary transmission with AMC.

In this chapter, we consider a single PU and single SU cognitive communication scenario, where the SU adopts a slotted transmission structure. Collision occurs with periodic spectrum sensing when PU starts transmission, however, SU has not sensed the channel yet. Different from previous works, we focus on collision, delay and throughput analysis of SU with slotted communication protocol. We propose a discrete-time Markov chain to characterize secondary transmission procedure. Steady

state probability is obtained to evaluate collision. We propose a two dimensional Markov model to study the queuing performance for slotted secondary transmission with AMC. We also study the effect of imperfect spectrum sensing on energy efficiency and queuing performance of secondary transmission.

4.2 System Model

We assume that SU opportunistically access a PU channel in an interweave fashion. The PU behaviour on the channel is modeled by a two-state homogeneous continuous-time Markov chain, where state B represents that PU is transmitting (i.e. channel unavailable for secondary transmission) and state I corresponds that PU is not transmitting. Researches on IEEE 802.11 Wireless LAN (WLAN) support a semi-Markov model for various traffic types. As such, Markov model serves as a reasonable approximation [63–65]. The sojourn time in states B and I follow independent non-identical (i.n.d.) exponential distribution with average λ and μ, respectively.

SU employs a slotted transmission strategy as illustrated in Fig. 4.1. SU periodically senses the PU spectrum with a fixed SU period T_{S}. Each T_{S} is divided into two phases, sensing phase T_{I}, and transmission phase T_{II}. SU performs spectrum sensing in the sensing phase and makes transmission decision according to the sensing result. If PU spectrum is sensed busy, SU will wait for T_{II} duration and sense again. Otherwise, SU starts its transmission immediately during the following T_{II}. Here, we assume that T_{S} is sufficiently small compared to λ and μ, and as such, the chance that PU activity changes more than once during one T_{S} is negligible [61, 80, 81]. As such, if the spectrum is sensed busy, the SU waits in the following T_{II}. If the spectrum is sensed free at two consecutive sensing phases, secondary transmission after the first sensing phase has not collided with PU transmission. However, if the spectrum is sensed busy after being sensed free in previous sensing phase, the secondary transmission has interfered with primary transmission.

We also assume that secondary transmission adopts AMC technique. Here, the transmission rate measured in bits/symbol remains unchanged in each T_{II}. However, between different SU periods, the transmission rate can be variant depending on the secondary channel quality. More specifically, the value range of received SNR is divided into $N + 1$ regions each of which corresponds to one possible data rate

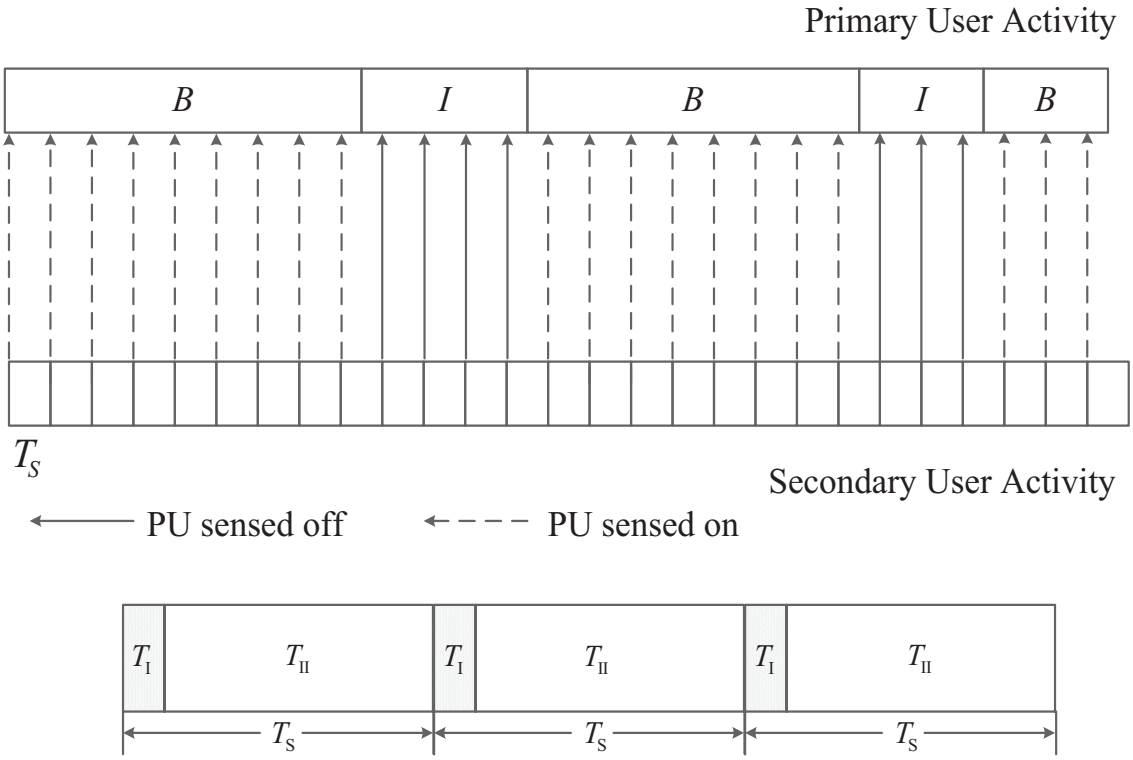

Figure 4.1: Slotted secondary transmission with periodic spectrum sensing strategy and the structure of SU period.

$R_i, i = 0, 1, ..., N$. R_i is selected with probability π_i as discussed in previous chapters.

4.3 Perfect Sensing Result

In this section, assuming perfect spectrum sensing results, we introduce Markov modeling of secondary slotted transmission. Close-form solution of stationary probability is used to investigate the collision probability. The queueing performance for small-size packet transmission with AMC is evaluated by construct a two-dimensional Markov chain with proposed secondary transmission model. The analytical results of EDT for large size packet transmission are also obtained considering both fixed-rate and variable-rate modulation.

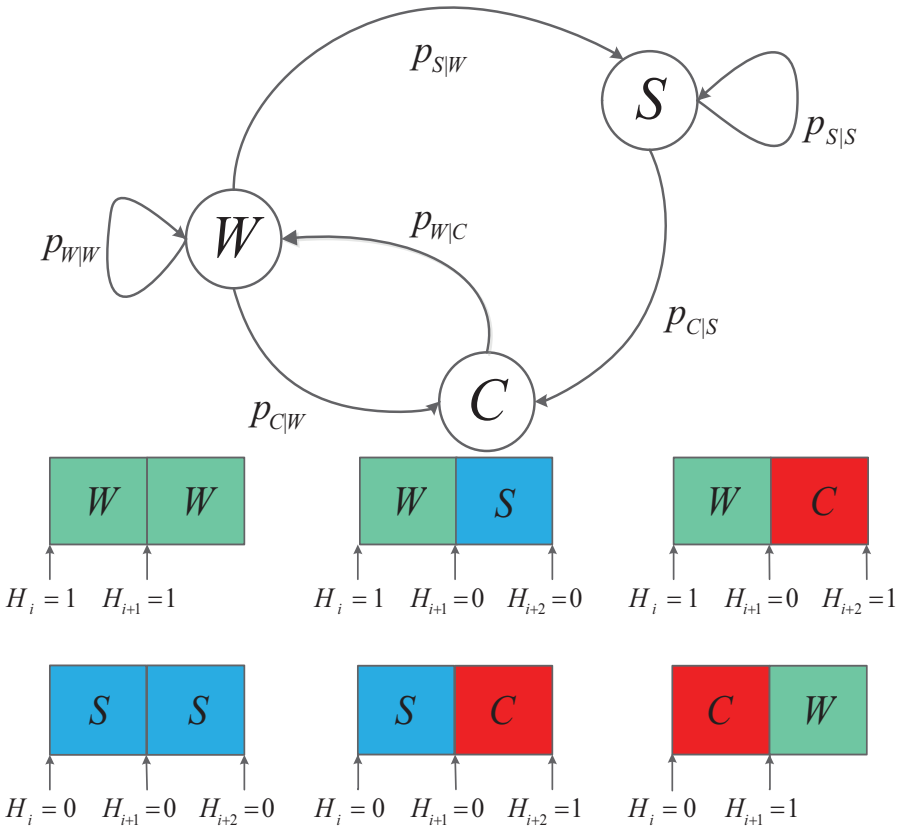

Figure 4.2: Markov modeling of secondary slotted transmission and state transition based on PU activity.

4.3.1 Markov Model for Secondary Transmission

We form a three-state discrete-time Markov chain to characterize SU activity, where state W represents the T_{S} that SU is waiting for transmission, state S that SU transmits without collision and state C that SU transmission collides with PU transmission, over a T_{S}, as illustrated in Fig. 4.2. Let H_i denote the PU activity at the start of ith T_{S}. Assume perfect sensing, we have $H_i = 1$ if PU is on and $H_i = 0$ if PU is off. The transition probability from state W to state S is given by

$$\begin{aligned} p_{S|W} &= \Pr[H_{i+1} = 0,\ H_{i+2} = 0 | H_i = 1] \\ &= \Pr[H_{i+2} = 0 | H_{i+1} = 0] \Pr[H_{i+1} = 0 | H_i = 1] \\ &= \beta_{\mathrm{off}}(1 - \beta_{\mathrm{on}}), \end{aligned} \tag{4.1}$$

where $\beta_{\text{on}} = \Pr[H_i = 1 | H_{i-1} = 1]$ is the probability that PU is sensed on at the sensing instant given PU is also on at previous sensing instant. Accordingly, $\beta_{\text{off}} = \Pr[H_i = 0 | H_{i-1} = 0]$ represents the probability that PU is sensed off given previous sensing result is also off. $\beta_{\text{on}}/\beta_{\text{off}}$ can be calculated as the probability that PU transmission/waiting duration is larger than T_{S} as [67]

$$\beta_{\text{on}} = e^{-\frac{T_{\text{S}}}{\lambda}}, \ \beta_{\text{off}} = e^{-\frac{T_{\text{S}}}{\mu}}, \tag{4.2}$$

respectively[1]. Similarly, the transition probability from state S to state S is calculated as

$$\begin{aligned} p_{S|S} &= \Pr[H_{i+1} = 0, \ H_{i+2} = 0 | H_i = 0, \ H_{i+1} = 0] \\ &= \Pr[H_{i+2} = 0 | H_{i+1} = 0] \\ &= \beta_{\text{off}}. \end{aligned} \tag{4.3}$$

Other transition probabilities can be obtained following similar step. Thus, the transition probability matrix of proposed three-state Markov chain is given by

$$\mathbf{P} = \begin{bmatrix} p_{S|S} & p_{S|W} & p_{S|C} \\ p_{W|S} & p_{W|W} & p_{W|C} \\ p_{C|S} & p_{C|W} & p_{C|C} \end{bmatrix} = \begin{bmatrix} \beta_{\text{off}} & (1-\beta_{\text{on}})\beta_{\text{off}} & 0 \\ 0 & \beta_{\text{on}} & 1 \\ 1-\beta_{\text{off}} & (1-\beta_{\text{on}})(1-\beta_{\text{off}}) & 0 \end{bmatrix}. \tag{4.4}$$

The stationary distribution of the Markov chain can be calculated from the eigenvector of $\mathbf{P}$ corresponding to eigenvalue one, given by

$$[(1-\beta_{\text{on}})\beta_{\text{off}}, \ 1-\beta_{\text{off}}, \ (1-\beta_{\text{on}})(1-\beta_{\text{off}})]. \tag{4.5}$$

After normalization, the stationary distribution of our three-state Markov chain is obtained as

$$[p_S, \ p_W, \ p_C] = \left[\frac{(1-\beta_{\text{on}})\beta_{\text{off}}}{2-\beta_{\text{on}}-\beta_{\text{off}}}, \ \frac{1-\beta_{\text{off}}}{2-\beta_{\text{on}}-\beta_{\text{off}}}, \ \frac{(1-\beta_{\text{on}})(1-\beta_{\text{off}})}{2-\beta_{\text{on}}-\beta_{\text{off}}} \right]. \tag{4.6}$$

[1]With continuous PU model and slotted secondary transmission, the exact expression of β_{off} is $\frac{\mu}{\lambda+\mu} + \frac{\lambda}{\lambda+\mu} e^{-\left(\frac{1}{\lambda}+\frac{1}{\mu}\right)T_{\text{S}}}$ [82]. In our analysis, β_{off} is approximately calculated by Eq. (4.2). When T_{S} is small compared to λ and μ, the approximation error is small. For the typical values we choose in our numerical results ($\lambda = 50$ ms, $\mu = 30$ ms), the error is approximately 0.02 when $T_{\text{S}} = 10$ ms.

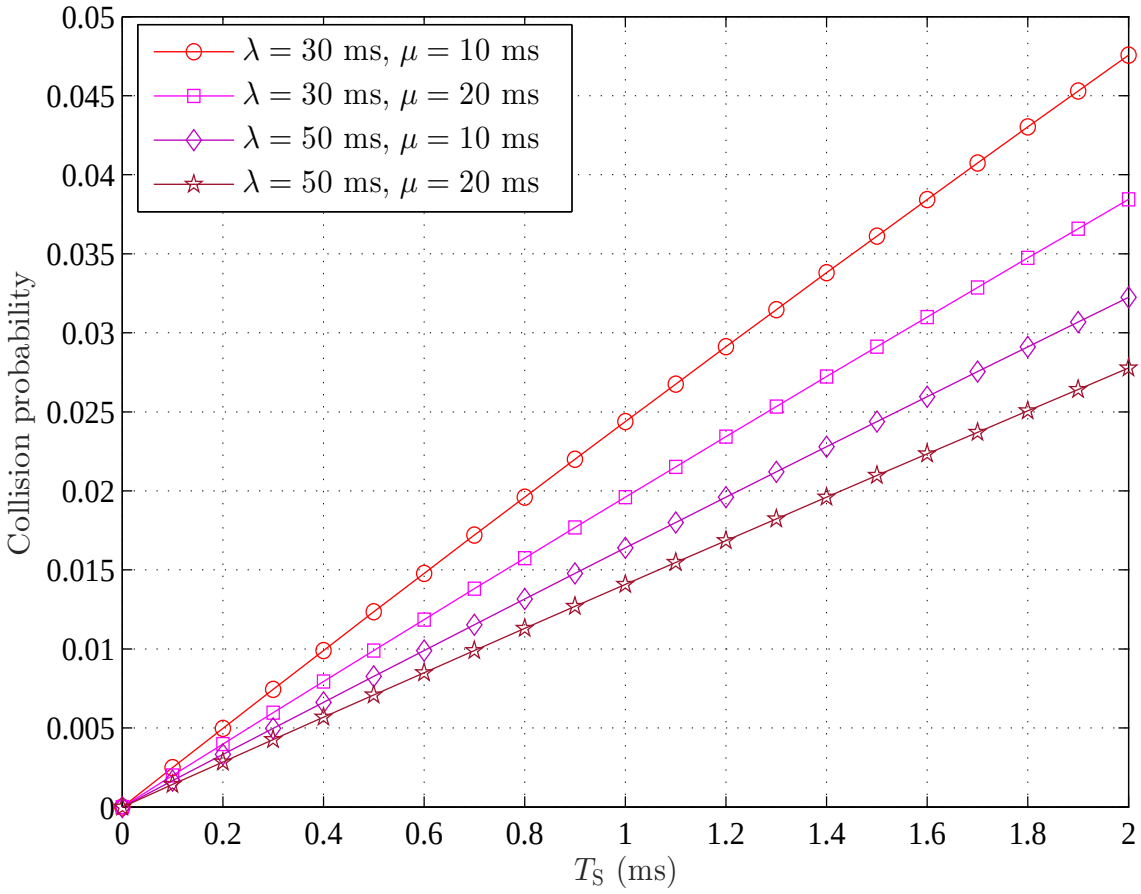

Figure 4.3: Correspondence of collision probability and sensing period for various PU activities.

The Markov model can be verified by solving Markov chain at equilibrium. As an illustration, for state C

$$\begin{aligned} p_W p_{C|W} + p_S p_{C|S} &= (1-\beta_{\text{off}})(1-\beta_{\text{on}})\frac{1-\beta_{\text{off}}}{2-\beta_{\text{on}}-\beta_{\text{off}}} + (1-\beta_{\text{off}})\frac{(1-\beta_{\text{on}})\beta_{\text{off}}}{2-\beta_{\text{on}}-\beta_{\text{off}}} \\ &= p_C p_{W|C} \end{aligned} \tag{4.7}$$

An immediate application of the Markov chain modeling is to evaluate the collision probability with secondary slotted transmission strategy. Fig. 4.3 plots the collision probability p_C as a function of sensing period T_{S} for different primary transmission parameters. Larger λ or larger μ results in smaller collision probability. Note that collision only occurs when PU restarts transmission. We also observe that collision

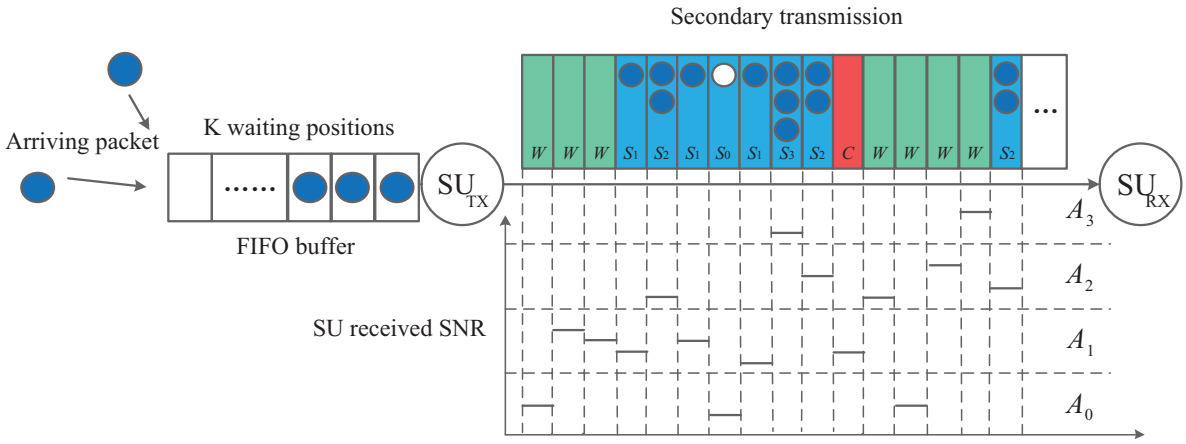

Figure 4.4: Secondary transmission with AMC for small-size packet.

probability increases for a longer sensing period as expected by intuition.

4.3.2 Queuing Analysis of Secondary Packet Transmission

In this subsection, we apply the proposed discrete-time Markov chain to evaluate the queueing performance of secondary packet transmission. We assume that SU information data is fragmented into equal-size packet. The packet size is chosen such that j packets can be transmitted over one T_{II} [83] when the primary channel is available and secondary link can support transmission rate $R_j, j = 0, 1, \cdots, N-1$, where $R_0 = 0$ corresponds to SU decides not to transmit due to unacceptable BER performance. During each T_{S}, at most one packet may arrive at the SU transmitter with probability p_a. The newly arrived packet will be put into a first-in-first-out (FIFO) buffer with K waiting positions before being delivered over the next available transmission slot as illustrated in Fig. 4.4. Only those packets that are successfully received will be removed from the buffer. We also assume that the SU received SNR remains unchanged over each T_{S} and changes independently afterwords. Let $\mathcal{A}_i \in \{0, 1\}$ represent no arrival or one packet arrival during the ith T_{S}. We have

$$\Pr[\mathcal{A}_i = a] = \begin{cases} p_a, & a = 1; \\ 1 - p_a, & a = 0. \end{cases} \tag{4.8}$$

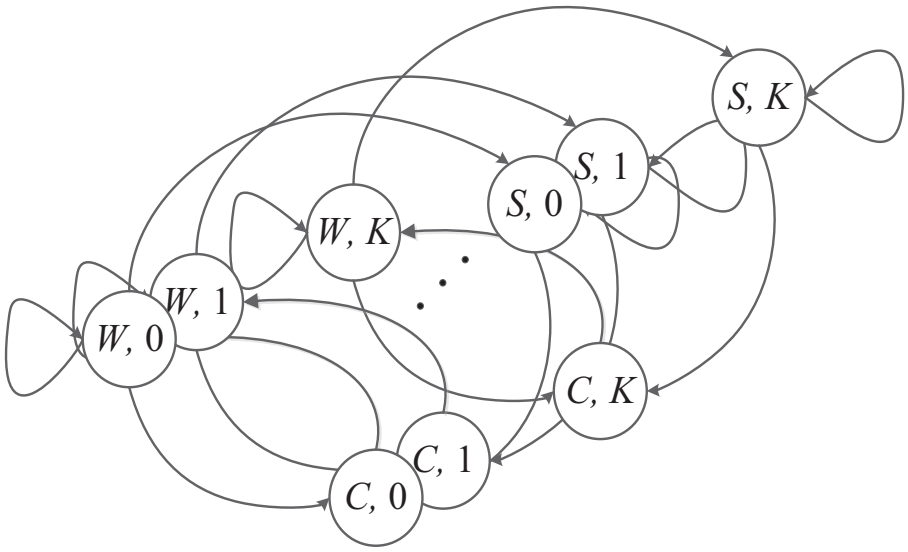

Figure 4.5: Two-dimensional discrete-time finite state Markov chain model for secondary transmission with AMC.

Unlike fixed-rate transmission, service time is a dynamic process in adaptive transmission system. Different from conventional adaptive transmission system, service time is bursty with cognitive radio implementation, since SU has to vacate the channel when PU transmits. With AMC, the number of packets can be transmitted over each T_{S} depends on channel availability and quality of secondary link. We denote the service state of the ith T_{S} as $\mathcal{D}_i$, where $\mathcal{D}_i \in \{S, W, C\}$.

Let $\mathcal{L}_i$ denote the instantaneous queue length of ith T_{S}, where $\mathcal{L}_i \in \{0, 1, ..., K\}$. New arrival will be dropped if the queue is full. The queue will be emptied if the number of queuing packets is less than the rate used. As illustrated in Fig. 4.6, the recursion of the queue length can be expressed as

$$\mathcal{L}_i = \min\{K,\ \max\{0,\ \mathcal{L}_{i-1} - \mathcal{D}_{i-1}\} + \mathcal{A}_{i-1}\}. \tag{4.9}$$

To investigate secondary queuing performance, we construct a two-dimensional Markov chain with state being the $(\mathcal{D}_i, \mathcal{L}_i)$ pair, as illustrated in Fig. 4.5. Let $p_{(\mathcal{D}_i,\mathcal{L}_i)|(\mathcal{D}_{i-1},\mathcal{L}_{i-1})}$ denote the transition probability from state $(\mathcal{D}_{i-1}, \mathcal{L}_{i-1})$ to state $(\mathcal{D}_i, \mathcal{L}_i)$. Accordingly, the state transition probability matrix, denoted by $\mathbf{P_Q}$, is

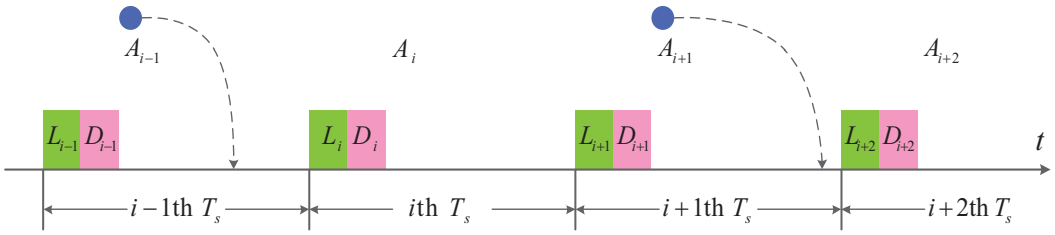

Figure 4.6: Queue recursion of secondary transmission.

organized as

$$\mathbf{P_Q} = \begin{bmatrix} \mathbf{P}_{(W,\mathcal{L}_i)|(W,\mathcal{L}_{i-1})} & \mathbf{P}_{(W,\mathcal{L}_i)|(S,\mathcal{L}_{i-1})} & \mathbf{P}_{(W,\mathcal{L}_i)|(C,\mathcal{L}_{i-1})} \\ \mathbf{P}_{(S,\mathcal{L}_i)|(W,\mathcal{L}_{i-1})} & \mathbf{P}_{(S,\mathcal{L}_i)|(S,\mathcal{L}_{i-1})} & \mathbf{P}_{(S,\mathcal{L}_i)|(C,\mathcal{L}_{i-1})} \\ \mathbf{P}_{(C,\mathcal{L}_i)|(W,\mathcal{L}_{i-1})} & \mathbf{P}_{(C,\mathcal{L}_i)|(S,\mathcal{L}_{i-1})} & \mathbf{P}_{(C,\mathcal{L}_i)|(C,\mathcal{L}_{i-1})} \end{bmatrix}, \tag{4.10}$$

where the $(K+1) \times (K+1)$ sub-matrix $\mathbf{P}_{(\mathcal{D}_i,\mathcal{L}_i)|(\mathcal{D}_{i-1},\mathcal{L}_{i-1})}$ is of the form

$$\mathbf{P}_{(\mathcal{D}_i,\mathcal{L}_i)|(\mathcal{D}_{i-1},\mathcal{L}_{i-1})} = \begin{bmatrix} p_{(\mathcal{D}_i,0)|(\mathcal{D}_{i-1},0)} & \cdots & p_{(\mathcal{D}_i,0)|(\mathcal{D}_{i-1},K)} \\ \vdots & \ddots & \vdots \\ p_{(\mathcal{D}_i,K)|(\mathcal{D}_{i-1},0)} & \cdots & p_{(\mathcal{D}_i,K)|(\mathcal{D}_{i-1},K)} \end{bmatrix}, \tag{4.11}$$

with $\mathcal{D}_{i-1} \in (W, S, C)$ and $\mathcal{D}_i \in (W, S, C)$. The transition probabilities can be further simplified, while noting that current service state is only dependent on previous service state, as

$$\begin{aligned} p_{(\mathcal{D}_i,\mathcal{L}_i)|(\mathcal{D}_{i-1},\mathcal{L}_{i-1})} &= \Pr[\mathcal{D}_i, \mathcal{L}_i | \mathcal{D}_{i-1}, \mathcal{L}_{i-1}] \\ &= \Pr[\mathcal{D}_i | \mathcal{D}_{i-1}] \Pr[\mathcal{L}_i | \mathcal{D}_{i-1}, \mathcal{L}_{i-1}] \\ &= p_{\mathcal{D}_i|\mathcal{D}_{i-1}} p_{\mathcal{L}_i|\mathcal{D}_{i-1},\mathcal{L}_{i-1}}. \end{aligned} \tag{4.12}$$

$p_{\mathcal{D}_i|\mathcal{D}_{i-1}}$ can be calculated by the transition probabilities given by Eq. (4.4). Accordingly, Eq. (4.10) is rewritten in a block form as

$$\mathbf{P_Q} = \begin{bmatrix} p_{W|W}\mathbf{P}_{\mathrm{N}} & \mathbf{O} & \mathbf{P}_{\mathrm{N}} \\ p_{S|W}\mathbf{P}_{\mathrm{N}} & p_{S|S}\mathbf{P}_{\mathrm{T}} & \mathbf{O} \\ p_{C|W}\mathbf{P}_{\mathrm{N}} & p_{C|S}\mathbf{P}_{\mathrm{T}} & \mathbf{O} \end{bmatrix}, \tag{4.13}$$

where $\mathbf{O}$ represents $(K+1)\times(K+1)$ zero matrix. When $\mathcal{D}_i = W$ or C, SU waits for channel availability or collision occurs. As such, no packet was assumed to be successfully transmitted. When $\mathcal{D}_i = S$ and rate R_j is used, j packets are transmitted successfully. As derived in Appendix B, sub-matrices $\mathbf{P}_{\mathrm{N}}$, $\mathbf{P}_{\mathrm{T}}$ are given by Eq. (4.14) and Eq. (4.15), respectively.

$$\mathbf{P}_{\mathrm{N}} = \begin{bmatrix} 1-p_a & 0 & 0 & \dots & 0 & 0 & 0 & \dots & 0 \\ p_a & 1-p_a & 0 & \dots & 0 & 0 & 0 & \dots & 0 \\ 0 & p_a & 1-p_a & \dots & 0 & 0 & 0 & \dots & 0 \\ 0 & 0 & p_a & \dots & 0 & 0 & 0 & \dots & 0 \\ \vdots & \vdots & \vdots & \vdots & \vdots & \vdots & \vdots & \vdots & \vdots \\ 0 & 0 & 0 & \dots & 0 & 0 & 0 & \dots & 1 \end{bmatrix}, \tag{4.14}$$

$$\mathbf{P}_{\mathrm{T}} = \begin{bmatrix} 1-p_a & (1-p_a)\sum_{j=1}^{N}\pi_j & (1-p_a)\sum_{j=2}^{N}\pi_j & \dots & 0 \\ p_a & (1-p_a)\pi_0 + p_a\sum_{j=1}^{N}\pi_j & (1-p_a)\pi_1 + p_a\sum_{j=2}^{N}\pi_j & \dots & 0 \\ 0 & p_a\pi_0 & (1-p_a)\pi_0 + p_a\pi_1 & \dots & 0 \\ 0 & 0 & p_a\pi_0 & \dots & 0 \\ \vdots & \vdots & \vdots & \vdots & \ddots \quad \vdots \\ 0 & 0 & 0 & \dots & (1-p_a)\pi_1 + p_a\pi_2 \\ 0 & 0 & 0 & \dots & \pi_0 + p_a\pi_1 \end{bmatrix} \tag{4.15}$$

The steady state probabilities for $\mathbf{P_Q}$, denoted by

$$\phi_{\mathbf{Q}} = [\phi_{W,0}, \cdots, \phi_{W,K}, \phi_{S,0}, \cdots, \phi_{S,K}, \phi_{C,0}, \cdots, \phi_{C,K}], \tag{4.16}$$

is the left eigenvector of $\mathbf{P_Q}$ corresponding to eigenvalue 1, which can be calculated by difference equations and normalization equation. The stationary distribution of queue length can be also found as $\phi_k = \sum_{\mathcal{D}=\mathrm{W,S,C}} \phi_{\mathcal{D},k},\ k = 0, 1, \cdots, K$.

Fig. 4.7 compares the analytical results of stationary distribution of the queue length against corresponding Monte Carlo simulations, where a four-state AM system

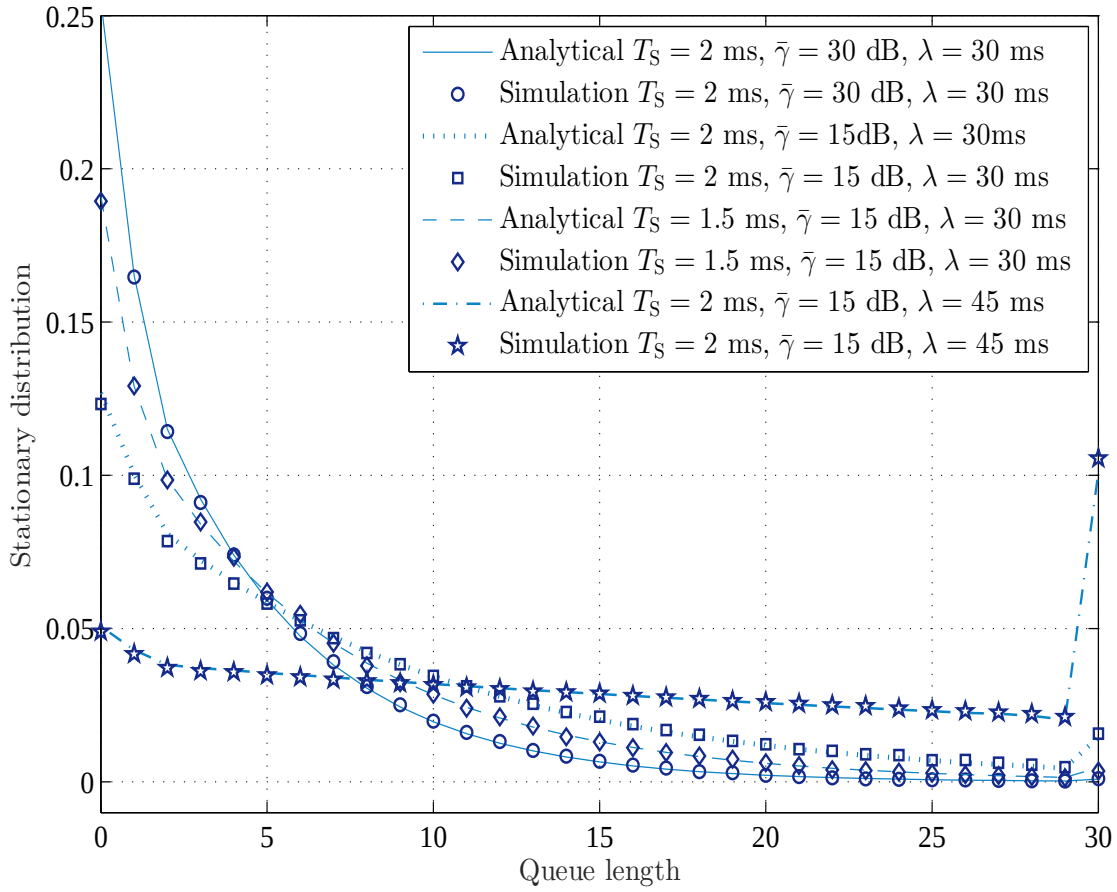

Figure 4.7: Analytical and simulation results on the stationary distribution of queue length with different sensing periods, primary user parameters and secondary channel condition, where $K = 30$ and $p_a = 0.16$.

with transmission rates $[R_0,\ R_1,\ R_2,\ R_3] = [0,\ 1,\ 2,\ 3]$ bits/symbol is introduced. The target BER is set to be 10^{-3}. The received SNR boundaries are set accordingly as $[\gamma_1, \gamma_2, \gamma_3] = [9.39, 13.95, 16.09]$ dB. We also assume that secondary link introduces Rayleigh fading with average received SNR $\bar{\gamma}$ dB (i.e. $f_\gamma(\gamma) = \frac{1}{\bar{\gamma}} e^{-\frac{\gamma}{\bar{\gamma}}}$). Identical AMC implementation is applied throughout this chapter. The perfect match here validates our analytical approaches. When PU channel is available for secondary transmission, the probability distribution decreases as k increases based on the assumption that average arriving rate is less than the average service rate. However, when PU transmits, the queue would continuously build up resulting in higher ϕ_K even for a small packet arriving probability. Smaller λ or larger μ leads to shorter waiting time or

longer transmission time, which can help reduce the queue length. For larger value of $\bar{\gamma}$, high order transmission rates have more chances to be used, which can increase the average service rate. Next, we will evaluate the queuing performance with stationary distribution of the queue length. The packet drop probability is, the one that new arrival finds out the queue is full, given by $P_{\text{drop}} = p_K p_a$. The average queue-length, denoted by $\mathbb{E}[Q]$, and average throughput, denoted by $\mathbb{E}[Th]$, of secondary system can be calculated as

$$\mathbb{E}[Q] = \sum_{k=0}^{K} k p_k, \ \mathbb{E}[Th] = p_S \sum_{k=0}^{K} \mathbb{E}[\mathcal{S}|k] p_k, \tag{4.17}$$

respectively, where p_S is the stationary probability that SU transmits without collision and $\mathbb{E}[\mathcal{S}|k]$ is the average number of packets been successfully transmitted per T_{s} given k packets waiting in the queue. Note that when $\mathcal{L}_{i-1} < \mathcal{D}_{i-1}$, $\mathcal{L}_{i-1}$ packets will be transmitted over the upcoming slot. $\mathbb{E}[Th|k]$ can be calculated as

$$\mathbb{E}[\mathcal{S}|k] = \begin{cases} 0, & k = 0; \\ \sum_{i=1}^{k} i\pi_i + k \sum_{j=k+1}^{N} \pi_j, & 0 < k < N; \\ \sum_{i=1}^{N} i\pi_i, & N \leq k \leq K. \end{cases} \tag{4.18}$$

The average queue-length, denoted by $\mathbb{E}[Q_L]$, can be calculated as $\mathbb{E}[Q_L] = \sum_{k=0}^{K} k\varphi_k$. Applying Little's law, the average queuing delay can be calculated as

$$\mathbb{E}[T_Q] = \frac{\mathbb{E}[Q]}{\mathbb{E}[Th]} = \frac{\sum_{k=0}^{K} k p_k}{p_S \sum_{k=0}^{K} \mathbb{E}[\mathcal{S}|k] p_k}. \tag{4.19}$$

We present the analytical results of secondary queuing performance. More chances to access the channel (i.e. larger μ or smaller λ) or better secondary link quality helps increase average throughput and results in lower average queuing time as expected by intuition (See Fig. 4.8 (a) and Fig. 4.8 (b)). The average delay saturates as input traffic intensity grows because packets are dropped when queue is full. When average throughput approaches its maximum, packet drop probability increases sharply as shown in Fig. 4.8 (c).

(a)

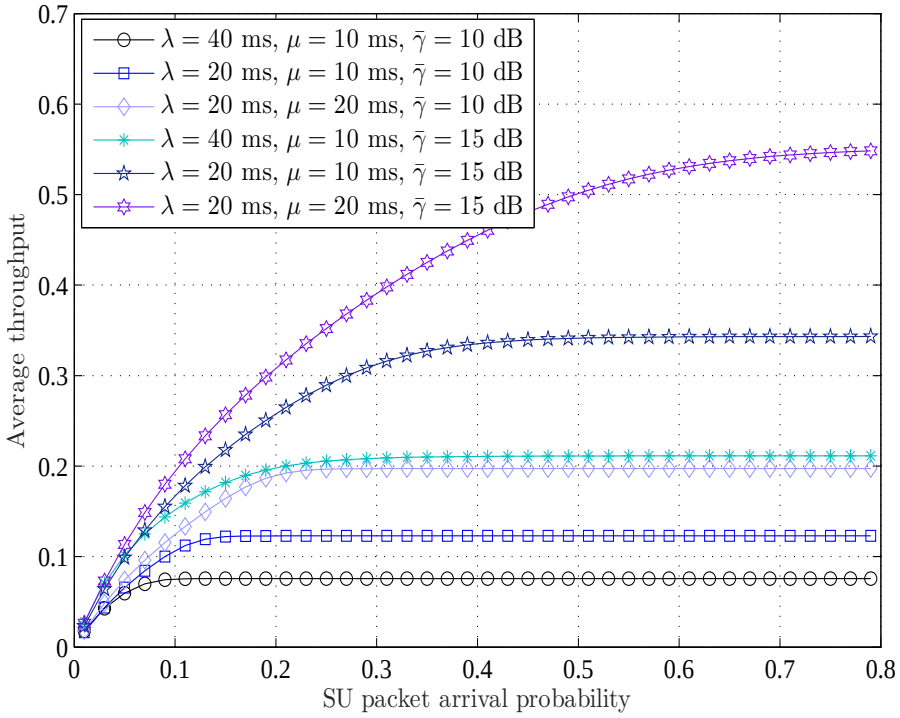
Average throughput
SU packet arrival probability
λ = 40 ms, μ = 10 ms, γ̄ = 10 dB
λ = 20 ms, μ = 10 ms, γ̄ = 10 dB
λ = 20 ms, μ = 20 ms, γ̄ = 10 dB
λ = 40 ms, μ = 10 ms, γ̄ = 15 dB
λ = 20 ms, μ = 10 ms, γ̄ = 15 dB
λ = 20 ms, μ = 20 ms, γ̄ = 15 dB
0
0.1
0.2
0.3
0.4
0.5
0.6
0.7
0.8

(b)

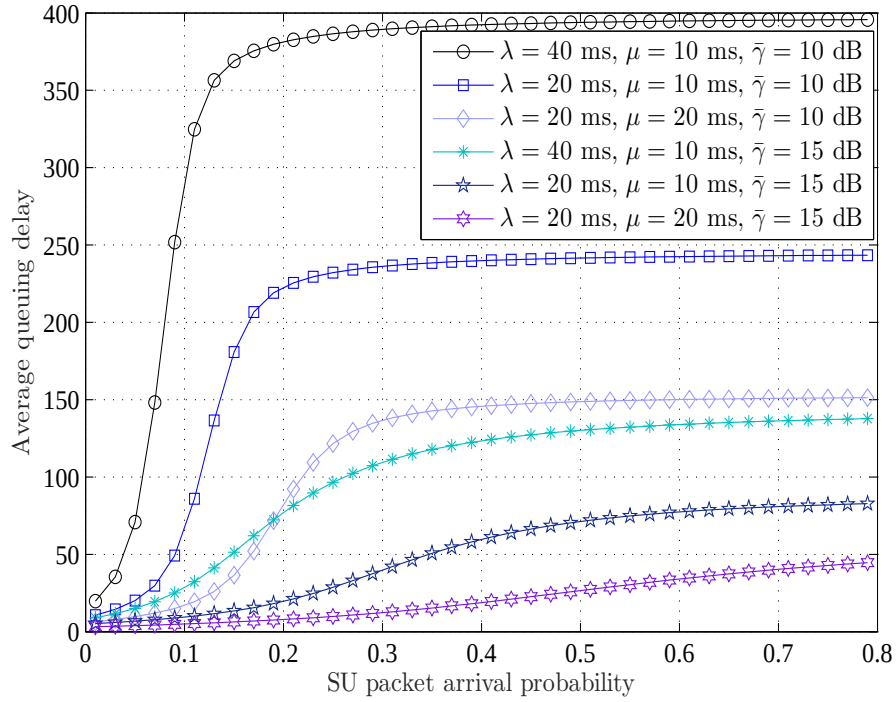
Average queuing delay
SU packet arrival probability
λ = 40 ms, μ = 10 ms, γ̄ = 10 dB
λ = 20 ms, μ = 10 ms, γ̄ = 10 dB
λ = 20 ms, μ = 20 ms, γ̄ = 10 dB
λ = 40 ms, μ = 10 ms, γ̄ = 15 dB
λ = 20 ms, μ = 10 ms, γ̄ = 15 dB
λ = 20 ms, μ = 20 ms, γ̄ = 15 dB
0
50
100
150
200
250
300
350
400
0.1
0.2
0.3
0.4
0.5
0.6
0.7
0.8

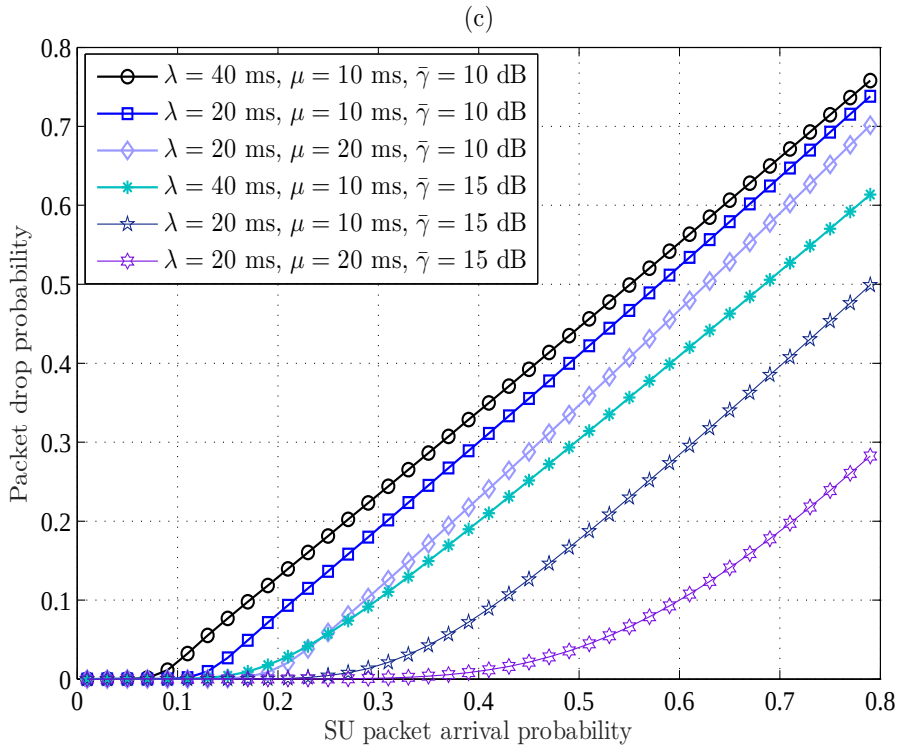

Figure 4.8: Average queuing delay, average throughput and packet drop probability versus various secondary channel quality and primary user parameters.

4.3.3 EDT analysis for slotted secondary transmission

For large-size packet, multiple T_Ss are required to complete single packet transmission. As such, packet service time consists of waiting time and transmission time. We derive the statistics of EDT assuming fixed-rate transmission and variable-rate transmission in the following subsections.

Fixed-Rate Transmission

Firstly, We derive the PMF of EDT (T_{ED}) for a fixed-size packet transmission with a fixed data rate. T_{ED} should include all the waiting periods, collision periods and transmission periods before transmission completed. Specifically, the statistics of T_{ED} depends on the state of the first T_S at the instant of packet arrival as illustrated in Fig. 4.9. Conditioning on the first T_S being in state S, W and C. The PMF of

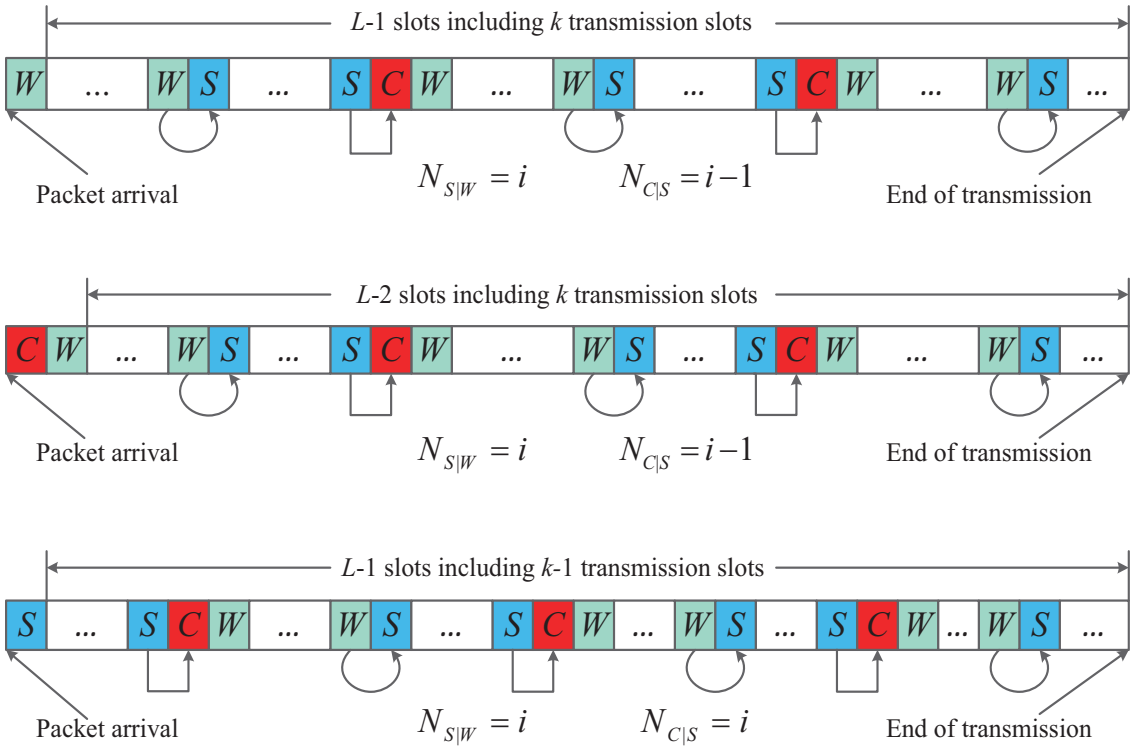

Figure 4.9: EDT sequence conditioning on the first slot is in state W, C and S, respectively.

T_{ED} can be calculated as

$$\Pr[T_{\mathrm{ED}} = LT_{\mathrm{S}}] = p_W \Pr\left[T_{\mathrm{ED}|W} = LT_{\mathrm{S}}\right] + p_S \Pr\left[T_{\mathrm{ED}|S} = LT_{\mathrm{S}}\right] + p_C \Pr\left[T_{\mathrm{ED}|C} = LT_{\mathrm{S}}\right], \tag{4.20}$$

where $\Pr[T_{\mathrm{ED}|W} = LT_{\mathrm{S}}]$, $\Pr[T_{\mathrm{ED}|S} = LT_{\mathrm{S}}]$, and $\Pr[T_{\mathrm{ED}|C} = LT_{\mathrm{S}}]$ denote the conditional probabilities that the first T_{S} is in state W, S, and C, respectively.

The number of transmission periods needed to complete transmission, denoted by θ, can be approximately calculated by

$$\theta = \left\lceil \frac{H_t}{RT_{\mathrm{H}}} \right\rceil, \tag{4.21}$$

where H_t represents the amount of data in a packet, and R is the pre-determined data rate. Let $N_{\cdot|\cdot}$ denote the number of certain transition of secondary transmission.

For example, $N_{S|W} = a$ represents that transition from state W to state S occurs a times. As such, the conditional PMF of $T_{\mathrm{ED}|W}$ can be written as

$$\Pr[T_{\mathrm{ED}|W} = LT_{\mathrm{S}}] = \Pr[N_{S|S} + N_{C|S} + N_{S|W} + N_{W|W} + N_{C|W} + N_{W|C} = L-1], \quad (4.22)$$

which can be further simplified, while noting $N_{C|S} + N_{C|W} = N_{W|C}$,as

$$\Pr[T_{\mathrm{ED}|W} = LT_{\mathrm{S}}] = \Pr[N_{S|S} + N_{S|W} + N_{W|W} + 2N_{C|W} + 2N_{C|S} = L-1] \quad (4.23)$$

Conditioning on that $N_{S|W} = i$, $i = 1, 2, \cdots, \theta$, Eq. (4.23) is written as

$$\begin{aligned} &\Pr[T_{\mathrm{ED}|W} = LT_{\mathrm{S}}] \\ &= \sum_{i=1}^{\theta} \Pr[N_{W|W} + 2N_{C|W} = L-1-\theta-2(i-1)] \Pr[N_{S|W} = i], \end{aligned} \quad (4.24)$$

while noting $N_{S|S} + N_{C|S} = \theta$ and $N_{C|S} = N_{S|W} - 1$. Applying the statistics of binomial random variable, we have

$$\Pr[N_{S|W} = i] = \binom{\theta-1}{i-1} p_{S|S}^{\theta-i} p_{C|S}^{i-1}. \quad (4.25)$$

Conditioned on $N_{C|W} = j$ and $N_{W|W} = m - j$ and applying negative-multinomial distribution, we have

$$\begin{aligned} \Pr[N_{W|W} + 2N_{C|W} &= L-1-\theta-2(i-1)] \\ &= \sum_{\substack{m,\ j \text{ s.t.} \\ m+2j=L-1-\theta-2(i-1)}} \binom{m+i-1}{i-1,\ j} p_{S|W}^{i} p_{C|W}^{j} p_{W|W}^{m-j}. \end{aligned} \quad (4.26)$$

Substituting Eq. (4.25) and Eq. (4.26) into Eq. (4.24), we have

$$\begin{aligned} &\Pr[T_{\mathrm{ED}|W} = LT_{\mathrm{S}}] = \\ &\sum_{i=1}^{\theta} \left[\sum_{\substack{m,\ j \text{ s.t.} \\ m+2j=L-1-\theta-2(i-1)}} \binom{m+i-1}{i-1,\ j} p_{S|W}^{i} p_{C|W}^{j} p_{W|W}^{m-j} \right] \binom{\theta-1}{i-1} p_{S|S}^{\theta-i} p_{C|S}^{i-1}. \end{aligned} \quad (4.27)$$

Conditioning on that SU transmission starts with C, the first two slots are in state C and W, respectively. We have

$$\Pr[T_{\mathrm{ED}|C} = LT_{\mathrm{S}}] = \sum_{i=1}^{\theta} \left[\sum_{\substack{m,\ j \text{ s.t.} \\ m+2j=L-2-\theta-2(i-1)}} \binom{m+i-1}{i-1,\ j} p_{S|W}^{i} p_{C|W}^{j} p_{W|W}^{m-j} \right] \binom{\theta-1}{i-1} p_{S|S}^{\theta-i} p_{C|S}^{i-1}. \tag{4.28}$$

Conditioning on starting with S, the differences are $N_{S|W} = N_{C|S} = i,\ i = 1, 2, \cdots, \theta - 1$ and $N_{S|W} + N_{S|S} = \theta - 1$. $\Pr[T_{\mathrm{ED}|S} = LT_{\mathrm{S}}]$ can be calculated as

$$\Pr[T_{\mathrm{ED}|S} = LT_{\mathrm{S}}] = \sum_{i=1}^{\theta-1} \sum_{\substack{m,\ j \text{ s.t.} \\ m+2j=L-\theta-2i}} \left[\binom{m+i-1}{i-1,\ j} p_{S|W}^{i} p_{C|W}^{j} p_{W|W}^{m-j} \binom{\theta-1}{i} p_{S|S}^{\theta-1-i} p_{C|S}^{i} \right] + \delta(\theta) p_{S|S}^{\theta-1}, \tag{4.29}$$

where $\delta(\cdot)$ represents impulse function. $\delta(\theta) p_{S|S}^{\theta-1}$ is the special case that T_{ED} is just a sequence of θ transmission slots without collision. The final PMF of T_{ED} is obtained as

$$\begin{aligned}
&\Pr[T_{\mathrm{ED}} = LT_{\mathrm{S}}] = \\
&\frac{(1-\beta_{\mathrm{on}})\beta_{\mathrm{off}}}{2-\beta_{\mathrm{on}}-\beta_{\mathrm{off}}} \left\{ \sum_{i=1}^{\theta-1} \sum_{\substack{m,\ j \text{ s.t.} \\ m+2j=L-\theta-2i}} \left[\binom{m+i-1}{i-1,\ j} p_{S|W}^{i} p_{C|W}^{j} p_{W|W}^{m-j} \binom{\theta-1}{i} p_{S|S}^{\theta-1-i} p_{C|S}^{i} \right] + \delta(\theta) p_{S|S}^{\theta-1} \right\} \\
&+ \frac{1-\beta_{\mathrm{off}}}{2-\beta_{\mathrm{on}}-\beta_{\mathrm{off}}} \sum_{i=1}^{\theta} \sum_{\substack{m,\ j \text{ s.t.} \\ m+2j=L-1-\theta-2(i-1)}} \binom{m+i-1}{i-1, j} p_{S|W}^{i} p_{C|W}^{j} p_{W|W}^{m-j} \binom{\theta-1}{i-1} p_{S|S}^{\theta-i} p_{C|S}^{i-1} \\
&+ \frac{(1-\beta_{\mathrm{on}})(1-\beta_{\mathrm{off}})}{2-\beta_{\mathrm{on}}-\beta_{\mathrm{off}}} \sum_{i=1}^{\theta} \sum_{\substack{m,\ j \text{ s.t.} \\ m+2j=L-2-\theta-2(i-1)}} \binom{m+i-1}{i-1, j} p_{S|W}^{i} p_{C|W}^{j} p_{W|W}^{m-j} \binom{\theta-1}{i-1} p_{S|S}^{\theta-i} p_{C|S}^{i-1}
\end{aligned} \tag{4.30}$$

Fig. 4.10 compares the analytical result of T_{ED} and corresponding Monte Carlo simulation. The perfect match validates our analysis. T_{ED} depends on the packet size and PU behaviour. Larger H_t results in longer transmission time, which leads to even longer waiting time. When SU has more chance to acquire the channel, both average and variance of T_{ED} decreases. (See Fig. 4.11)

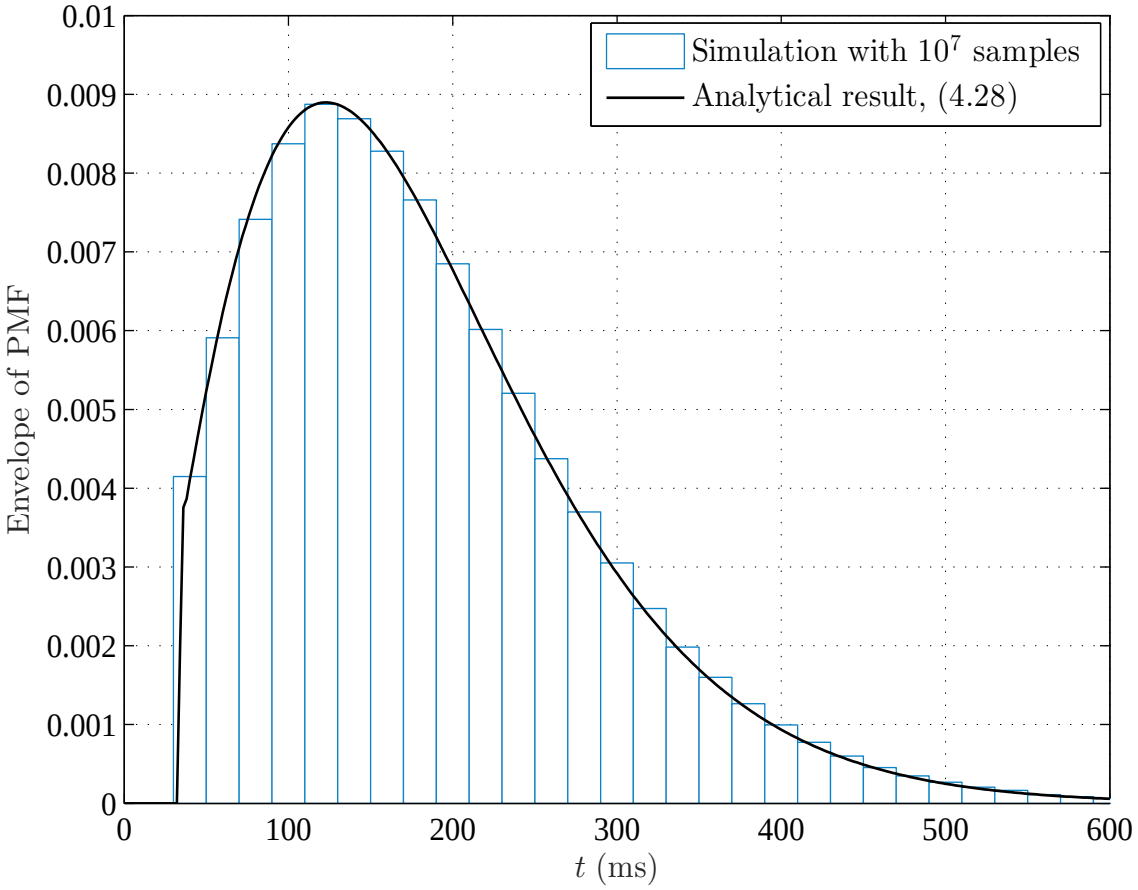

Figure 4.10: Monte Carlo verification of T_{ED} analysis ($H_t = 8$ kb, $\lambda = 30$ ms, $\mu = 10$ ms, $\bar{\gamma} = 20$ dB).

Variable-Rate Transmission

When AMC is used, transmission slots required to complete transmission is no longer constant but a random variable depending on secondary channel quality. θ transmission slots are needed only if data transmitted over $\theta - 1$ transmission slots is less than packet size H_t, whereas data transmitted over θ transmission slots is greater than the packet size. The probability that transmission time, denoted by T_{tr}, is equal to θ T_{S}s can be formulated as

$$\Pr[T_{\mathrm{tr}} = \theta T_{\mathrm{S}}] = \Pr\left[H_t - R^{(\theta)} T_{\mathrm{S}} \leq \mathbb{H}_{\theta-1} \leq H_t\right], \tag{4.31}$$

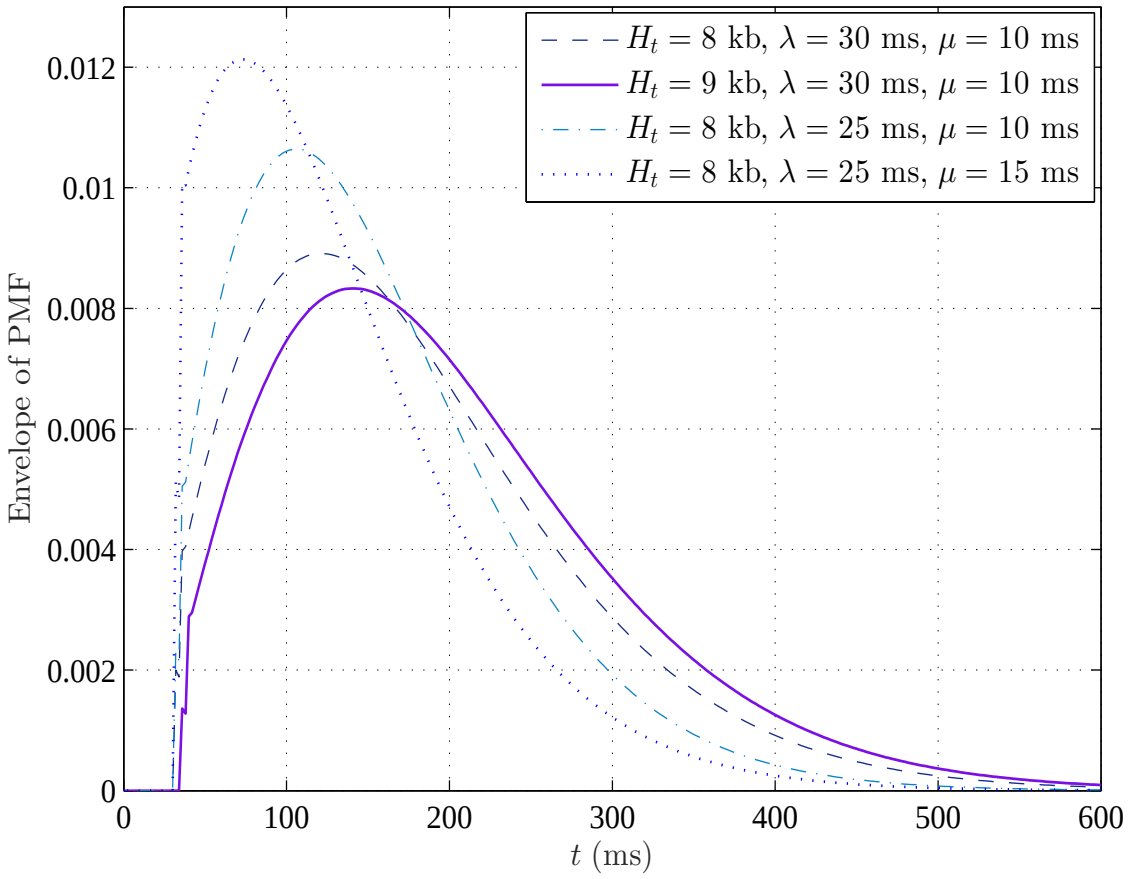

Figure 4.11: PMF of EDT with fixed-rate transmission for various PU activities and secondary packet size.

where $R^{(\theta)}$ denotes the data rate used in the last transmission slot without channel information. As such, $R^{(\theta)}$ is a random variable (i.e. $R^{(\theta)} = R_l$ with probability $\pi_l,\ l = 1, 2, \cdots, N$). $\mathbb{H}_{\theta-1}$ denotes the data transmitted over the first $\theta - 1$ periods. If secondary user received SNR falls into region A_l at the θth period, then R_l is used (i.e. $R^{(\theta)} = R_l$). By conditioning on the channel realization of the θth transmission period, we have

$$\Pr\left[T_{\text{tr}} = \theta T_{\text{S}}\right] = \sum_{l=1}^{N} \Pr\left[H_t - R_l T_{\text{S}} \leq \mathbb{H}_{\theta-1} \leq H_t\right] \pi_l. \tag{4.32}$$

Then $\Pr\left[T_{\rm tr} = \theta T_{\rm S}\right]$ can be calculated by Eq. (2.11) and given by

$$\Pr[T_{\rm tr} = \theta T_{\rm S}] = \sum_{l=1}^{N} \left(\sum_{\substack{\overrightarrow{\mathbf{n}} \text{ s.t.} \\ \mathbb{H}_{\theta-1} \in [H_t - R_l T_{\rm S},\ H_t]}} \binom{\theta-1}{n_1, n_2, ..., n_N} \prod_{i=1}^{N} \pi_i^{n_i} \right) \pi_l,$$

where $\overrightarrow{\mathbf{n}} = [n_1, n_2, \cdots, n_N]$ represents certain channel realization of the first $k-1$ transmission slots satisfying $\sum_{i=1}^{N} n_i = \theta - 1$. The inner sum is carried out over all $\overrightarrow{\mathbf{n}}$s satisfying that $\mathbb{H}_{\theta-1}$ falls into region $[H_t - R_l T_{\rm S},\ H_t]$. The distribution of $T_{\rm ED}$ can be obtained by conditioning on θ as

$$\Pr[T_{\rm ED} = L T_{\rm S}] = \sum_{\theta=1}^{\infty} \Pr[T_{{\rm ED}|\theta} = L T_{\rm S}] \Pr[T_{\rm tr} = \theta T_{\rm S}], \tag{4.33}$$

where $\Pr[T_{{\rm ED}|\theta} = L T_{\rm S}]$ is the distribution of EDT given θ periods required, shown in Eq. (4.30). In practical, the value of θ can not be infinity, since the packet size H_t is fixed. Fig. 4.12 compares the envelope of PMF of $T_{\rm ED}$ versus various secondary channel quality. As channel quality gets better, both average and variance of $T_{\rm ED}$ decreases since less periods are required to complete transmission. Note that, when channel quality is poor, more time is required to accomplish transmission even with AM, compared to fixed-rate transmission. This is because that lower rates are frequently used, or SU decides not to transmit mostly.

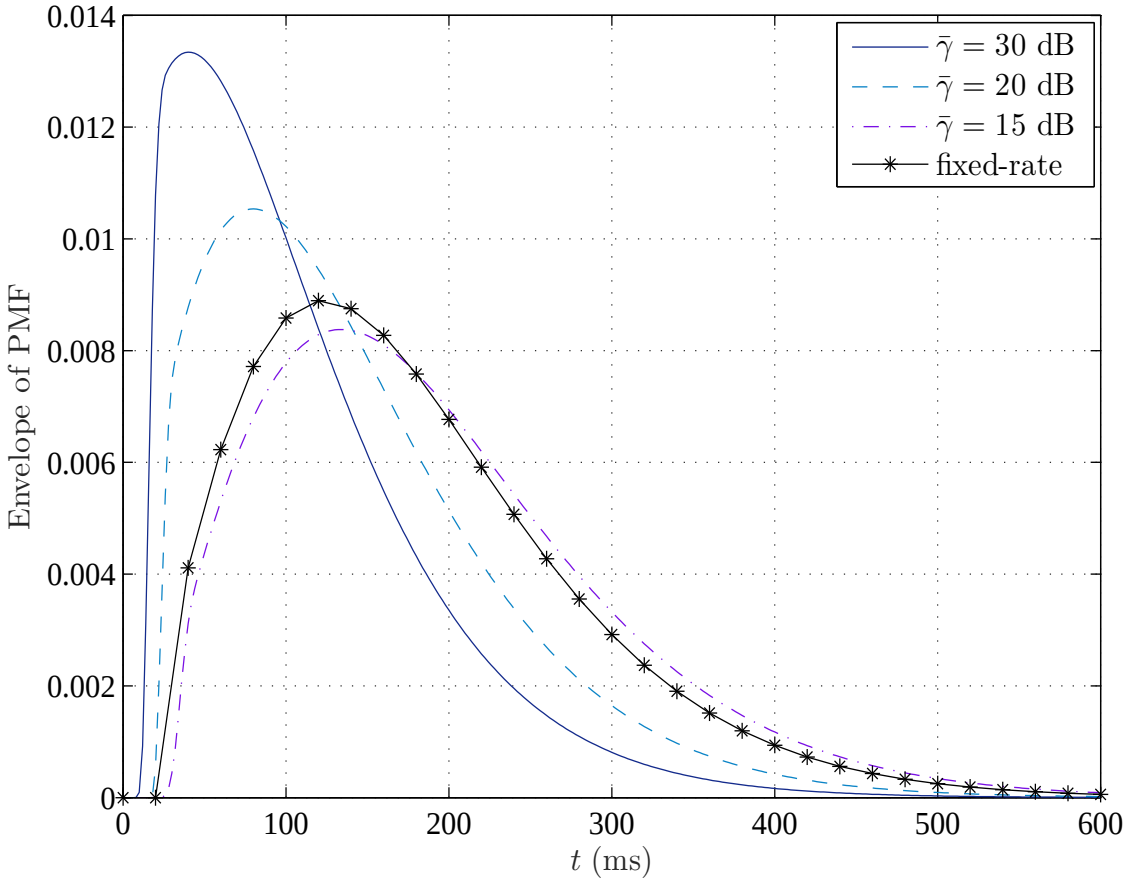

Figure 4.12: PMF of EDT for secondary transmission with four-state AMC.

4.4 Imperfect Spectrum Sensing

SU performs spectrum sensing on the target frequency band to identify transmission opportunity. Due to the presence of noise, hidden terminals, and other factors, sensing errors might occur. Sensing errors can greatly affect the performance of secondary transmission. With slotted transmission protocol, collision occurs when PU restarts transmission. We investigate SU transmission activity assuming imperfect spectrum sensing results, where *false alarm* occurs with probability p_f. False alarm is defined as PU has stopped transmission, however, SU still waits for channel availability due to sensing errors. Another kind of sensing error miss detection is defined as the event that PU is transmitting but SU senses the channel to be free. According to the IEEE 802.22 standard, both false alarm probability and miss detection prob-

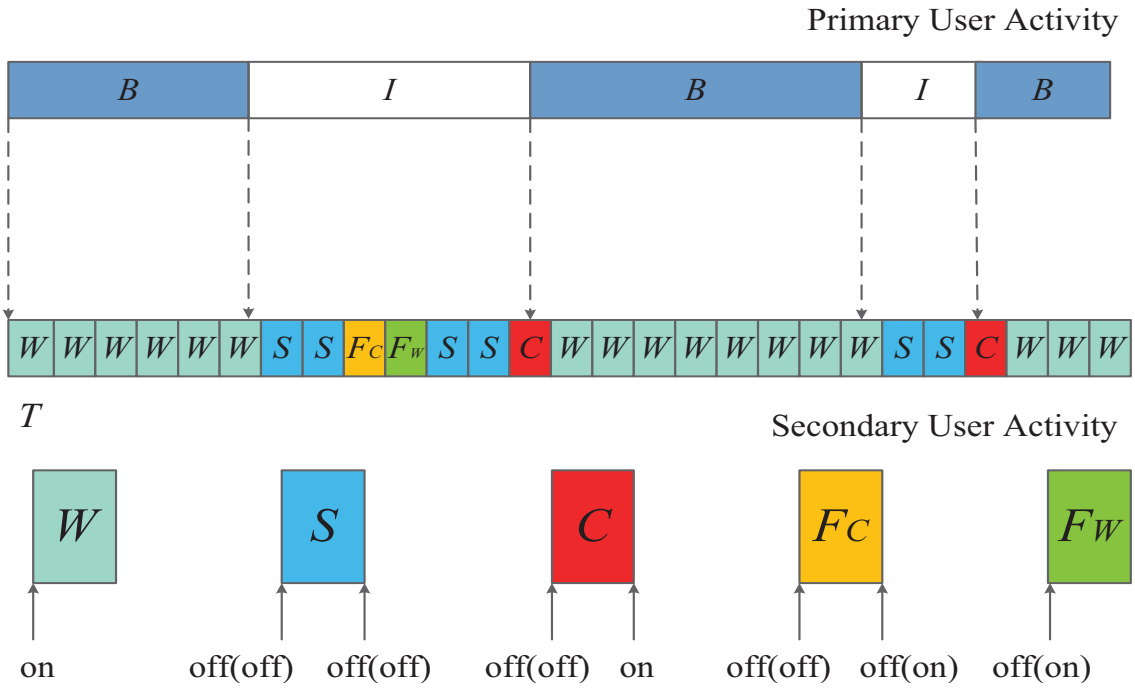

Figure 4.13: Slotted secondary transmission under false alarm.

ability should be less than 0.1 [84]. We first assume that the SU adopts very strict sensing policy to protect PU transmission. As such, the probability of miss detection is ignorable [71, 85, 86]. The effect of miss detection will be discussed at the end of this section. The slotted secondary transmission with false alarm is illustrated in Fig. 4.13.

4.4.1 Markov Model of Secondary Transmission with False Alam

We form a five-state discrete-time Markov chain to characterize SU activity assuming false alarm might occur. Except for state W, S and C, two new states are formed. If false alarm occurs at the ith sensing phase, SU affirms that collision occurs in the $i-1$th T_{S}. We introduce a false collision state, denoted by F_C, for such scenario. Consequently, SU waits in the ith period due to the incorrect sensing result at the ith sensing phase, which corresponds to a false waiting state, denoted by F_W. The Markov model is illustrated in Fig. 4.14.

State transition depends on the variation of PU activity and sensing results. With

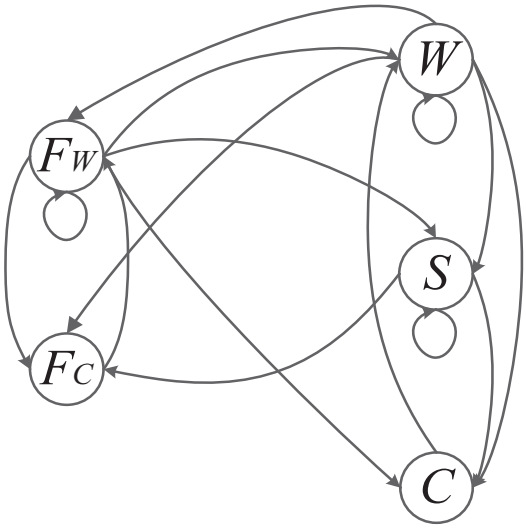

Figure 4.14: Markov model and state transitions of slotted secondary transmission with false alarm.

slotted protocol, SU periodically senses PU activity on the target frequency band. Similarly, let H_i represent PU activity at the ith sensing instant. $H_i = 1$ if PU is on and $H_i = 0$ if PU is off. In addition, H_i^* represents the sensing result at the ith sensing instant. $H_i^* = 1$ if the channel is sensed busy, whereas $H_i^* = 0$ if the channel is sensed free. We show the proposed Markov chain and illustrate the state transmission determined by sensing results in Fig. 4.15. The false alarm probability p_f is defined as

$$p_f = \Pr[H_i^* = 1 | H_i = 0], \tag{4.34}$$

Accordingly, we can determine the transition probability matrix. As an example, the transition probability from state F_W to state F_C is calculated as

$$\begin{aligned}
&p'_{F_C|F_W} \\
&= \Pr[H_{i+1} = 0,\ H_{i+2} = 0,\ H_{i+1}^* = 0,\ H_{i+2}^* = 1 | H_i = 0,\ H_i^* = 1] \\
&= \Pr[H_{i+2} = 0,\ H_{i+2}^* = 1 | H_{i+1} = 0,\ H_{i+1}^* = 0] \Pr[H_{i+1} = 0,\ H_{i+1}^* = 0 | H_i = 0,\ H_i^* = 1] \\
&= \Pr[H_{i+2}^* = 1 | H_{i+2} = 0] \Pr[H_{i+2} = 0 | H_{i+1} = 0] \Pr[H_{i+1}^* = 0 | H_{i+1} = 0] \Pr[H_{i+1} = 0 | H_i = 0] \\
&= \beta_{off}^2 (1 - p_f) p_f,
\end{aligned} \tag{4.35}$$

where the second equality results from that H_i^* only depends on H_i, and H_{i+1} only depends on H_i. Other transition probabilities can be obtained following similar steps.

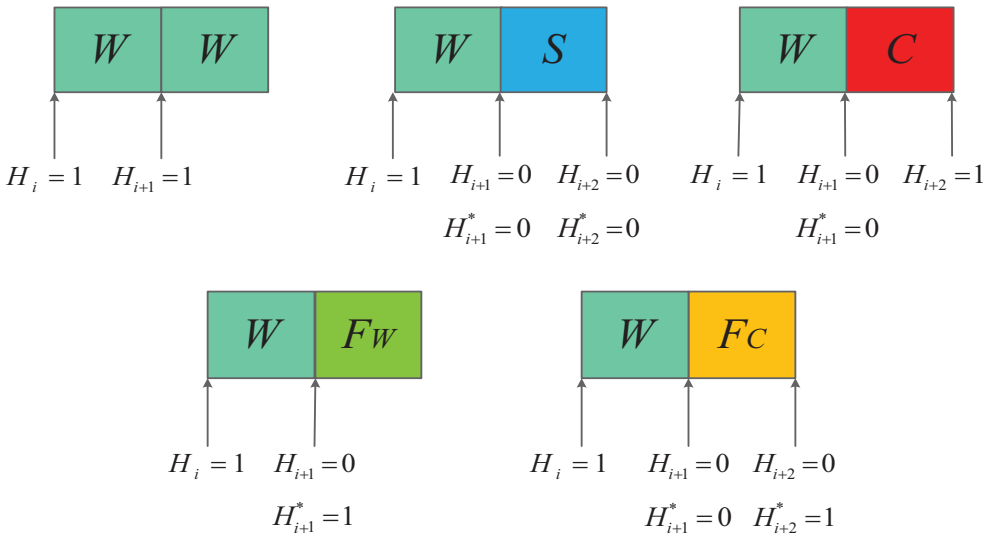

Figure 4.15: State transition illustration.

Thus, the transition probability matrix of proposed five-state Markov chain is given by

$$\mathbf{P}' = \begin{bmatrix} p'_{W|W} & p'_{W|S} & p'_{W|C} & p'_{W|F_W} & p'_{W|F_C} \\ p'_{S|W} & p'_{S|S} & p'_{S|C} & p'_{S|F_W} & p'_{S|F_C} \\ p'_{C|W} & p'_{C|S} & p'_{C|C} & p'_{C|F_W} & p'_{C|F_C} \\ p'_{F_W|W} & p'_{F_W|S} & p'_{F_W|C} & p'_{F_W|F_W} & p'_{F_W|F_C} \\ p'_{F_C|W} & p'_{F_C|S} & p'_{F_C|C} & p'_{F_C|F_W} & p'_{F_C|F_C} \end{bmatrix}$$

$$= \begin{bmatrix} \beta_{on} & 0 & 1 & 1-\beta_{off} & 0 \\ (1-\beta_{on})\beta_{off}(1-p_f)^2 & \beta_{off}(1-p_f) & 0 & \beta_{off}^2(1-p_f)^2 & 0 \\ (1-\beta_{on})(1-\beta_{off})(1-p_f) & 1-\beta_{off} & 0 & \beta_{off}(1-\beta_{off})(1-p_f) & 0 \\ (1-\beta_{on})p_f & 0 & 0 & \beta_{off}p_f & 1 \\ (1-\beta_{on})\beta_{off}(1-p_f)p_f & \beta_{off}p_f & 0 & \beta_{off}^2(1-p_f)p_f & 0 \end{bmatrix}. \tag{4.36}$$

The stationary distribution of the Markov chain can be calculated from the eigenvector of $\mathbf{P}'$ corresponding to eigenvalue one. After carrying out manipulations and

normalization, the stationary distribution of proposed Markov chain is obtained as

$$[p'_W,\ p'_S,\ p'_C,\ p'_{F_W},\ p'_{F_C}] = \tag{4.37}$$

$$\left[\frac{1-\beta_{off}}{2-\beta_{on}-\beta_{off}},\ \frac{(1-\beta_{on})\beta_{off}(1-p_f)^2}{2-\beta_{on}-\beta_{off}},\ \frac{(1-\beta_{on})(1-\beta_{off})(1-p_f)}{2-\beta_{on}-\beta_{off}},\right. \tag{4.38}$$

$$\left.\frac{(1-\beta_{on})p_f}{2-\beta_{on}-\beta_{off}},\ \frac{\beta_{off}(1-\beta_{on})p_f(1-p_f)}{2-\beta_{on}-\beta_{off}}\right] \tag{4.39}$$

An immediate application of the Markov chain modeling is to evaluate the successful transmission probability. Fig. 4.4.1 (a) plots p'_S as a function of SU period for different false alarm probabilities and PU parameter pairs. We can see that p'_S is smaller for larger false alarm probability as expected by intuition. Larger average PU busy period λ or smaller average PU idle period μ results in smaller p'_S since SU wastes more time in waiting for channel availability. Fig. 4.4.1 (b) shows the effect of false alarm probability and PU parameters on the collision probability. Note that collision only occurs when PU restarts transmission. Hence, larger μ or larger λ leads to smaller p'_C. We also observe that p'_C decreases slightly as false alarm probability increases. This attributes to that if false alarm occurs right before PU restarts transmission, secondary transmission will be in state F_W or F_C instead of state C.

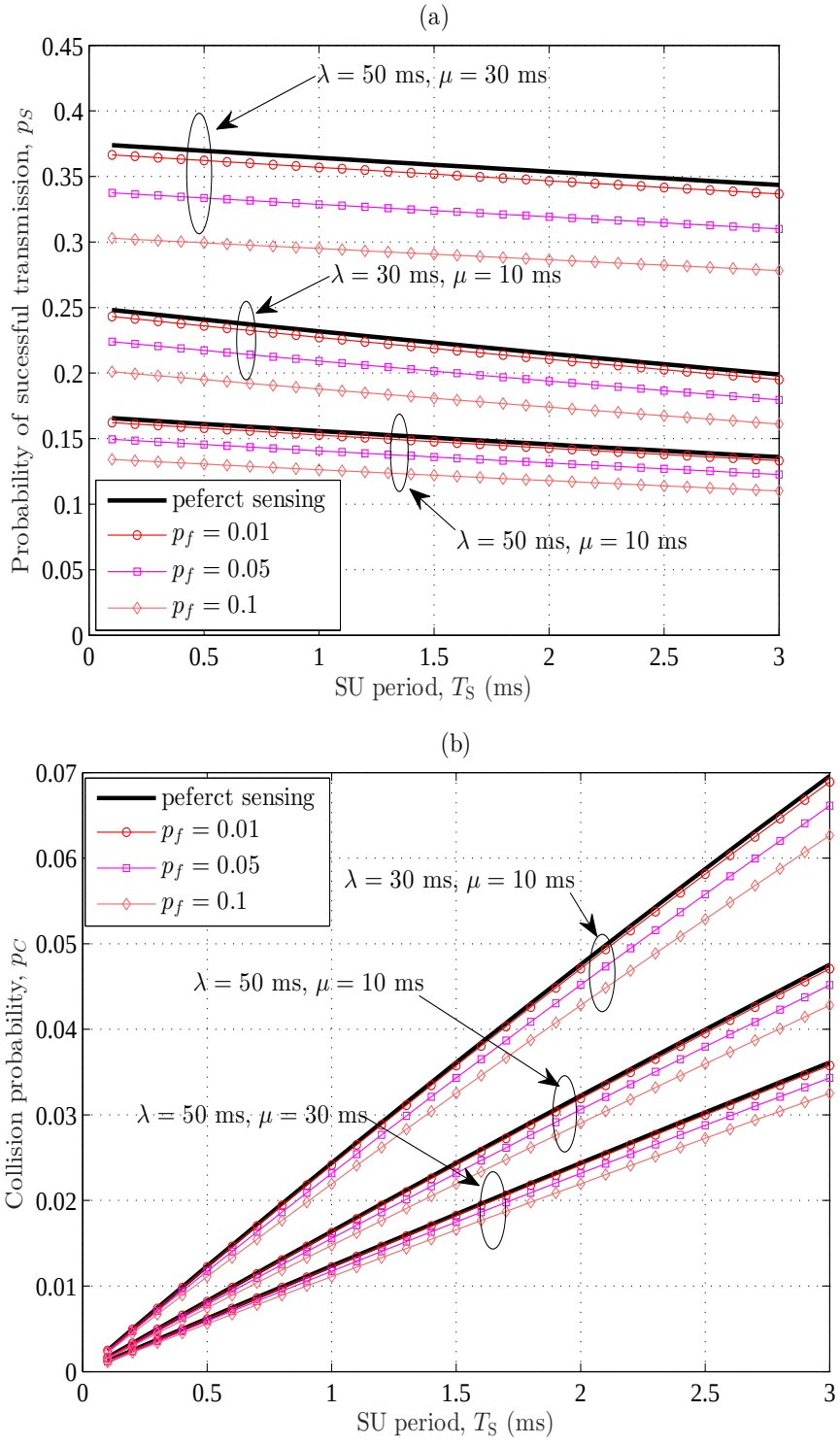

Figure 4.16: Collision probability/successful transmission probability versus SU period for various false alarm probabilities and PU parameters.

4.4.2 Energy Efficiency of Slotted Secondary Transmission

In this section, we apply the analytical results in previous section to investigate energy efficiency of secondary transmission by taking sensing energy consumption into account. SU performs spectrum sensing during the sensing phase and makes transmission decision according to the sensing result in T_{I}. If PU channel is sensed busy, SU will wait for T_{II} duration and sense again. Otherwise, SU starts its transmission immediately during the following T_{II}. At the sensing phase, SU performs spectrum sensing with power P_{sen}, which depends on the target false alarm/mis-detection probability [87]. The energy consumed in spectrum sensing is calculated as $P_{\mathrm{sen}}T_{\mathrm{I}}$. We also assume that SU transmits with constant power P_{tr}. Then, if SU decides to transmit, the energy consumed in transmission is calculated as $P_{\mathrm{tr}}T_{\mathrm{II}}$. We obtain the average energy consumption of slotted secondary transmission as

$$\mathcal{E}_{\mathrm{all}} = (p'_S + p'_C + p'_{F_C})P_{\mathrm{tr}}T_{\mathrm{II}} + P_{\mathrm{sen}}T_{\mathrm{I}}. \tag{4.40}$$

If collision or false collision occurs, SU declares a transmission failure and retransmits the data packet in next transmission availability. Hence, energy consumed in previous SU period is wasted. Energy consumed in successful transmission is characterized as

$$\mathcal{E}_{\mathrm{T}} = p'_S(P_{\mathrm{tr}}T_{\mathrm{II}} + P_{\mathrm{sen}}T_{\mathrm{I}}). \tag{4.41}$$

We define the energy efficiency as the ratio of the energy consumed in successful transmission over the total energy consumption as

$$R_{\mathrm{suc}} = \frac{\mathcal{E}_{\mathrm{T}}}{\mathcal{E}_{\mathrm{all}}}. \tag{4.42}$$

Typically, T_{I} is invariant to guarantee a certain sensing reliability, whereas T_{II} can be adjusted.

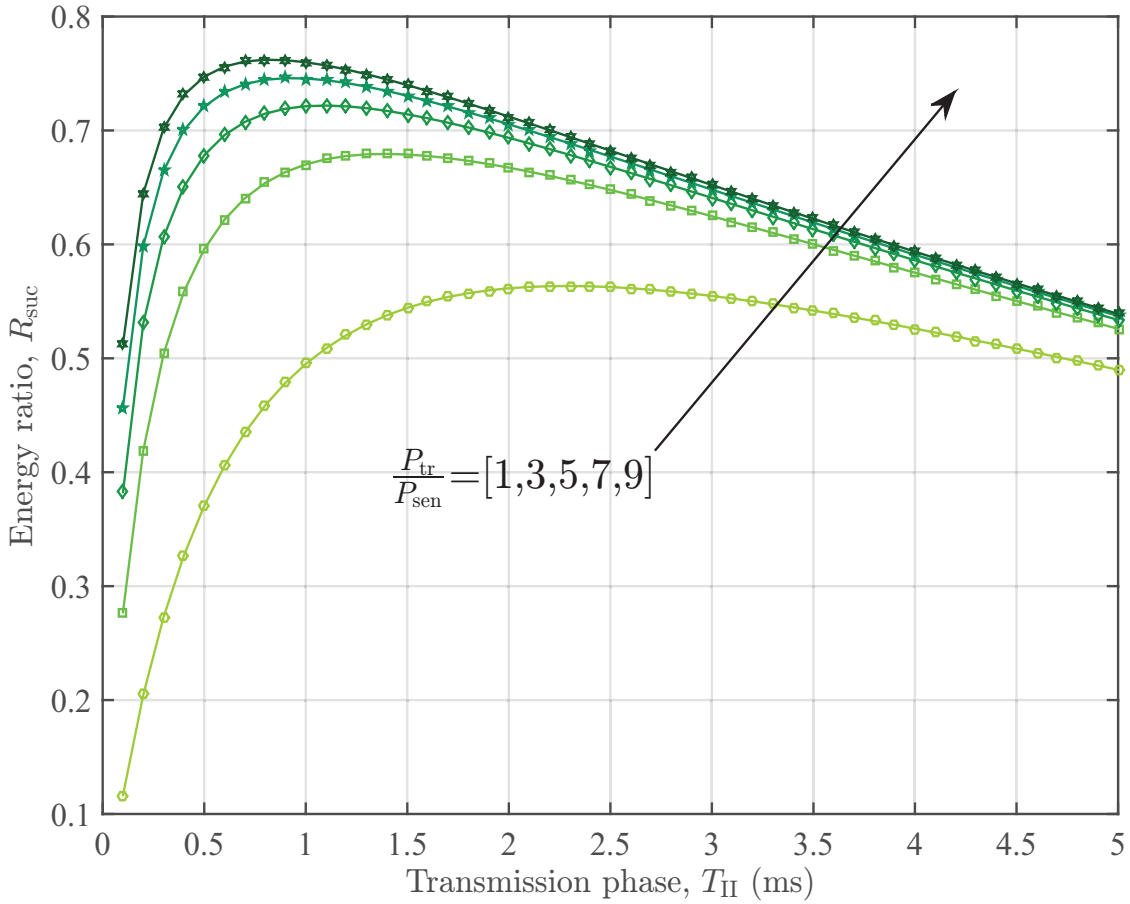

Figure 4.17: Energy ratio of energy consumed in successful transmission over the total energy consumption, where $p_f = 0.1$, $\lambda = 50$ ms and $\mu = 10$ ms.

Fig. 4.17 plots R_{suc} as a function of T_{II} for different ratios of transmission power over sensing power. R_{suc} increases at first because both $\mathcal{E}_{\text{all}}$ and $\mathcal{E}_{\text{T}}$ get larger by similar increment. R_{suc} starts decreasing when T_{II} keeps increasing since more energy is wasted. For larger $\frac{P_{\text{tr}}}{P_{\text{sen}}}$, R_{suc} reaches its maximum at a smaller T_{II} because energy consumed in transmission increases faster.

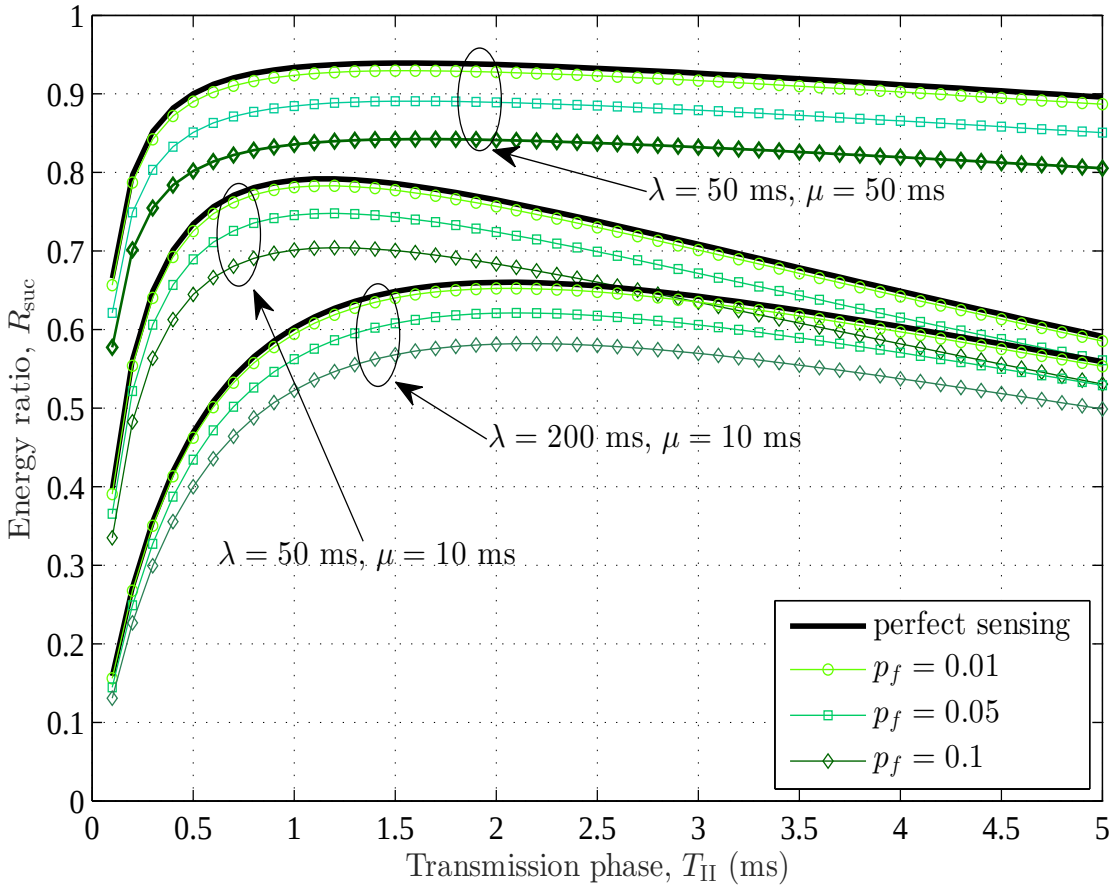

Figure 4.18: Energy ratio versus transmission phase for various false alarm probabilities and PU parameter pairs.

Fig. 4.18 presents the effect of p_f on R_{suc} for various PU parameter pairs. We observe that R_{suc} is smaller for larger p_f as expected intuitively. For larger μ or smaller λ, R_{suc} maximizes to a larger value at a smaller T_{II} mainly because SU has more chances to transmit successfully.

Note that the collision probability is a function of SU period, which monotonically increases in $T_{\rm S}$, and then in $T_{\rm II}$. To protect PU transmission, the collision probability must be restricted to be smaller than a tolerable collision probability $C_{\max}$ (i.e. $p'_C(T_{\rm II}) \leq C_{\max}$). Hence, given SU parameters (i.e. $P_{\rm sen}$, $P_{\rm tr}$ and $T_{\rm I}$) and PU parameter pair (i.e. λ and μ), the optimal transmission phase can be determined by solving the optimization problem, given by

$$\begin{aligned} &\max_{T_{\rm II}} R_{\rm suc} \\ &\text{s.t. } p'_C(T_{\rm II}) \leq C_{\max}. \end{aligned} \tag{4.43}$$

The first-order derivative of p'_C with respect to $T_{\rm II}$ is calculated by

$$\frac{\partial p'_C(T_{\rm II})}{\partial T_{\rm II}} = \frac{\left[\frac{1}{\lambda}\beta_{on}(1-\beta_{off})^2 + \frac{1}{\mu}\beta_{off}(1-\beta_{on})^2\right](1-p_f)}{(2-\beta_{on}-\beta_{off})^2}, \tag{4.44}$$

which is positive for $T_{\rm II} > 0$. $p'_C(T_{\rm II})$ is monotonically increasing of $T_{\rm II}$ for fixed $T_{\rm I}$. The optimal value of $T_{\rm II}$ is given by $T^*_{\rm II} = \min\left[\arg\max_{T_{\rm II}} R_{\rm suc},\ p_C^{-1'}(p_{\max})\right]$, where $p_C^{-1'}(\cdot)$ is the inverse of $p'_C(\cdot)$.

4.4.3 Effect of False Alarm on Queuing Performance

In this section, we evaluate the queuing performance of slotted secondary transmission with AMc. We assume that SU information data is fragmented into equal-size small packets, the size of which is chosen such that j packets can be transmitted over one $T_{\rm II}$ when the primary channel is available and secondary link can support transmission rate $R_j, j = 0, 1, \cdots, N$. $R_0 = 0$ corresponds to the case that SU decides not to transmit because of unacceptable secondary link quality. The newly arrived packets will be put into a first-in-first-out (FIFO) buffer with K waiting positions before being delivered over the next available transmission phase. New arrivals will be dropped if the queue is full. Only those packets that are successfully received will be removed from the buffer. Let $\mathcal{A}_i \in \{0, 1, \cdots\}$ represent the number of packets arrived in the ith $T_{\rm S}$, which is assumed to be poisson distributed. We have

$$p_a = \Pr[\mathcal{A}_i = a] = \frac{(\eta T_{\rm S})^a e^{-\eta T_{\rm S}}}{a!},\ a = 0, 1, \cdots, \tag{4.45}$$

where η is the average packet arrival rate.

The service process is independent of the arrival process. We denote the service state of the ith T_{S} as $\mathcal{D}_i$, where $\mathcal{D}_i \in \{C, W, S, F_W, F_C\}$. When $\mathcal{D}_i = W, C, F_W$ or F_C, no packet was successfully transmitted since SU waits for channel availability or collision/sensing error occurs. When $\mathcal{D}_i = S$ and rate R_j is used, j packets are transmitted successfully. Let $\mathcal{L}_i$ denote the instantaneous queue length at the beginning of ith T_{S}, where $\mathcal{L}_i \in \{0, 1, ..., K\}$. As such, $\mathcal{L}_i$ depends on $\mathcal{L}_{i-1}$, $\mathcal{D}_{i-1}$ and $\mathcal{A}_{i-1}$. Specifically, the queue length will be updated as Eq. (4.9). To investigate secondary queuing performance, we construct a two-dimensional Markov chain with state being the $(\mathcal{D}_i, \mathcal{L}_i)$ pair. Based on the analysis in the previous subsection, the probability transition matrix $\mathbf{P}'_{\mathbf{Q}}$ is rewritten in a block form as

$$\mathbf{P}'_{\mathbf{Q}} = \begin{bmatrix} p'_{W|W}\mathbf{P}'_{\mathrm{N}} & \mathbf{O} & \mathbf{P}'_{\mathrm{N}} & p'_{W|F_W}\mathbf{P}'_{\mathrm{N}} & \mathbf{O} \\ p'_{S|W}\mathbf{P}'_{\mathrm{N}} & p'_{S|S}\mathbf{P}'_{\mathrm{T}} & \mathbf{O} & p'_{S|F_W}\mathbf{P}'_{\mathrm{N}} & \mathbf{O} \\ p'_{C|W}\mathbf{P}'_{\mathrm{N}} & p'_{C|S}\mathbf{P}'_{\mathrm{T}} & \mathbf{O} & p'_{C|F_W}\mathbf{P}'_{\mathrm{N}} & \mathbf{O} \\ p'_{F_W|W}\mathbf{P}'_{\mathrm{N}} & \mathbf{O} & \mathbf{O} & p'_{F_W|F_W}\mathbf{P}'_{\mathrm{N}} & \mathbf{P}'_{\mathrm{N}} \\ p'_{F_C|W}\mathbf{P}'_{\mathrm{N}} & p'_{F_C|S}\mathbf{P}'_{\mathrm{T}} & \mathbf{O} & p'_{F_C|F_W}\mathbf{P}'_{\mathrm{N}} & \mathbf{O} \end{bmatrix}, \tag{4.46}$$

where $\mathbf{O}$ represents $(K+1) \times (K+1)$ zero matrix. When $\mathcal{D}_{i-1} = W, C, F_W$ or F_C, no packet was successfully transmitted. Hence, $\mathcal{L}_i$ only depends on $\mathcal{L}_{i-1}$ and $\mathcal{A}_{i-1}$. Sub-matrices $\mathbf{P}'_{\mathrm{N}}$ can be calculated by

$$\mathbf{P}'_{\mathrm{N}} = \begin{bmatrix} p_0 & 0 & 0 & \dots & 0 \\ p_1 & p_0 & 0 & \dots & 0 \\ p_2 & p_1 & p_0 & \dots & 0 \\ p_3 & p_2 & p_1 & \dots & 0 \\ \vdots & \vdots & \vdots & \ddots & \vdots \\ M_K & M_{K-1} & M_{K-2} & \dots & 1 \end{bmatrix}, \tag{4.47}$$

where M_j denotes the probability that more than j arrivals in T_{S}, given by

$$M_j = \sum_{a=j}^{\infty} p_a = 1 - \frac{\Gamma(j+1, \eta T_{\mathrm{S}})}{j!}, \tag{4.48}$$

where $\Gamma(\cdot, \cdot)$ is the incomplete gamma function.

When $\mathcal{D}_{i-1} = S$, j packets are successfully transmitted if secondary link supports rate $R_j, j = 0, 1, \cdots, N$. According to Eq. (4.9), $\mathbf{P}'_{\mathrm{T}}$ is given by

$$\mathbf{P}'_{\mathrm{T}} = \begin{bmatrix} p_0 & p_0 \sum_{j=1}^{N} \pi_j & p_0 \sum_{j=2}^{N} \pi_j & \cdots & 0 \\ p_1 & p_0\pi_0 + p_1 \sum_{j=1}^{N} \pi_j & p_0\pi_1 + p_1 \sum_{j=2}^{N} \pi_j & \cdots & 0 \\ p_2 & p_1\pi_0 + p_2 \sum_{j=1}^{N} \pi_j & p_0\pi_0 + p_1\pi_1 + p_2 \sum_{j=2}^{N} \pi_j & \cdots & p_0\pi_N \\ \vdots & \vdots & \vdots & \ddots & \vdots \\ p_{K-1} & p_{K-2}\pi_0 + p_{K-1} \sum_{j=1}^{N} \pi_j & p_{K-3}\pi_0 + p_{K-2}\pi_1 + p_{K-1} \sum_{j=2}^{N} \pi_j & \cdots & \sum_{i=1}^{K} p_{i-1}\pi_i \\ M_K & M_{K-1}\pi_0 + M_K \sum_{j=1}^{N} \pi_j & M_{K-2}\pi_0 + M_{K-1}\pi_1 + M_K \sum_{j=2}^{N} \pi_j & \cdots & \pi_0 + \sum_{j=1}^{N} M_j\pi_j \end{bmatrix}. \tag{4.49}$$

The steady state probabilities of the two-dimensional Markov chain, denoted by

$$\begin{aligned} \varphi_{\mathbf{Q}} = [&\varphi_{W,0}, \cdots, \varphi_{W,K}, \varphi_{S,0}, \cdots, \varphi_{S,K}, \varphi_{C,0}, \cdots, \varphi_{C,K} \\ &\varphi_{F_W,0}, \cdots, \varphi_{F_W,K}, \varphi_{F_C,0}, \cdots, \varphi_{F_C,K}], \end{aligned} \tag{4.50}$$

is the left eigenvector of $\mathbf{P}_{\mathbf{Q}}$ corresponding to eigenvalue one, which can be calculated from the forward equations and the normalization equation. The stationary distribution of queue length can be found as $\varphi_k = \sum_{\mathcal{D}=W,S,C,F_W,F_C} \varphi_{\mathcal{D},k},\ k = 0, 1, \cdots, K$.

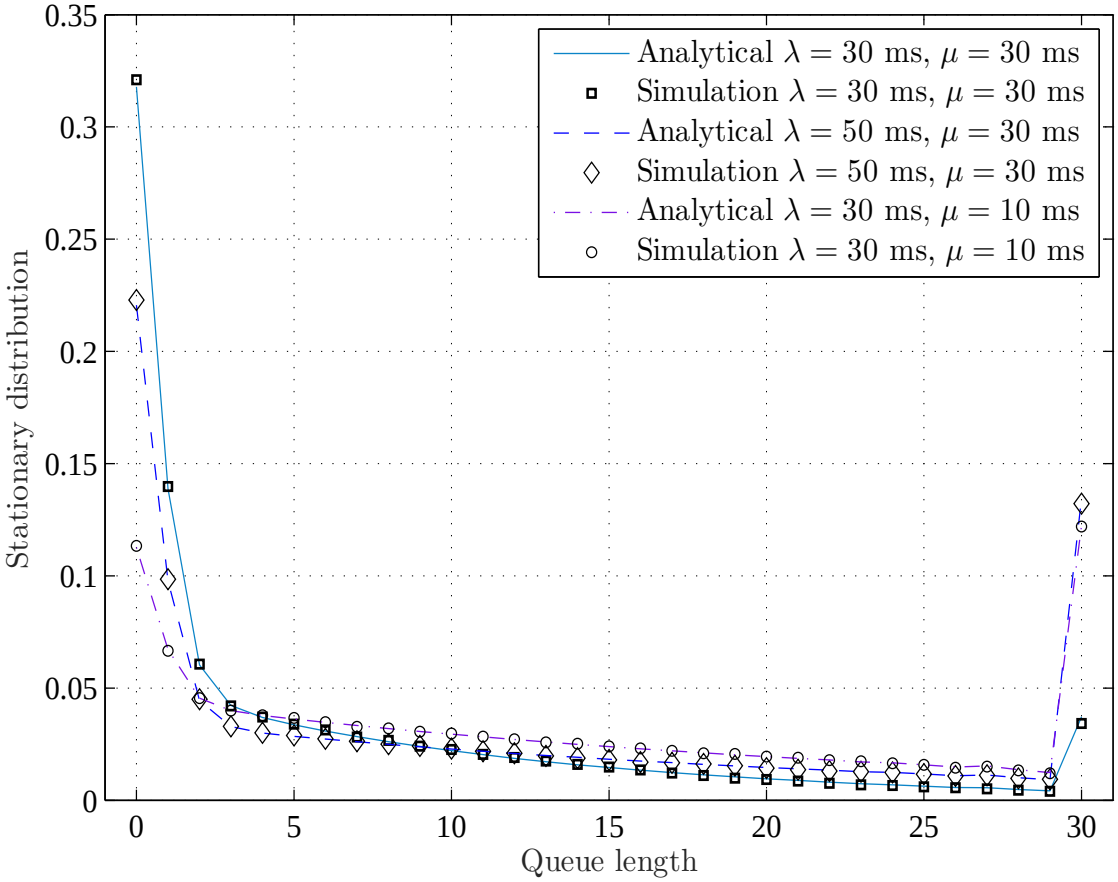

Figure 4.19: Analytical and simulation results on the stationary distribution of queue length with different PU parameters, where $K = 30$ and $\bar{\gamma} = 20$ dB.

Fig. 4.19 compares the analytical results of stationary distribution of the queue length against corresponding Monte Carlo simulations. The perfect match here validates our analytical approaches. For larger μ or smaller λ, since SU can acquire the PU channel for longer time duration, φ_k is larger for smaller k.

We evaluate the queuing performance in term of throughput, queuing delay and packet drop rate. The average throughput of secondary system, denoted by $\mathbb{E}[Th]$, can be calculated as

$$\mathbb{E}[Th] = p_S \sum_{k=0}^{K} \mathbb{E}[Th|k]\varphi_k, \tag{4.51}$$

where $\mathbb{E}[Th|k]$ is the average number of packets successfully transmitted per SU

period, given k packets waiting in the queue, which can be calculated as

$$\mathbb{E}[Th|k] = \begin{cases} 0, & k = 0; \\ \sum_{i=1}^{k} i\pi_i + k \sum_{j=k+1}^{N} \pi_j, & 0 < k < N; \\ \sum_{i=1}^{N} i\pi_i, & N \leq k \leq K. \end{cases} \tag{4.52}$$

The average queue-length, denoted by $\mathbb{E}[Q_L]$, can be calculated as $\mathbb{E}[Q_L] = \sum_{k=0}^{K} k\varphi_k$. Applying the Little's law, the average queuing delay $\mathbb{E}[T_Q]$ can be evaluated by

$$\mathbb{E}[T_Q] = \frac{\mathbb{E}[Q_L]}{\mathbb{E}[Th]} = \frac{\sum_{k=0}^{K} k\varphi_k}{p_S \sum_{k=0}^{K} \mathbb{E}[Th|k]\varphi_k}. \tag{4.53}$$

Let N_d denote the number of dropped packets over one T_{II}, whose probability mass function is calculated as

$$\begin{aligned} \Pr[N_d = m] &= \sum_{k=0}^{K} \Pr[N_d = m, k \text{ packets in queue}] \\ &= \sum_{k=0}^{K} \Pr[\mathcal{A} = K - k + m]\varphi_k, \end{aligned} \tag{4.54}$$

where the second equality follows that, given k packets waiting in the queue, m packets will be dropped only when $K - k + m$ packets arrive. The average number of dropped packets can be calculated as

$$\mathbb{E}[N_d] = \sum_{m=1}^{\infty} m \left[\sum_{k=0}^{K} \frac{(\eta T)^{K-k+m} e^{-\eta T}}{(K-k+m)!} \varphi_k \right]. \tag{4.55}$$

Fig. 4.20 (a) shows the average throughput versus arriving rate for various average SU received SNRs and false alarm probabilities. The throughput saturates as input traffic intensity grows because packets are dropped when the queue is full. Intuitively, secondary system suffers throughput loss from spectrum sensing error. In Fig. 4.20 (b), we plot the average queuing delay as a function of average arrival rate. As p_f increases, the average queuing delay gets larger and saturates at a smaller η because SU has less chances to transmit successfully. For lager $\bar{\gamma}$, transmission schemes with

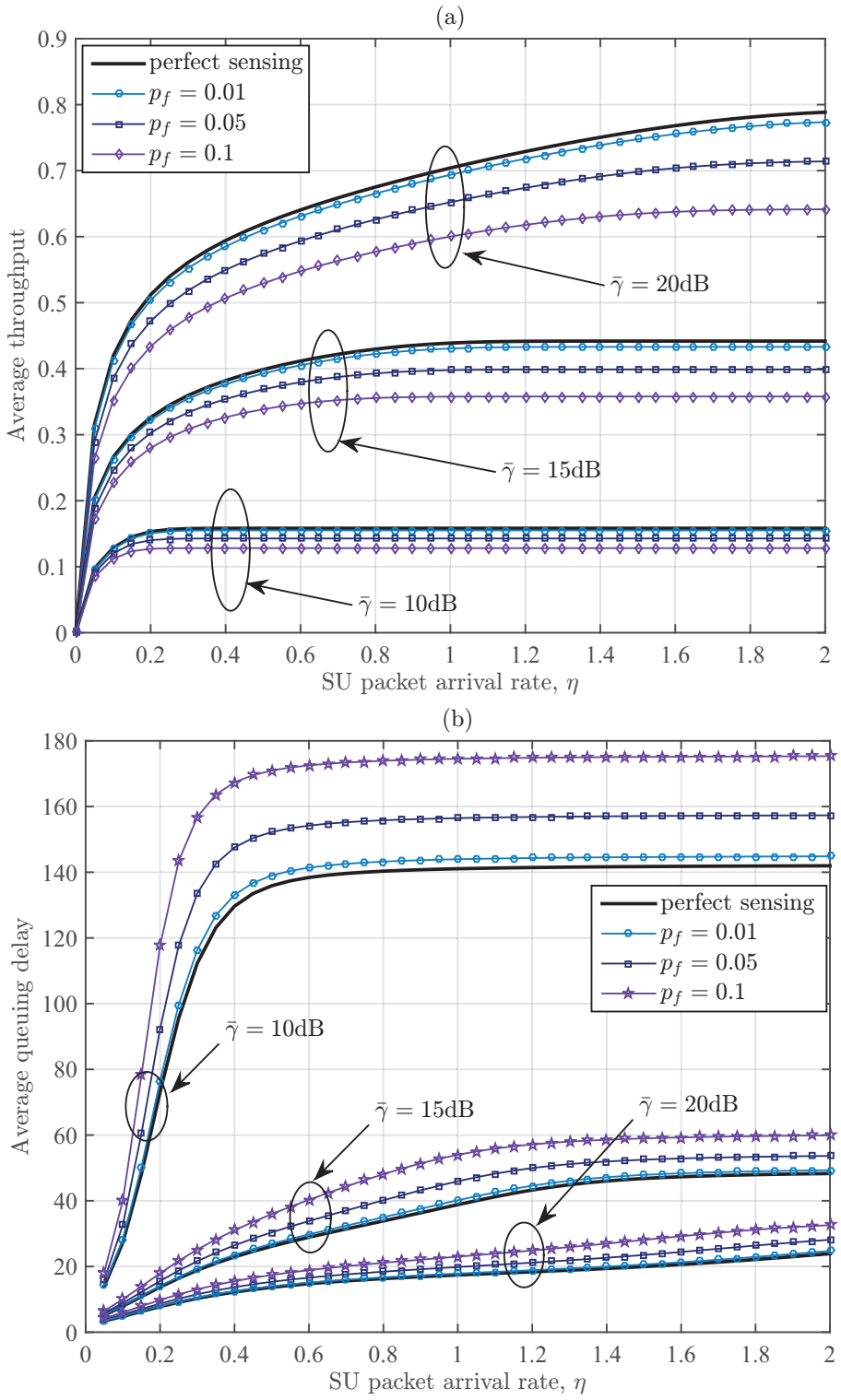
(a)
perfect sensing
$p_f = 0.01$
$p_f = 0.05$
$p_f = 0.1$
$\bar{\gamma} = 20$dB
$\bar{\gamma} = 15$dB
$\bar{\gamma} = 10$dB
Average throughput
SU packet arrival rate, η
(b)
perfect sensing
$p_f = 0.01$
$p_f = 0.05$
$p_f = 0.1$
$\bar{\gamma} = 10$dB
$\bar{\gamma} = 15$dB
$\bar{\gamma} = 20$dB
Average queuing delay
SU packet arrival rate, η

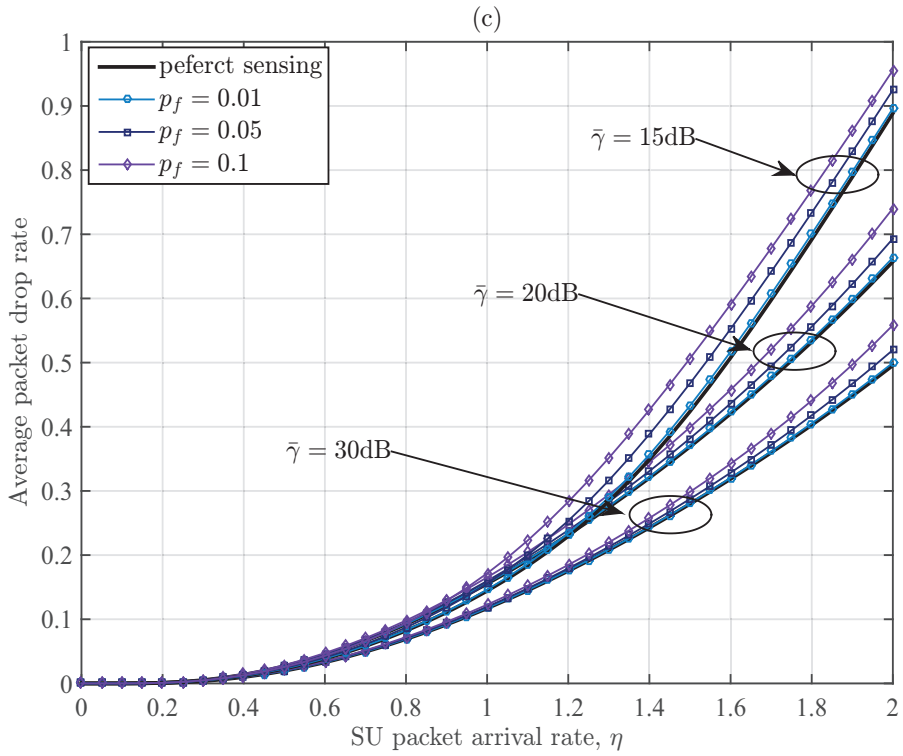

Figure 4.20: The effect of sensing error on average queuing delay, average throughput and packet drop probability versus various secondary channel quality.

higher data rate are used more frequently, which helps improve the throughput and reduce the queuing delay. The queue is filled up at a faster rate for smaller $\bar{\gamma}$ because of the lower throughput. Therefore, the packet drop rate increases more sharply (see Fig. 4.20 (c)).

4.4.4 Effect of Miss Detection

When the miss detection probability is not zero (i.e. $p_m = \Pr[H_i^* = 0 | H_i = 1] \neq 0$), we can introduce two new states and construct a seven-state discrete-time Markov chain to characterize the slotted secondary transmission. The Markov chain modeling and state definition are presented in Fig. 4.21. State C_M corresponds to the case that, due to miss detection in the ith sensing phase, SU transmits in the ith transmission phase and causes collision. State C_N represents the event that miss detection occurs in the $i+1$th sensing phase and the secondary transmission over the ith transmission

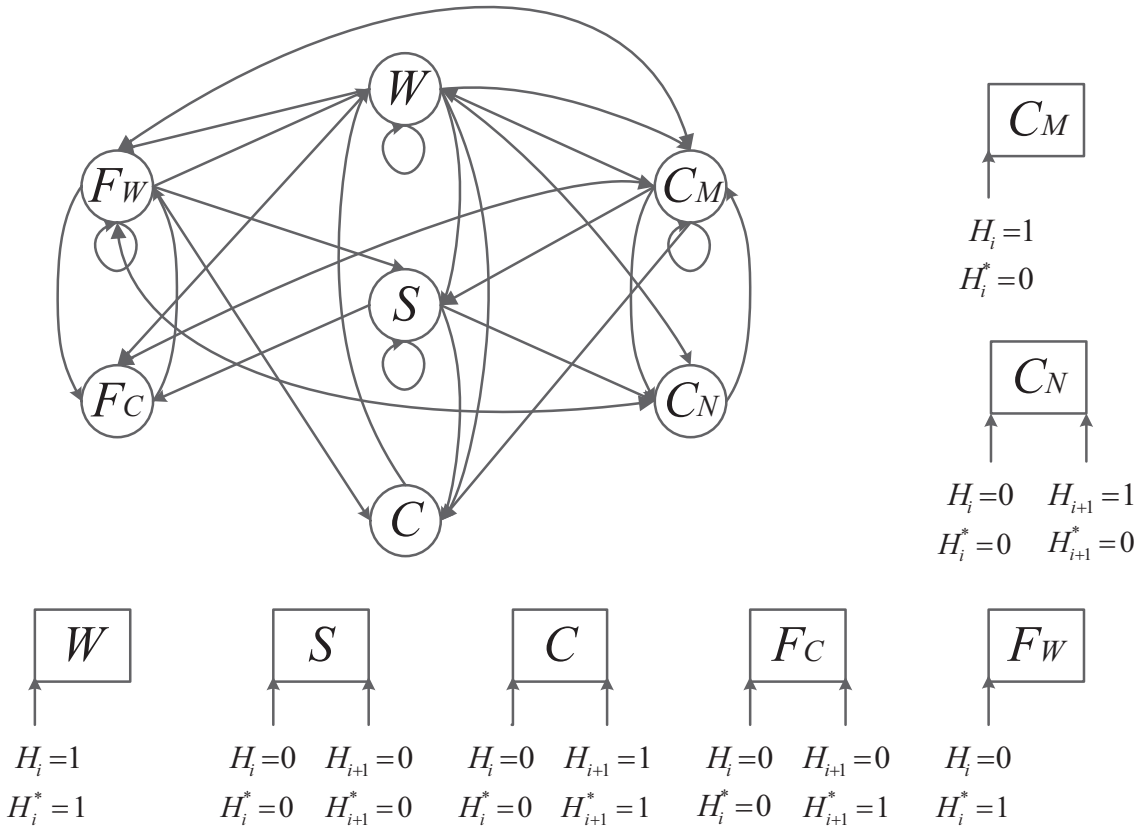

Figure 4.21: Seven-state Markov model of slotted secondary transmission under spectrum sensing imperfection.

phase collides with PU transmission. The stationary distribution can be obtained by solving the forward equations and normalization equation and applied to performance evaluation.

In particular, the total collision probability can be calculated as $P_C^* = p_C + p_{C_M} + p_{C_N}$, where p_{C_M} and p_{C_N} are the stationary probabilities in state C_M and state C_N, respectively. p_C characterizes the inevitable collision due to slotted secondary transmission scheme and $p_{C_M} + p_{C_N}$ accounts for the extra collision because of miss detection. The queueing performance can be evaluated by the tow dimensional Markov chain approach. Note that, when $\mathcal{D}_{i-1} = C_M$ or C_N and rate R_j is used, j packets are transmitted and lost due to miss detection. The transition probability matrix $\mathbf{P}''_{\mathrm{Q}}$

is written in a compact form given by

$$\mathbf{P}''_{\mathrm{Q}} = \begin{bmatrix} p_{W|W}\mathbf{P}_{\mathrm{N}} & \mathbf{O} & \mathbf{P}_{\mathrm{N}} & p_{W|F_W}\mathbf{P}_{\mathrm{N}} & \mathbf{O} & p_{W|C_M}\mathbf{P}_{\mathrm{T}} & \mathbf{O} \\ p_{S|W}\mathbf{P}_{\mathrm{N}} & p_{S|S}\mathbf{P}_{\mathrm{T}} & \mathbf{O} & p_{S|F_W}\mathbf{P}_{\mathrm{N}} & \mathbf{O} & p_{S|C_M}\mathbf{P}_{\mathrm{T}} & \mathbf{O} \\ p_{C|W}\mathbf{P}_{\mathrm{N}} & p_{C|S}\mathbf{P}_{\mathrm{T}} & \mathbf{O} & p_{C|F_W}\mathbf{P}_{\mathrm{N}} & \mathbf{O} & p_{C|C_M}\mathbf{P}_{\mathrm{T}} & \mathbf{O} \\ p_{F_W|W}\mathbf{P}_{\mathrm{N}} & \mathbf{O} & \mathbf{O} & p_{F_W|F_W}\mathbf{P}_{\mathrm{N}} & \mathbf{P}_{\mathrm{N}} & p_{F_W|C_M}\mathbf{P}_{\mathrm{T}} & \mathbf{O} \\ p_{F_C|W}\mathbf{P}_{\mathrm{N}} & p_{F_C|S}\mathbf{P}_{\mathrm{T}} & \mathbf{O} & p_{F_C|F_W}\mathbf{P}_{\mathrm{N}} & \mathbf{O} & p_{F_C|C_M}\mathbf{P}_{\mathrm{T}} & \mathbf{O} \\ p_{C_M|W}\mathbf{P}_{\mathrm{N}} & p_{C_M|S}\mathbf{P}_{\mathrm{T}} & \mathbf{O} & p_{C_M|F_W}\mathbf{P}_{\mathrm{N}} & \mathbf{O} & p_{C_M|C_M}\mathbf{P}_{\mathrm{T}} & \mathbf{O} \\ p_{C_N|W}\mathbf{P}_{\mathrm{N}} & \mathbf{O} & \mathbf{O} & p_{C_N|F_W}\mathbf{P}_{\mathrm{N}} & \mathbf{O} & p_{C_N|C_M}\mathbf{P}_{\mathrm{T}} & \mathbf{P}_{\mathrm{T}} \end{bmatrix}. \tag{4.56}$$

With the stationary distribution of the queue length, the throughput of secondary transmission can be obtained by Eq. (4.3.2). Arriving packets will be dropped at the secondary transmitter if the buffer is full. Additionally, buffered secondary packets will be lost at the secondary receiver due to collision with PU transmission as the result of miss detection. The total packet loss probability can be evaluated by

$$P''_L = P_D + (1 - P_D)(p_{C_M} + p_{C_N}). \tag{4.57}$$

Accordingly, the average energy consumption can be calculated as

$$R''_{\mathrm{suc}} = \frac{p_S(P_{\mathrm{tr}}T_{\mathrm{II}} + P_{\mathrm{sen}}T_{\mathrm{I}})}{(p_S + p_C + p_{F_C} + p_{C_M} + p_{C_N})P_{\mathrm{tr}}T_{\mathrm{II}} + P_{\mathrm{sen}}T_{\mathrm{I}}}. \tag{4.58}$$

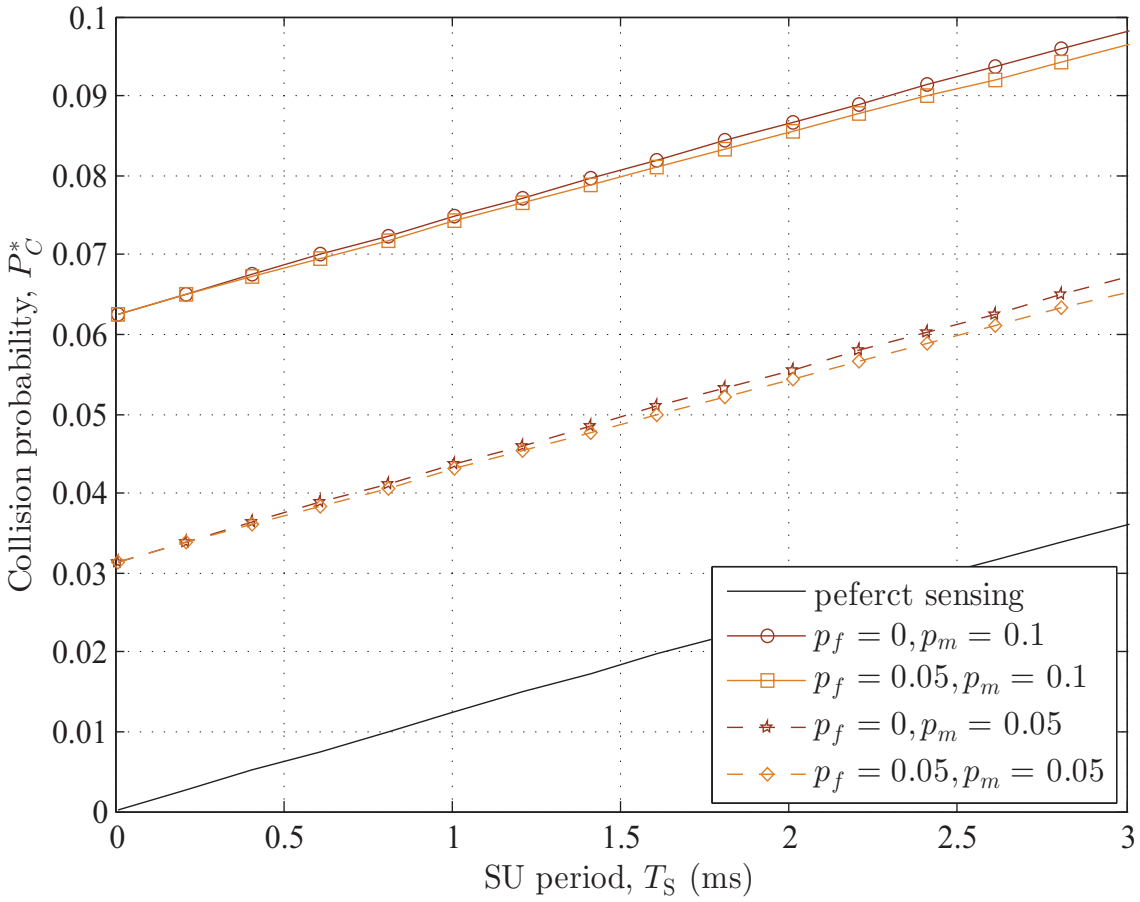

Figure 4.22: Effect of sensing imperfection on total collision probability, where $\lambda = 50$ ms and $\mu = 30$ ms.

Fig. 4.22 illustrates the effect of sensing imperfection on the total collision probability. We can see that miss detection dramatically increases the total collision probability, whereas false alarm reduces total collision probability slightly. Therefore, to protect PU transmission, the miss detection probability should be made as small as possible in practice.

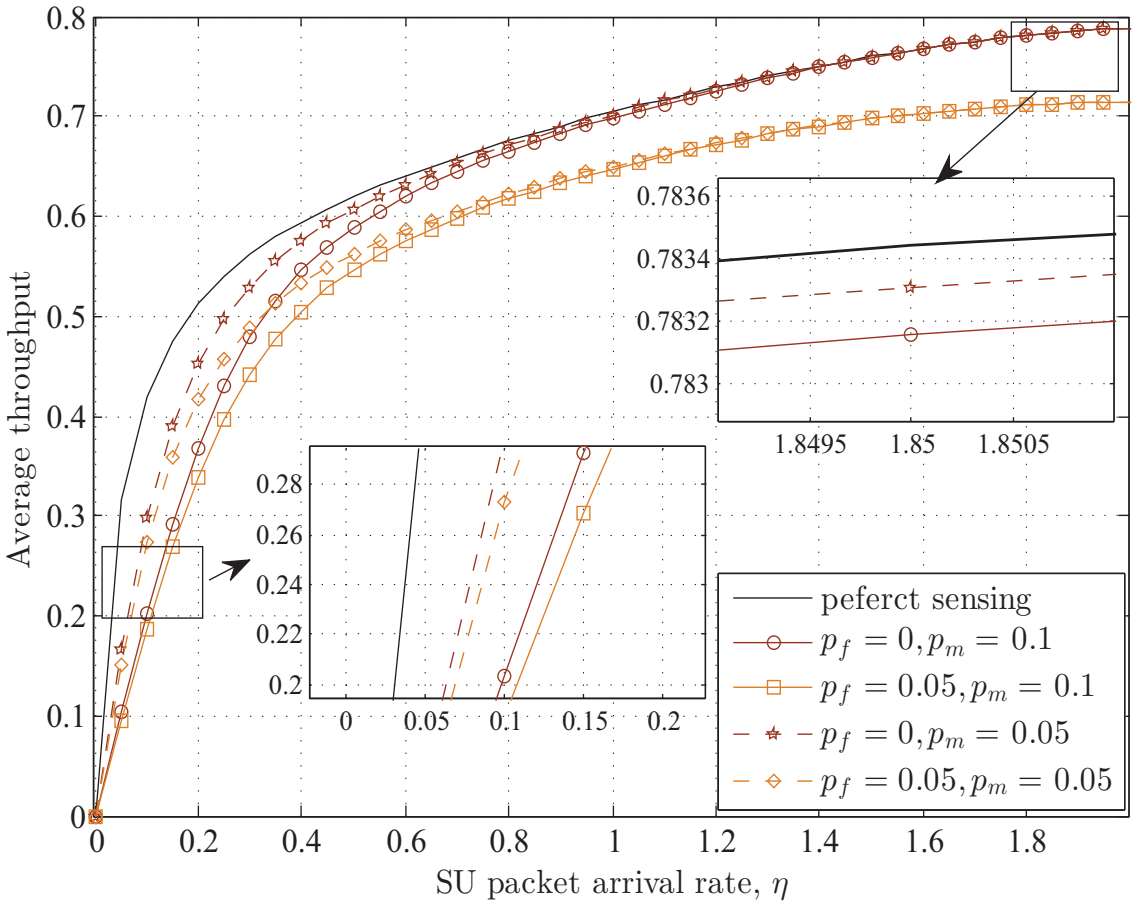

Figure 4.23: Effect of sensing imperfection on secondary throughput, where $T_S = 2$ ms, $\lambda = 50$ ms and $\mu = 30$ ms.

Fig. 4.23 presents the secondary throughput as a function of SU packet arrival rate for various false alarm probability and miss detection probability pairs. We observe that both false alarm and miss detection have deleterious effect on the secondary throughput. When SU packet arrival rate is low, buffer overflow barely occurs. Hence, packet loss due to miss detection is the main factor that reduces secondary throughput. While SU packet arrival rate grows, packet drop because of buffer overflow becomes dominant in limiting the secondary throughput, and the effect of miss detection diminishes. Meanwhile, false alarm reduces the SU transmission capability and has more significant impact on secondary throughput. Packet loss due to miss detection only slightly reduces the secondary throughput when the SU packet arrival rate is high.

4.5 Concluding Remarks

We studied secondary transmission performance of slotted transmission. We first proposed a three-state discrete-time Markov chain to model slotted secondary transmission with periodic spectrum sensing. The stationary probabilities that SU waits/transmits/collides with PU transmission are calculated. The Markov model is then applied to analyze the delay performance of secondary packet transmission. For short packet transmission, a two dimensional Markov chain is formed to evaluate the queuing delay, average throughput and packet drop probability assuming SU adopts adaptive modulation. When packet size is large, we derive the PMF of EDT considering both fixed-rate and variable-rate transmission, respectively.

We propose a five-state discrete-time Markov chain to model slotted secondary transmission with imperfect sensing. The stationary probabilities are calculated in closed form to analyze collision probability and SU successful transmission probability. The stationary distribution is then applied to select optimal transmission phase duration by maximizing the energy efficiency, subject to a collision probability constrain. A two dimensional Markov chain is formed to evaluate the throughput, queuing delay and packet drop rate assuming SU adopts adaptive modulation and coding. We show that false alarm has significant effect on the secondary throughput, whereas miss detection only notably reduces the secondary throughput when the packet arrival rate is low.

Derivation of transition probability for two-dimensional Markov chain

In this appendix, we derive the transition probabilities in $\mathbf{P}_{\mathrm{T}}$ and $\mathbf{P}_{\mathrm{N}}$, respectively. We firstly derive each entry in matrix $\mathbf{P}_{\mathrm{T}}$, denoted by $\Pr[\mathcal{L}_i = m|S, \mathcal{L}_{i-1} = n]$. Note that j packets are successfully transmitted when rate R_j is used, which is selected with probability $\pi_j,\ j = 0, 1, \cdots, N$. For $m = 0$, given $\mathcal{D}_{i-1} = S$ and $\mathcal{L}_{i-1} = n,\ n = 0, 1, \cdots, K$, the queue can not be emptied even the highest rate is used if $n > N$. If $n \leq N$, $\mathcal{L}_i = 0$ only when the secondary link can support rate n or higher as well as no packet arrives in the $i-1$th T_{S}. Hence, the entries in first row in $\mathbf{P}_{\mathrm{T}}$ can be

calculated by

$$\Pr[\mathcal{L}_i = 0|S, \mathcal{L}_{i-1} = n] = \begin{cases} 0, & n > N; \\ (1-p_a)\sum_{j=n}^{N-1} \pi_j, & n \leq N. \end{cases} \tag{4.59}$$

If $n = 0$, based on the queue recursion, $m = 1$ when one packet arrives in the $i-1$th T_{S}. If $1 \leq n \leq N$, $m = 1$ only when $n-1$ departures and no arrival, or at least n packets departed and one packet arrives. If $n = N+1$, $m = 1$ only when highest rate, R_N, is used and no packet arrives. For $n > N+1$, m can not be one. Then, the entries in second row can be calculated as

$$\Pr[\mathcal{L}_i = 1|S, \mathcal{L}_{i-1} = n] = \begin{cases} p_a, & n = 0; \\ (1-p_a)\pi_{n-1} + p_a \sum_{j=n}^{N-1} \pi_j, 1 \leq & n \leq N; \\ (1-p_a)\pi_N, & n = N+1; \\ 0, & n > N+1. \end{cases} \tag{4.60}$$

Following similar analytical step, when $2 \leq m \leq K$, the entries can be calculated by

$$\Pr[\mathcal{L}_i = m|S, \mathcal{L}_{i-1} = n] = \begin{cases} 0, & n-m > N-1; \\ & \text{or } n-m < -1; \\ (1-p_a)\pi_{n-m}, & n-m = N-1; \\ (1-p_a)\pi_{n-m} + p_a\pi_{n-(m-1)}, & 0 \leq n-m < N-1; \\ p_a\pi_0, & n-m = -1. \end{cases} \tag{4.61}$$

The special case $m = n = K$ can be calculated by

$$\Pr[\mathcal{L}_i = K|S, \mathcal{L}_{i-1} = K] = \pi_0 + p_a\pi_1. \tag{4.62}$$

Substituting all the entries, $\mathbf{P}_{\mathrm{T}}$ is given by Eq. (4.15).

If $\mathcal{D}_{i-1} = W$ or $\mathcal{D}_{i-1} = C$, the queue length would remain unchanged or add up one, depending absolutely on the arrival process. Hence,

$$\Pr[\mathcal{L}_i = m|W,\, \mathcal{L}_{i-1} = n] = \Pr[\mathcal{L}_i = m|C,\ \mathcal{L}_{i-1} = n] = \begin{cases} p_a, & 0 \leq m = n+1 \leq K; \\ 1 - p_a, & 0 \leq m = n < K; \\ 1, & m = n = K; \\ 0, & \text{otherwise.} \end{cases} \tag{4.63}$$

As such, the corresponding $(K+1) \times (K+1)$ transition matrix given SU waits or collides with PU transmission at current T_{S} is given by Eq. (4.14).

Chapter 5

Conclusions

Adaptive transmission is attractive technology to improve both spectrum efficiency and energy efficiency with guaranteed bit error performance in wireless communication systems. As the wireless data traffic is expected to continue its growth in the near future, adaptive transmission is a promising candidate to support intensive wireless transmission.

Different from conventional systems, transmission time is no longer constant but is random variable due to rate adaptation. We studied the statistics of transmission time for block fading channels, where selected rate remains unchanged over a fixed-length time interval, and Markov channels, where selected rate has been invariant for random-length time duration. We extended the analytical results to EDT evaluation of secondary packet transmission under interweave cognitive radio system. We studied the statistics of EDT assuming SU adopts continuous spectrum sensing and semi-periodic sensing. The numerical examples are presented to illustrate and validate the analytical results.

With more practical sensing policy, we proposed a discrete-time Markov model to characterize secondary slotted transmission under sensing perfection. The stationary distribution is applied to evaluate the collision probability with PU transmission. An optimal length of SU period is calculated by maximizing the energy efficiency. To analyze the secondary queuing performance with adaptive modulation and coding, we construct a two dimensional Markov model. The queuing performance in term of throughput, queuing delay and packet loss probability are studied. We also discussed the effect of sensing imperfection.

Chapter 6

Future Work

6.1 Secondary Sensor Transmission with RF Energy Harvesting

For certain wireless implementations, charging or replacing the batteries can be of high cost, (e.g. the large scale wireless sensor networks). Due to its convenience and flexibility, radio frequency (RF) energy harvesting becomes a promising solution for powering wireless sensors. Recently, because of the intensive deployment of WiFi and small-cell cellular systems, RF energy harvesting receives great research interest. The feasibility of RF energy harvesting is experimentally proved from a hardware implementation perspective [88]. In [89], a prototype design has been presented to enable two devices communicate with RF energy as the only power source. However, there is insufficient analytical results on the statistics of harvested RF energy over fading wireless channels.

The amount of harvested RF energy is a critical design metric for RF energy harvesting based wireless transmission. Previous works typically use an energy queue to characterize the dynamics of the RF energy harvesting process, where a fixed amount of RF energy is assumed to reach the sensor at a random time instant. The overall transmission completion time is analyzed in [90]. The maximum total throughput is studied for a communication network with RF energy harvesting in [91], based on the assumption that a node harvests one unit of energy with a certain probability in a time slot. The energy arrival process is inherently time-varying. Exponential and Gamma distributions are widely used for characterizing the amount

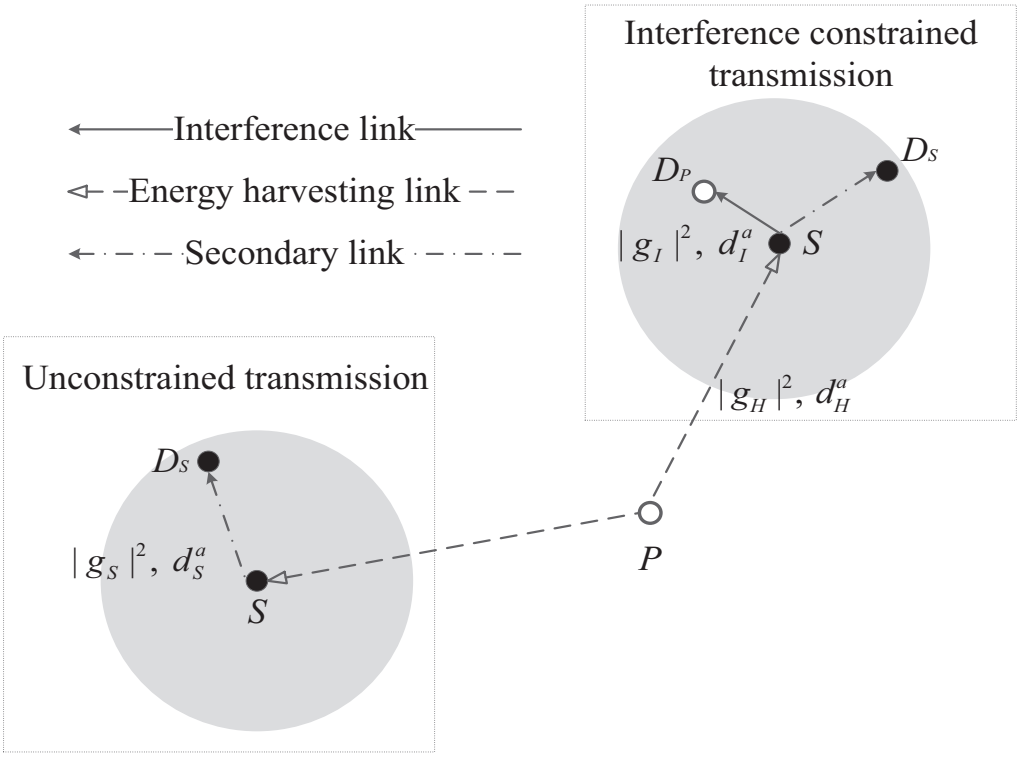

Figure 6.1: Unconstrained/interference constrained secondary sensor transmission with RF harvested energy.

of harvested RF energy over a channel coherence time [92–94]. [93] investigates the packet loss probability of overlaid wireless sensor transmission with harvested RF energy, where the sensor is assumed to be harvesting RF energy over multiple channel coherence time. In [95], the optimal mode switching rule achieving desired trade-offs between wireless information transfer and RF energy harvesting is investigated. In [96], the transmission probability of a RF powered user is investigated in a cognitive radio network. [97] proposes statistical models for battery recharging time over fading channels, where the recharging time is inversely proportional to the received power. Applying the Markov modeling, an optimal mode switch policy is proposed in [98] for the sensor to decide to transmit information or to harvest RF energy, where the sensor nodes are able to harvest RF energy from primary transmission. [99] investigates statistics of RF harvested energy, where the wireless sensor node harvests the RF energy from a multi user MIMO system.

Different from previous work, we intend to investigate the statistics of harvested

RF energy in a time-varying fading channel over a random-length time duration. For delay sensitive traffic, assuming that sensor uses all the harvested RF energy to transmit, we can derive the exact statistics of received SNR. To better protect primary transmission, we can also derive the PDF of the received SNR, where secondary sensor transmission must satisfy an interference constraint as shown in Fig. 6.1. For delay insensitive traffic, we intent to propose two low-complexity transmission strategies, depending on if the channel information is available at the sensor or not. The delay performance can be evaluated.

6.2 Performance Evaluation for Multiple PU Multiple SU Cognitive Radio Network

Multiple PU channels provide the secondary system with more flexibility. A secondary system with multiple SUs can explore the transmission availability of the PU system more effectively. Assume that there are N PUs modeled by an i.i.d. homogeneous continuous-time Markov chain. With the analytical results obtained in Chapter 3, we construct a two dimensional Markov chains, whose state space is the number of PU channels in state S and the number of PU channels in state C pair at the ith SU period, denoted by (NS_i, NC_i). The transition probability from (NS_{i-1}, NC_{i-1}) to (NS_i, NC_i) can be calculated by

$$\Pr[NS_i = a, NC_i = b | NS_{i_1} = a', NC_{i-1} = b'] =$$

$$\begin{cases} 0, & M - b' < a + b < a'; \\ \binom{N - a' - b'}{N - b' - a - b} p_{W|W}^{N-b'-a-b} & \\ \times \left[\sum_{k=\max(0,a'-b)}^{\min(a,a')} \binom{a'}{k} p_{S|S}^{k} p_{C|S}^{a'-k} \binom{a + b - a'}{a - k} p_{S|W}^{a-k} p_{C|W}^{b-a'+k} \right] & \text{otherwise} \end{cases}$$

To analyze the performance of the secondary system, we observe that

1. Contention occurs if *more than one* SU chooses the PU channel in state S to transmit.

2. If *at least one* SU accesses a PU channel in state C, SU transmission collides with PU transmission.

3. Successful secondary transmission occurs when *only one* SU access a PU channel in state S.

Ongoing effort has been carried out to derive the probability of the number of successful transmissions.

List of Publication

[J1] W.-J. Wang and H.-C. Yang "Effect of imperfect spectrum sensing on slotted secondary transmission: energy efficiency and queuing performance", *IEEE Trans. Cognit. Commun. and Netw.*, accepted.

[J2] W.-J. Wang, H.-C. Yang and M.-S. Alouini "Wireless transmission of big data: a transmission time analysis over fading channel", *IEEE Trans. Wireless Commun.*, vol. 17, no. 7, pp. 4315-4325, July 2018.

[J3] W.-J. Wang, M. Usman, H.-C. Yang and M. S. Alouini, "Extended delivery time analysis for secondary packet transmission with adaptive modulation under interweave cognitive implementation", in *IEEE Trans. Cognit. Commun. and Netw.*, vol. 3, no. 2, pp. 180-189, June 2017.

[J4] W.-J. Wang and H.-C. Yang and M.-S. Alouini, "Energy consumption analysis of adaptive transmission over fading wireless channels: a statistical characterization", submitted to *IEEE Trans. Wireless Commun.*.

[J5] W.-J. Wang, H.-C. Yang and H.-S. Zhang "Performance analysis of underlay sensor transmission with RF energy harvesting", submitted to *IEEE Trans. Commun.*.

[C1] W.-J. Wang and H.-C. Yang "Queuing analysis for slotted secondary transmission with imperfect spectrum sensing", *IEEE VTC fall*, Chicago, IL, Aug. 2018.

[C2] W.-J. Wang and H.-C. Yang "Secondary sensor transmission with RF energy harvesting: energy statistics and performance analysis", *IEEE VTC fall*, Chicago, IL, Aug. 2018.

[C3] W.-J. Wang and H.-C. Yang, "Transmission time analysis for adaptive modulation system over block fading channels", *IEEE WCNC*, San Francisco, CA, Mar. 2017, pp. 1-5.

[C4] W.-J. Wang, H.-C. Yang, "Service time analysis for secondary packet transmission with adaptive modulation", *IEEE WCNC*, San Francisco, CA, Mar. 2017, pp. 1-5.

[C5] W.-J. Wang and H.-C. Yang and M.-S. Alouini, "A statistical characterization of energy consumption for adaptive transmission of big data over fading channels", submitted to *IEEE ICC 2019.*.

Bibliography

[1] H. Tran, T. Duong, and H. J. Zepernick, "Delay performance of cognitive radio networks for point-to-point communications," *EURASIP J. on Wireless Commun. and Networking*, vol. 2012, pp. 1–14, Jan. 2012.

[2] L. Sibomana, H. J. Zepernick, H. Tran, and C. Kabiri, "Packet transmission time for cognitive radio networks considering interference from primary user," in *Proc. International Wireless Communications and Mobile Computing Conference*, Jul. 2013, pp. 791–796.

[3] M. Usman, H. C. Yang, and M. S. Alouini, "Extended delivery time analysis for cognitive packet transmission with application to secondary queuing analysis," *IEEE Trans. Wireless Commun.*, vol. 14, no. 10, pp. 5300–5312, Oct. 2015.

[4] H. Liu, Y. Zhou, L. Tian, and J. Shi, "How can vehicular communication reduce rear-end collision probability on highway," in *Proc. IEEE Global Communications Conference*, Dec 2015, pp. 1–6.

[5] Y.-C. Lai and W.-H. Li, "A novel scheduler for proportional delay differentiation by considering packet transmission time," *IEEE Commun. Lett.*, vol. 7, no. 4, pp. 189–191, Apr. 2003.

[6] T. M. C. Chu, H. Phan, and H. J. Zepernick, "On the performance of underlay cognitive radio networks using M/G/1/K queueing model," *IEEE Commun. Lett.*, vol. 17, no. 5, pp. 876–879, May 2013.

[7] S. G. Cui, A. J. Goldsmith, and A. Bahai, "Energy-constrained modulation optimization," *IEEE Trans. Wireless Commun.*, vol. 4, no. 5, pp. 2349–2360, Sep. 2005.

[8] S. G. Cui, A. J. Goldsmith, and Bahai, "Energy-efficiency of MIMO and cooperative MIMO techniques in sensor networks," *IEEE J. Sel. Areas Commun.*, vol. 22, no. 6, pp. 1089–1098, Aug. 2004.

[9] R. Vaze, "Competitive ratio analysis of online algorithms to minimize packet transmission time in energy harvesting communication system," in *Proceedings IEEE INFOCOM*, Apr. 2013, pp. 115–1123.

[10] A. F. Molisch, N. B. Mehta, J. S. Yedidia, and J. Zhang, "Performance of fountain codes in collaborative relay networks," *IEEE Trans. Wireless Commun.*, vol. 6, no. 11, pp. 4108–4119, Nov. 2007.

[11] J. Hayes, "Adaptive feedback communications," *IEEE Trans. Commun. Technol.*, vol. 16, no. 1, pp. 29–34, Feb. 1968.

[12] S. Sampei and H. Harada, "System design issues and performance evaluations for adaptive modulation in new wireless access systems," *Proceedings of the IEEE*, vol. 95, no. 12, pp. 2456–2471, Dec. 2007.

[13] M. Abdallah, A. Salem, M. Alouini, and K. Qaraqe, "Discrete rate and variable power adaptation for underlay cognitive networks," in *European Wireless Conference*, Apr. 2010, pp. 733–737.

[14] *IEEE Standard for Telecommunications and Information Exchange Between Systems - LAN/MAN Specific Requirements - Part 11: Wireless Medium Access Control (MAC) and physical layer (PHY) specifications: High Speed Physical Layer in the 5 GHz band*, IEEE Std 802.11a, Dec. 1999.

[15] A. Doufexi, S. Armour, M. Butler, A. Nix, D. Bull, J. McGeehan, and P. Karlsson, "A comparison of the hiperlan/2 and ieee 802.11a wireless lan standards," *IEEE Commun. Mag.*, vol. 40, no. 5, pp. 172–180, May 2002.

[16] *IEEE Draft Standard for Information Technology– Local and Metropolitan Area Networks– Specific Requirements– Part 15.3: Wireless Medium Access Control (MAC) and Physical Layer (PHY) Specifications for High Rate Wireless Personal Area Networks (WPAN) Amendment: High-Rate Close Proximity Point-to-Point Communications*, pp. 1–152, IEEE P802.15, Oct. 2016.

[17] *Unapproved Draft IEEE Standard for Local and Metropolitan Area Networks-Part 16: Air Interface for Fixed Broadband Wireless Access Systems*, IEEE Std P802.16, Jan. 2005.

[18] S. Bi, R. Zhang, Z. Ding, and S. Cui, "Wireless communications in the era of big data," *IEEE Commun. Mag.*, vol. 53, no. 10, pp. 190–199, Oct. 2015.

[19] T. Hu, E. Bigelow, J. Luo, and H. Kautz, "Tales of two cities: Using social media to understand idiosyncratic lifestyles in distinctive metropolitan areas," *IEEE Transactions on Big Data*, vol. 3, no. 1, pp. 55–66, Mar. 2017.

[20] F. Xia, W. Wang, T. M. Bekele, and H. Liu, "Big scholarly data: A survey," *IEEE Transactions on Big Data*, vol. 3, no. 1, pp. 18–35, Mar. 2017.

[21] M. M. Najafabadi, F. Villanustre, T. M. Khoshgoftaar, N. Seliya, R. Wald, and E. Muharemagic, "Deep learning applications and challenges in big data analytics," *J. Big Data*, vol. 2, no. 1, Mar. 2015.

[22] P. K. Agyapong, M. Iwamura, D. Staehle, W. Kiess, and A. Benjebbour, "Design considerations for a 5G network architecture," *IEEE Commun. Mag.*, vol. 52, no. 11, pp. 65–75, Nov. 2014.

[23] H.-C. Yang and M.-S. Alouini, "Wireless transmission of big data: Data-oriented performance limits and their applications," [Online]. Available: https://arxiv.org/pdf/1805.09923.pdf.

[24] X. Zheng and Z. Cai, "Real-time big data delivery in wireless networks: A case study on video delivery," *IEEE Trans. Ind. Informat.*, vol. 13, no. 4, pp. 2048–2057, Aug. 2017.

[25] A. R. Ekti, M. Z. Shakir, E. Serpedin, and K. A. Qaraqe, "End-to-end downlink power consumption of heterogeneous small-cell networks based on the probabilistic traffic model," in *Proc. IEEE Wireless Communication and Networking Conference*, Apr. 2014, pp. 1138–1142.

[26] E. Gelenbe and Y. Caseau, "The impact of information technology on energy consumption and carbon emissions," *Ubiquity*, no. 1, pp. 1–15, Jun. 2015.

[27] Z. Hasan, H. Boostanimehr, and V. K. Bhargava, "Green cellular networks: A survey, some research issues and challenges," *IEEE Communications Surveys Tutorials*, vol. 13, no. 4, pp. 524–540, 4th Quart 2011.

[28] Y. Li, B. Bakkaloglu, and C. Chakrabarti, "A system level energy model and energy-quality evaluation for integrated transceiver front-ends," *IEEE Transactions on Very Large Scale Integr. Syst.*, vol. 15, no. 1, pp. 90–103, Jan. 2007.

[29] C. Yi, L. Wang, and Y. Li, "Energy efficient transmission approach for wban based on threshold distance," *IEEE Sensors Journal*, vol. 15, no. 9, pp. 5133–5141, Sep. 2015.

[30] B. Li, W. Wang, Q. Yin, R. Yang, Y. Li, and C. Wang, "A new cooperative transmission metric in wireless sensor networks to minimize energy consumption per unit transmit distance," *IEEE Communications Letters*, vol. 16, no. 5, pp. 626–629, May 2012.

[31] Z. Nan, T. Chen, X. Wang, and W. Ni, "Energy-efficient transmission schedule for delay-limited bursty data arrivals under nonideal circuit power consumption," *IEEE Trans. Veh. Technol.*, vol. 65, no. 8, pp. 6588–6600, Aug. 2016.

[32] Y. Xiao, Y. Cui, P. Savolainen, M. Siekkinen, A. Wang, L. Yang, A. Yl-Jski, and S. Tarkoma, "Modeling energy consumption of data transmission over Wi-Fi," *IEEE Trans. Mobile Comput.*, vol. 13, no. 8, pp. 1760–1773, Aug. 2014.

[33] A. Goldsmith, *Wireless Communications*. Cambridge University Press, 2005.

[34] A. J. Goldsmith and S.-G. Chua, "Variable-rate variable-power MQAM for fading channels," *IEEE Trans. Commun.*, vol. 45, no. 10, pp. 1218–1230, Oct. 1997.

[35] I. S. Gradshteyn and I. M. Ryzhik, *Table of Integrals, Series and Products*. 7th ed. Academic Press, 2007.

[36] W. Michael, D. R. Insua, and F. Ruggeri, "Mixtures of Gamma distributions with applications," *Journal of Computational and Graphical Statistics*, vol. 10, no. 3, pp. 440–454, 2001.

[37] A. Dempster, N. Laird, and D. Rubin, "Maximum likelihood from incomplete data via the em algorithm," *J. Roy. Stat. Soc. B (Met.)*, vol. 39, no. 1, pp. 1–38, 1977.

[38] G. McLachlan and T. Krishnan, *The EM Algorithm and Extensions*. New York: John Wiley & Sons, 1996.

[39] T. H. Lee, *The Design of CMOS Radio-Frequency Integrated Circuits*. Cambridge, U.K.: Cambridge Univ. Press, 1998.

[40] J. Cioffi, *Digital Communications*. Stanford, CA: Stanford Univ. Press, Fall 2001.

[41] J. Mitola and G. Q. Maguire, "Cognitive radio: making software radios more personal," *IEEE Trans. Wireless Commun.*, vol. 6, no. 4, pp. 13–18, Aug. 1999.

[42] S. Haykin, "Cognitive radio: brain-empowered wireless communications," *IEEE J. Sel. Areas Commun.*, vol. 23, no. 2, pp. 201–220, Feb. 2005.

[43] I. F. Akyildiz, W.-Y. Lee, M. C. Vuran, and S.Hohanty, "Next generation/dynamic spectrum access/cognitive radio wireless networks: A survey," *Comput. Netw. J.*, vol. 50, no. 13, pp. 2127–2159, Sep. 2006.

[44] Q. Zhao, L. Tong, A. Swami, and Y. Chen, "Decentralized cognitive mac for opportunistic spectrum access in ad hoc networks: A pomdp framework," *IEEE J. Sel. Areas Commun.*, vol. 25, no. 3, pp. 589–600, Apr. 2007.

[45] Q. Zhao, S. Geirhofer, L. Tong, and B. M. Sadler, "Opportunistic spectrum access via periodic channel sensing," *IEEE Trans. Signal Process.*, vol. 56, no. 2, pp. 785–796, Feb. 2008.

[46] M. H. Islam, C. L. Koh, S. W. Oh, X. Qing, Y. Y. Lai, C. Wang, Y. C. Liang, B. E. Toh, F. Chin, G. L. Tan, and W. Toh, "Spectrum survey in singapore: Occupancy measurements and analyses," in *Proc. International Conference on Cognitive Radio Oriented Wireless Networks and Communications*, May. 2008, pp. 1–7.

[47] B. Hamdaoui, "Adaptive spectrum assessment for opportunistic access in cognitive radio networks," *IEEE Trans. Wireless Commun.*, vol. 8, no. 2, pp. 922–930, Feb. 2009.

[48] F. Borgovono, M. Cesana, and L.Fratta, "Throughput and delay bounds for cognitive transmission," *Advances in Ad Hoc Networking*, pp. 170–190, 2008.

[49] L. C. Wang, C. W. Wang, and F. Adachi, "Load-balancing spectrum decision for cognitive radio networks," *IEEE J. Sel. Areas Commun.*, vol. 29, no. 4, pp. 757–769, Apr. 2011.

[50] C. W. Wang and L. C. Wang, "Analysis of reactive spectrum handoff in cognitive radio networks," *IEEE J. Sel. Areas Commun.*, vol. 30, no. 10, pp. 2016–2028, Nov. 2012.

[51] D. J. C. MacKay, "Fountain codes," *IEE Proceedings Communications*, vol. 152, no. 6, pp. 1062–1068, Dec. 2005.

[52] J. Castura and Y. Mao, "Rateless coding over fading channels," *IEEE Commun. Lett.*, vol. 10, no. 1, pp. 46–48, Jan. 2006.

[53] F. Gaaloul, H. C. Yang, R. M. Radaydeh, and M. S. Alouini, "Switch based opportunistic spectrum access for general primary user traffic model," *IEEE Commun. Lett.*, vol. 1, no. 5, pp. 424–427, 2012.

[54] Z. Liang and D. Zhao, "Quality of service performance of a cognitive radio sensor network," in *Proc. IEEE International Conference on Communications*, May 2010, pp. 1–5.

[55] X. Li, J. Wang, H. Li, and S. Li, "Delay analysis and optimal access strategy in multichannel dynamic spectrum access system," in *Proc. ICNC*, Jan. 2012, pp. 376–380.

[56] S. Kandeepan, C. V. Saradhi, M. Filo, and R. Piesiewicz, "Delay analysis of cooperative communication with opportunistic relay access," in *Proc. IEEE Vehicular Technology Conference-Spring*, May 2011, pp. 1–5.

[57] A. P. Namanya and J. Pagna-Disso, "Performance modelling and analysis of the delay aware routing metric in cognitive radio Ad Hoc networks," in *Proc. Joint Joint IFIP Wireless and Mobile Networking Conference*, Apr. 2013, pp. 1–8.

[58] H. Li and Z. Han, "Queuing analysis of dynamic spectrum access subject to interruptions from primary users," in *Proc. of International Conference on Cognitive Radio Oriented Wireless Networks and Communications*, Jun. 2010, pp. 1–5.

[59] M. Kahvand, M. T. Soleimani, and M. Dabiranzohouri, "Channel selection in cognitive radio networks: A new dynamic approach," in *Proc. IEEE Malaysia International Conference on Communications*, Nov 2013, pp. 407–411.

[60] V. Asghari and S. Aissa, "Adaptive rate and power transmission in spectrum-sharing systems," *IEEE Trans. Wireless Commun.*, vol. 9, no. 10, pp. 3272–3280, Oct. 2010.

[61] Y. Chen, M. S. Alouini, L. Tang, and F. Khan, "Analytical evaluation of adaptive-modulation-based opportunistic cognitive radio in nakagami- m fading channels," *IEEE Trans. Veh. Technol.*, vol. 61, no. 7, pp. 3294–3300, Sep. 2012.

[62] S. T. Chung and A. J. Goldsmith, "Degrees of freedom in adaptive modulation: a unified view," *IEEE Trans. Commun.*, vol. 49, no. 9, pp. 1561–1571, Sep. 2001.

[63] S. Geirhofer, L. Tong, and B. M. Sadler, "A measurement-based model for dynamic spectrum access in wlan channels," in *Prec. IEEE Military Communications Conference*, Oct. 2006, pp. 1–7.

[64] H. Yu, "Approximation solution methods for partially observable markov and semi-markov decision processes," Ph.D. dissertation, Massachusetts Inst. Technol.,Cambridge, MA, 2007.

[65] S. Geirhofer, L. Tong, and B. M. Sadler, "Cognitive radios for dynamic spectrum access - dynamic spectrum access in the time domain: Modeling and exploiting white space," *IEEE Commun. Mag.*, vol. 45, no. 5, pp. 66–72, May. 2007.

[66] D. Cabric, S. Mishra, and R. Brodersen, "Implementation issues in spectrum sensing for cognitive radios," in *Conference Record of the Asilomar Conference on Signals, Systems and Computers*, vol. 1, Nov 2004, pp. 772–776 Vol.1.

[67] E. Cinlar, *Introduction to stochastic process.* Englewood Cliff, NJ, USA: Prentice-Hall, 1975.

[68] I. F. Akyildiz, W. y. Lee, M. C. Vuran, and S. Mohanty, "A survey on spectrum management in cognitive radio networks," *IEEE Computer*, vol. 46, no. 4, pp. 40–48, Apr. 2008.

[69] X. Li, H. Liu, S. Roy, J. Zhang, P. Zhang, and C. Ghosh, "Throughput analysis for a multi-user, multi-channel ALOHA cognitive radio system," *IEEE Trans. Wireless Commun.*, vol. 11, no. 11, pp. 3900–3909, Nov. 2012.

[70] W. S. Jeon and D. G. Jeong, "Combined channel access and sensing in cognitive radio slotted-ALOHA networks," *IEEE Trans. Veh. Technol.*, vol. 64, no. 5, pp. 2128–2133, May 2015.

[71] Z. Khan, J. J. Lehtomki, L. A. DaSilva, and M. Latva-aho, "Autonomous sensing order selection strategies exploiting channel access information," *IEEE Trans. Mobile Comput.*, vol. 12, no. 2, pp. 274–288, Feb. 2013.

[72] X. Xing, T. Jing, H. Li, Y. Huo, X. Cheng, and T. Znati, "Optimal spectrum sensing interval in cognitive radio networks," *IEEE Trans. Parallel Distrib. Syst.*, vol. 25, no. 9, pp. 2408–2417, Sep. 2014.

[73] L. Zhang, M. Xiao, G. Wu, S. Li, and Y. C. Liang, "Energy-efficient cognitive transmission with imperfect spectrum sensing," *IEEE J. Sel. Areas Commun.*, vol. 34, no. 5, pp. 1320–1335, May 2016.

[74] D. T. C. Wong, S. Zheng, and Y. C. Liang, "Cognitive multi-channel mac protocols with perfect and imperfect sensing," in *Proc. IEEE International Conference on Communications*, Jun. 2011, pp. 1–5.

[75] J. Jeon, M. Codreanu, M. Latva-aho, and A. Ephremides, "The stability property of cognitive radio systems with imperfect sensing," *IEEE J. Sel. Areas Commun.*, vol. 32, no. 3, pp. 628–640, Mar. 2014.

[76] G. Ozcan, M. C. Gursoy, and S. Gezici, "Error rate analysis of cognitive radio transmissions with imperfect channel sensing," *IEEE Trans. Wireless Commun.*, vol. 13, no. 3, pp. 1642–1655, March 2014.

[77] H. J. Lim, D. Y. Seol, and G. H. Im, "Joint sensing adaptation and resource allocation for cognitive radio with imperfect sensing," *IEEE Trans. Commun.*, vol. 60, no. 4, pp. 1091–1100, April 2012.

[78] Q. Liu, S. Zhou, and G. B. Giannakis, "Queuing with adaptive modulation and coding over wireless links: cross-layer analysis and design," *IEEE Trans. Wireless Commun.*, vol. 4, no. 3, pp. 1142–1153, May 2005.

[79] W. J. Wang, M. Usman, H. C. Yang, and M. S. Alouini, "Extended delivery time analysis for secondary packet transmission with adaptive modulation under interweave cognitive implementation," *IEEE Transactions on Cognitive Communications and Networking*, vol. 3, no. 2, pp. 180–189, June 2017.

[80] K. W. Choi, "Adaptive sensing technique to maximize spectrum utilization in cognitive radio," *IEEE Trans. Veh. Technol.*, vol. 59, no. 2, pp. 992–998, Feb. 2010.

[81] B. Li, P. Yang, J. Wang, Q. Wu, S. Tang, X. Y. Li, and Y. Liu, "Almost optimal dynamically-ordered channel sensing and accessing for cognitive networks," *IEEE Trans. Mobile Comput.*, vol. 13, no. 10, pp. 2215–2228, Oct. 2014.

[82] A. Papoulis and U. Pillai, *Probability, Random Variables and Stochastic Process.* McGraw-Hill Europe; 4th edition, 2002.

[83] H. C. Yang and S. Sasankan, "Analysis of channel-adaptive packet transmission over fading channels with transmit buffer management," *IEEE Trans. Veh. Technol.*, vol. 57, no. 1, pp. 404–413, Jan. 2008.

[84] C. R. Stevenson, G. Chouinard, Z. Lei, W. Hu, S. J. Shellhammer, and W. Caldwell, "IEEE 802.22: The first cognitive radio wireless regional area network standard," *IEEE Commun. Mag.*, vol. 47, no. 1, pp. 130–138, Jan. 2009.

[85] E. Peh and Y. C. Liang, "Optimization for cooperative sensing in cognitive radio networks," in *Proc. IEEE Wireless Communications and Networking Conference*, Mar. 2007, pp. 27–32.

[86] Ghasemi and E. S. Sousa, "Collaborative spectrum sensing for opportunistic access in fading environments," in *Proc. IEEE International Symposium on New Frontiers in Dynamic Spectrum Access Networks*, Nov. 2005, pp. 131–136.

[87] M. Zheng, C. Xu, W. Liang, H. Yu, and L. Chen, "A novel comac-based cooperative spectrum sensing scheme in cognitive radio networks," in *Proc. IEEE International Conference on Communication Workshop*, June 2015, pp. 1009–1013.

[88] U. Baroudi, A. u. d. Qureshi, S. Mekid, and A. Bouhraoua, "Radio frequency energy harvesting characterization: An experimental study," in *Proc. IEEE International Conference on Trust, Security and Privacy in Computing and Communications*, Jun. 2012, pp. 1976–1981.

[89] V. Liu, A. Parks, V. Talla, S. Gollakota, D. Wetherall, and J. R. Smith, "Ambient backscatter: Wireless communication out of thin air," in *Proc. ACM SIGCOMM*, Aug. 2013, pp. 1–13.

[90] J. Yang and S. Ulukus, "Transmission completion time minimization in an energy harvesting system," in *Proc. Annual Conference on Information Sciences and Systems*, Mar. 2010, pp. 1–6.

[91] P. Blasco, D. Gndz, and M. Dohler, "Low-complexity scheduling policies for energy harvesting communication networks," in *Proc. IEEE International Symposium on Information Theory*, July 2013, pp. 1601–1605.

[92] A. A. Nasir, X. Zhou, S. Durrani, and R. A. Kennedy, "Wireless-powered relays in cooperative communications: Time-switching relaying protocols and throughput analysis," *IEEE Trans. Commun.*, vol. 63, no. 5, pp. 1607–1622, May 2015.

[93] T. Q. Wu and H. C. Yang, "On the performance of overlaid wireless sensor transmission with RF energy harvesting," *IEEE J. Sel. Areas Commun.*, vol. 33, no. 8, pp. 1693–1705, Aug. 2015.

[94] S. Luo, R. Zhang, and T. J. Lim, "Optimal save-then-transmit protocol for energy harvesting wireless transmitters," *IEEE Trans. Wireless Commun.*, vol. 12, no. 3, pp. 1196–1207, Mar. 2013.

[95] L. Liu, R. Zhang, and K. C. Chua, "Wireless information transfer with opportunistic energy harvesting," *IEEE Trans. Wireless Commun.*, vol. 12, no. 1, pp. 288–300, Jan. 2013.

[96] S. Lee, R. Zhang, and K. Huang, "Opportunistic wireless energy harvesting in cognitive radio networks," *IEEE Trans. Wireless Commun.*, vol. 12, no. 9, pp. 4788–4799, Sep. 2013.

[97] D. Altinel and G. K. Kurt, "Statistical models for battery recharging time in rf energy harvesting systems," in *Proc. IEEE Wireless Communications and Networking Conference*, Apr. 2014, pp. 636–641.

[98] S. Park, J. Heo, B. Kim, W. Chung, H. Wang, and D. Hong, "Optimal mode selection for cognitive radio sensor networks with RF energy harvesting," in *Proc. IEEE International Symposium on Personal, Indoor and Mobile Radio Communications*, Sep. 2012, pp. 2155–2159.

[99] T. Wu and H. Yang, "RF energy harvesting with cooperative beam selection for wireless sensors," *IEEE Wireless Communications Letters*, vol. 3, no. 6, pp. 585–588, Dec. 2014.